THESIS

THE BEHAVIOR OF ALPHA-TOCOPHEROL AND CHOLESTEROL IN THE OXIDIZED PLPC LIPID BILAYERS: A MOLECULAR DYNAMICS STUDY

PHANSIRI BOONNOY

GRADUATE SCHOOL, KASETSART UNIVERSITY
Academic Year 2021

THESIS APPROVAL
GRADUATE SCHOOL, KASETSART UNIVERSITY

DEGREE: Doctor of Philosophy (Physics)

MAJOR FIELD: Physics

DEPARTMENT: Physics

TITLE: The Behavior of Alpha-Tocopherol and Cholesterol in the Oxidized PLPC Lipid Bilayers: A Molecular Dynamics Study

NAME: Miss Phansiri Boonnoy

THIS THESIS HAS BEEN ACCEPTED BY

.... **THESIS ADVISOR**

(Associate Professor Jirasak Wong-Ekkabut, Ph.D.)

.... **DEPARTMENT HEAD**

(Associate Professor Pongsakorn Jantaratana, Ph.D.)

.... **DEAN**

(Associate Professor Srijidtra Charoenlarpnopparut, Ph.D.)

THESIS

THE BEHAVIOR OF ALPHA-TOCOPHEROL AND CHOLESTEROL IN THE
OXIDIZED PLPC LIPID BILAYERS: A MOLECULAR DYNAMICS STUDY

PHANSIRI BOONNOY

A Thesis Submitted in Partial Fulfillment of
the Requirements for the Degree of
Doctor of Philosophy (Physics)
Graduate School, Kasetsart University
Academic Year 2021

Phansiri Boonnoy : The Behavior of Alpha-Tocopherol and Cholesterol in the Oxidized PLPC Lipid Bilayers: A Molecular Dynamics Study. Doctor of Philosophy (Physics), Major Field: Physics, Department of Physics. Thesis Advisor: Associate Professor Jirasak Wong-Ekkabut, Ph.D. Academic Year 2021

Membrane lipids are particularly susceptible to oxidative attack by free radicals due to their high content of polyunsaturated phospholipids. Alpha-tocopherols (α-toc; vitamin E) and cholesterol (Chol) are two antioxidant molecules that effectively protect membranes lipids from free radical oxidative damage. Although the interactions of α-toc/Chol with lipid membranes have been shown, the roles by which it stabilizes membranes under oxidative stress are debated. In this research, the activity of α-toc and Chol in non-oxidized and oxidized lipid bilayers was investigated. Using molecular dynamics (MD) simulations of a PLPC lipid bilayer and a binary combination of PLPC and its oxidation products were done in this work. Two hydroperoxide lipids and two aldehyde lipids were considered as the primary and secondary oxidation products of PLPCs, respectively. α-toc at concentrations of 0-11.1% or Chol at concentrations of 0-50% were applied to the lipid bilayer. The effects of α -toc and Chol on lipid bilayer physical characteristics, as well as their positions and behaviors within the bilayers, were investigated. The result showed that pore development was seen in the aldehyde-containing oxidized lipid bilayers without α-toc and Chol. Pore in aldehyde bilayers is inhibited by the presence of α-toc or Chol at concentrations more than 11%. At either α-toc and Chol concentration, no pores were seen in the PLPC bilayer and the hydroperoxide-containing oxidized lipid bilayer. Furthermore, increasing cholesterol concentration in the lipid bilayer studies led to a change of the phase state from the liquid-disordered to the liquid-ordered phase for all systems. The free energy profiles were calculated using the umbrella sampling approach to obtain the free energy barrier and to calculate the rate for α-toc/Chol flip-flop within the bilayers. The results demonstrated that in the presence of oxidized lipids, the free energy barrier for both α-toc and Chol flip-flop decreases significantly. The flip-flop rate varies depending on the lipid bilayer type, with the highest rate reported in aldehyde bilayers. The oxidized lipid bilayer is stabilized by α-toc and Chol, which reduces water permeability across the bilayer by restricting the distribution of the oxidized functional groups.

_____   _____   ____ / ____ / ____

   Student's signature   Thesis Advisor's signature

ACKNOWLEDGEMENTS

Phansiri Boonnoy

TABLE OF CONTENTS

List of tables

List of figures

List of abbreviations

MD	Molecular Dynamics
PLPC	1-palmitoyl-2-linoleoyl-*sn*-glycero-3-phosphatidylcholine
13-tc	1-palmitoyl-2-(13-hydroperoxy-trans-11, cis-9-octadecadienoyl)-*sn*-glycero-3-phosphocholine
9-tc	1-palmitoyl-2-(9-hydroperoxy-trans-10, cis-12-octadecadienoyl)-sn-glycero-3-phosphocholine
12-al	1-palmitoyl-2-(12-oxo-cis-9-dodecenoyl)-sn-glycero-3-phosphocholine
9-al	1-palmitoyl-2-(9-oxo-nonanoyl)-sn-glycero-3-phosphocholine
α-toc	Alpha-Tocopherol
Chol	Cholesterol

List of publications

1. Does alpha-tocopherol flip-flop help to protect membranes against oxidation?

Phansiri Boonnoy, Mikko Karttunen, and Jirasak Wong-Ekkabut. (2018). *The Journal of Physical Chemistry B*, 122(45), 10362-10370.

2. Role of cholesterol flip-flop in oxidized lipid bilayers

Phansiri Boonnoy, Viwan Jarerattanachat, Mikko Karttunen, and Jirasak Wong-Ekkabut. (2021). *Biophysical Journal*. 120(20), 4525–4535.

SCOPE OF STUDYS

To better understand the role of α-toc and cholesterol in lipid membranes under oxidative stress, a comprehensive series of molecular dynamics simulations of α-toc and cholesterol in a model of lipid membrane were carried out in this study. The study looked at how alpha-tocopherol and cholesterol behave in the non-oxidized 1-palmitoyl-2-linoleoyl-sn-glycero-3-phosphatidylcholine (PLPC) lipid bilayer and the 50 percent oxidized-PLPC lipid bilayer, as well as their effects on physical properties in different lipid bilayers. Four main oxidation products of PLPC lipid were considered, namely, two hydroperoxides (1-palmitoyl-2-(9-hydroperoxytrans-10, cis-12-octa- decadienoyl)-sn-glycero-3-phosphocholine, 9-tc and 1-palmitoyl-2-(13-hydroperoxy-trans-11,cis-9-octadecadienoyl)-sn- glycero-3-phosphocholine, 13-tc), and two aldehydes (1- palmitoyl-2-(9-oxo-nonanoyl)-sn-glycero-3-phosphocholine, 9-al and 1-palmitoyl-2-(12-oxo-cis-9-dodecenoyl)-sn-glycero-3- phosphocholine, 12-al). α-toc and cholesterol concentrations ranged from 0-11.1 percent and 0-50 percent, respectively. Firstly, the position of α-toc and cholesterol in lipid bilayers was investigated to determine their antioxidant activity zone. Secondly, their impact on pore prevention was studied. Next, using the biased umbrella sampling method, the free energy profile of transporting a single molecule of α-toc and cholesterol through lipid bilayers was estimated. The free energy barrier for the α-toc /cholesterol flip-flop within the bilayer was calculated using the profiles. Finally, the kinetics and thermodynamics of the α-toc /cholesterol flip-flop rate were determined in various oxidized and non-oxidized bilayers.

INTRODUCTION

The cell membrane is made up of a variety of components, including lipids, membrane proteins, and other small molecules. Proteins and other molecules are embedded in a bilayer formed by lipid molecules. Lipid bilayers play an important function in cellular transport and signaling. They are semi-permeable partitions, allowing or stimulating the flow of substances into, out of, or through cells, as well as between cells.[1] The oxidative stress in biological membrane caused by an imbalance between production and elimination of oxidizing species leads to lipid peroxidation in cell membrane.[2] The double bond in unsaturated acyl chains of lipid molecules are targets of free radicals (OH^-, O_2^-, etc.). [3] Products of the lipid peroxidation process, oxidized lipids, have polar moieties at their terminals chain. Two major oxidized functional group are typically produced: hydroperoxide, and truncated chains with an aldehyde or carboxylic group.[4] Previous experimental and computer simulation studies [5-12] have demonstrated the influence of oxidized lipids in various model membrane. Oxidized lipids have a significant impact on the biophysical properties of lipid membrane particularly in terms of increasing water permeability, an increase in lipid membrane area, and a decrease in lipid chain ordering. Furthermore, an increase in oxidized lipid concentration containing an aldehyde or carboxylic group in the polar chain leads to the formation of water pores across the membrane.[6, 7, 10, 13-16] Pore formation plays an important role in biological transportation, intracellular ion concentration control, and apoptosis. Interestingly, it can potentially be applied for deverloping of cancer killing by using cold plasma treatments. Plasma induced massive lipid peroxidation in the cell membrane, resulting in a pore across the cancer cell membrane and leading to cell death.[17, 18]

α-tocopherol (Vitamin E, α-toc) is the most abundant and important lipophilic antioxidant found in cell membranes. It acts as an essential radical scavenging protecting the membrane from being oxidative attack.[19, 20] Under oxidative stress in biological membranes , α-toc is able to inhibit the initial stage of lipid peroxidation process by donating an electron in the chomanol head group to a lipid-peroxyl radical and become α-tocopheroxyl radical. [21] Although the chemical assessments of α-

toc's antioxidant abilities have been proved, its biological activities of how α-toc stabilizes membrane are still under discussion, especially in the membrane containing oxidized phospholipid. In deep understanding of α-toc's antioxidant action in the oxidized lipid membranes, the previous experimental and computational studies have focused on the location and interaction of α-toc in various model membranes. The biophysical studies have demonstrated that the chromanol ring of α-toc is placed in the neighborhood of the lipid water interface. This location suggested that the α-toc's antioxidant activity would be occurred at the membrane surface.[22-24] A molecular insight of the recycling of α-tocopheroxyl radical was observed in a computational simulation of Fabre et al. [23] They showed that α-toc can interact with vitamin C which also place close to the membrane surface and bring α-tocopheroxyl radical into the energetic ground state. Moreover, the presence of α-toc transmembrane within the lipid bilayers (α-toc flip-flop) was observed in the MD simulation studies at high temperature. Qin et al. (2009, 2011) showed that the flip-flop of α-toc in lipid bilayer depend on the temperatures, the degree of unsaturated lipid chain, and the fluidity of lipid membrane.[25, 26] Interestingly, Leng et al. performed both experiment and MD simulation of α-toc in unsaturated lipid membranes and suggested that α-toc is well designed to be efficient antioxidant molecule in cell membrane by which the location of α-toc's hydroxyl group at the lipid-water interface and the flip-flop behavior within the bilayer can trap the free radical near the lipid-water interface and can rid the lipid peroxyl radical within the bilayer. [27] However, no evidence to explain of how α-toc behaves after lipid peroxidation is occurred in membrane, the functions and the molecular insight of α-toc under oxidative in cell membrane are still unclear. Recently previous MD simulation of Boonnoy et al. has shown the inhibition of pore formation in the oxidized lipid bilayer caused by the presence of high concentration of α-toc in oxidized lipid bilayer, α-tocs help to stabilize the bilayer structure by trapping the polar oxidized functional group in the water interface and reducing water permeability across the bilayer. In addition the flip-flop of α-toc was observed in oxidized and non-oxidized bilayer even at room temperature (298 K).[28] The associations of α-toc flip-flop need to be investigated by additional studies.

Cholesterol is a foundation component in the cell membrane. It help to stabilize the fluidity of the cell membrane. [29, 30] Both experimental and computational studies have been reported that the presence of cholesterol in the lipid bilayer could affect the permeation of small molecule across the lipid bilayer such as water molecule, a drug molecule, nanoparticle as well as a free radical.[30-34] In the oxidized lipid membrane, cholesterol have showed the important role to inhibit pore formation in the oxidized lipid membrane.

In 2015, Jonas Van der Paal et al. performed molecular dynamics (MD) simulations to investigate the effect of oxidized lipids on the structural and dynamic properties of the bilayer.[13] This study has shown the mechanism of how plasma can selectively treat the cancer cell while a normal cell undamaged that help the researcher to develop a promising application in plasma medicine for anticancer therapy. Based on the deferent levels of cholesterol in the healthy normal cell and cancer cell, they performed a series of MD simulations of oxidized lipid bilayers with and without cholesterol. First, they investigated the influence of the oxidized lipids type and the degree of oxidation, three type of oxidized lipid such as OX1 (a hydroperoxide functional group), OX2 (an aldehyde functional group) and OX3 (an aldehyde functional group and the aldehyde shot chain product) were carried out in this work. The concentrations of oxidized lipids were varied from 0 to 100%. The results showed that pore formation was observed in the oxidized bilayer with the aldehyde functional group (OX2 and OX3) at the concentration of oxidized lipid up to 60% for the case of OX2 and up to 80% for the case of OX3. They suggested that the presence of the shot chain has shown the significant to prevent pore formation in the aldehyde membrane. In contrast, no pore formation was observed in the oxidized bilayer with the hydroperoxide functional group even fully oxidation at 100% of hydroperoxide lipid. To study the influence of cholesterol on the effect of oxidation, they simulated fully lipid oxidation condition. Oxidized lipid bilayers with cholesterol consist of oxidized lipid with aldehyde functional group, the shot chain product (OX3) and varying cholesterol concentrations between 0 to 50%. The results showed that at low concentrations of cholesterol (0-11%), pore formation in the oxidized

bilayer remain observed. At higher cholesterol concentrations (16-50%), the water pore was inhibited.

In 2018, Schumann-Gillett and Mara used MD simulation to study the influence of cholesterol on POPC and 10 % of oxidized POPC lipid bilayer. [35] They investigated the location and orientation of cholesterol in the lipid bilayer. The data show that in all system of pure POPC and oxidized POPC bilayer, the cholesterol's hydroxyl group prefer to stay at the aqueous phase with the ring structure till about 15 degree as respect to the bilayer normal. They did not observe the flip flop of cholesterol during the simulation for over 500 ns. However, it can be occur on microsecond times scale in various model of normal membrane without oxidized lipid [36-40], the study of cholesterol flip-flop in the oxidized lipid bilayer require the longer simulation times scale. The changes of physical properties in oxidized lipid bilayer cause by the presence of cholesterol were observed in this work. Interestingly, Cholesterol reduced the distribution of aldehyde functional group in the oxidized lipid tail. This effect is a key role that α-toc help to protect the oxidized lipid bilayer to form a pore as reported in the previous study of how α-toc inhibit pore formation in the oxidized lipid bilayer.[28]

Cholesterol, interestingly, is also considered as an antioxidant molecule. Cholesterol has a significant effect on the penetration of reactive species through membranes, according to free energy calculations: it increases the free energy barrier for certain reactive nitrogen oxide species, preventing their translocation into the lipid bilayer [41]. Thus, Membranes are protected from oxidative attack by free radicals as a result of this.

Structurally, α-toc and cholesterol have a similar molecular structure (see Figure 1) by which the ring structure of the head group consisting a hydroxyl group. This suggest that they may show the similar behavior in the oxidized lipid membrane to stabilize the membrane under oxidative stress.

The flip-flop behavior of α-toc and cholesterol has been hypothesized to help stabilize the membrane under oxidative stress. The previous study has suggested that α-toc flip-flops in a non-oxidized membrane prevent free radicals from damaging

unsaturated phospholipid molecules [42]. However, no information on how α-toc response to lipid peroxidation has been discovered. In the context of cholesterol, the activity of cholesterol flip-flop helps to stabilize oxidized membrane by balancing the area and relaxing differential-density stress in an asymmetrical oxidized lipid membrane [43]. The rate and mechanism of cholesterol flip-flop have been explored in various model membranes. [44-48] Its rate in oxidized lipid bilayers, however, is unknown. In this study, the role of α-toc and cholesterol in lipid membranes under oxidative stress, a comprehensive series of molecular dynamics simulations of α-toc and cholesterol in a model of lipid membrane were carried. The study looked at how alpha-tocopherol and cholesterol behave in the non-oxidized 1-palmitoyl-2-linoleoyl-sn-glycero-3-phosphatidylcholine (PLPC) lipid bilayer and the 50 percent oxidized-PLPC lipid bilayer, as well as their influence on physical properties in various lipid bilayers. Four main oxidation products of PLPC lipid were considered. To begin, study looked at the position of α-toc and cholesterol in lipid bilayers to establish their antioxidant activity zone. Second, their effects on pore prevention were investigated. The free energy profile of transporting a single molecule of α-toc and cholesterol into lipid bilayers was then calculated using the biased umbrella sampling method. Using the free energy profiles, the free energy cost for the α-toc /cholesterol flip-flop within the bilayer was determined.Finally, the kinetics and thermodynamics of the α-toc /cholesterol flip-flop rate were determined in various oxidized and non-oxidized bilayers. Temperature, the degree of unsaturated lipid chains, and the fluidity of the lipid membrane have all been demonstrated to influence the flip-flop rate of α-toc and cholesterol in earlier research. [44-51] As this study's key discovery revealed, oxidized lipid has an effect on the flip-flop rate of these two molecules with the rate depending on the degree of lipid oxidation and the oxidized lipid type.

BACKGROUND AND RATIONAL

Membrane lipids are particularly susceptible to oxidative attack by free radicals due to their high content of polyunsaturated phospholipids. Oxidized lipids, products of the lipid peroxidation process extremely influence the change of biophysical properties of cellular membranes. The presence of high concentrations of oxidized lipid especially aldehyde lipids in the lipid membrane caused pore formation and lipid membrane deformation. α-toc and cholesterol are two antioxidant molecules that effectively protect membranes lipids from free radical oxidative damage. In previous studies have shown that the presence of high concentrations of α-toc and cholesterol could inhibit pore formation in oxidized lipid bilayers. Although the interactions of α-toc/cholesterol with oxidized lipid membranes have been shown, the roles by which it stabilizes membranes under oxidative stress are debated. To better understand the role of α-toc and cholesterol in lipid membranes under oxidative stress, a comprehensive series of molecular dynamics (MD simulations of α-toc and cholesterol in a model of lipid membrane were carried out in this study. The aims of this work are to investigate the position of α-toc and cholesterol in lipid bilayers to establish their antioxidant activity zone. The effects of α-toc and cholesterol on pore prevention were investigated. The flip-flop behavior of α-toc and cholesterol are proposed to be the activity of these two molecules to help stabilize the oxidized membrane. Thus, the free energy profile of transporting a single molecule of α-toc and cholesterol into lipid bilayers was then calculated using the biased umbrella sampling method to determine the free energy barrier for the α-toc /cholesterol flip-flop within the oxidized membrane, as well as the α-toc /cholesterol flip-flop rate in various oxidized and non-oxidized bilayers.

Molecular dynamic (MD) simulations of α-toc in lipid bilayers

First, MD simulations of 1-palmitoyl-2-linoleoyl-sn-glycero-3-phosphatidylcholine (100% PLPC) bilayer and 50% oxidized bilayer with the mixture bilayer between PLPC and its oxidation products were performed. PLPC is unsaturated phospholipid containing 2 double bonds in the sn-2 of fatty acid chain. It can be oxidized by free radicals especially reactive oxygen spices (ROS) and provided

four main oxidation product namely 1-palmitoyl-2-(13-hydroperoxy-trans-11,cis-9-octadecadienoyl)-sn-glycero-3-phosphocholine (13-tc), 1-palmitoyl-2-(9-hydroperoxy-trans-10, cis-12-octadecadienoyl)-sn-glycero-3-phosphocholine (9-tc) , 1-palmitoyl-2-(12-oxo-cis-9-dodecenoyl)-sn-glycero-3-phosphocholine (12-al) and 1-palmitoyl-2-(9-oxo-nonanoyl)-sn-glycero-3-phosphocholine (9-al). A lipid bilayer consist of 128 phospholipid molecules (64 molecules per leaflet) and solvate by 10628 simple point charge water molecules. [52] The chemical structure of all lipid molecules are shown in Figure 1. The lipid bilayer at 100 ns of MD simulations were used as the initial structure to prepare the bilayer containing α-toc. The concentrations of α-toc were varied at 0%, 1.5%, 3.0%, 5.9%, and 11.1% (equivalent to the number of 0, 2, 4, 8, and 16 α-toc molecules in the lipid bilayer, respectively). All simulation system studies were listed in Table 1. The united force field parameters of both PLPC and the oxidized lipids were taken from the previous study.[5, 8, 10, 53] For the detailed descriptions of the topologies and force-field parameters of α-toc were optimized by Qin et al. [49, 50] After energy minimization with steepest descents algorithm, MD simulations were run for over 3 microseconds with an integration time step of 2 fs by using GROMACS 5.1.2 program package. [54] The NPT ensemble (constant of the number of atoms, pressure, and temperature) were applied. The temperature was set to 298 K controlling by the v-rescale algorithm [55] with a time constant of 0.1 ps. An equilibrium semi-isotropic pressure was applied using Parrinello-Rahman algorithm [56, 57] with a time constant of 4.0 and compressibility of 4.5 x 10-5 bar-1 to keep a constant of pressure at 1 bar. All bond lengths were constrained by the P-LINCG algorithm.[58] Periodic boundary conditions were applied in all xyz directions and the neighbor list was updated every at every integration time step. A cutoff value of 1.0 was used to for the real space part of van der Waal and electrostatic interactions. The particle-mesh Ewald method was applied to compute the long-rang electrostatic interaction with a 0.12 nm grid in the reciprocal-space interaction and cubic interaction of order four. [59-61] Visual Molecular Dynamics (VMD), a molecular visualization program was used to display the trajectory of molecular movement for all systems. [62]

Molecular dynamic (MD) simulations of cholesterol in lipid bilayers

A series of molecular dynamic (MD) simulations of cholesterol in PLPC bilayer and the binary mixture bilayer with 1:1 ratio of PLPC:Oxidized lipids were performed to investigate the behavior of cholesterol in the PLPC and oxidized PLPC lipid bilayers. A lipid bilayer had 128 phospholipid molecules with 64 molecules in each upper and lower leaflets. The concentrations of 0%, 1.5%, 3%, 6%, 11%, 17%, 20%, 23%, 29%, 33%, 40% and 50% of cholesterol (equivalent to the number of 0, 2, 4, 8, 16, 26, 32, 38, 52, 64, 86 and 128 cholesterol molecules in the lipid bilayer, respectively) were prepared in this work. Each system was generated using MemGen program [63] with cholesterol molecules were randomly added in the lipid bilayer, which were divided equally in both upper and lower leaflets as shown in Figure 2. All systems were solvated in 10,560 simple point charged (SPC) water molecules. [52] Detailed descriptions of the system are shown in Table 2. The structure and force field parameter of cholesterol are taken from Höltje et al. [64] After energy minimization with steepest descents algorithm, MD simulations were run for over 3 microseconds by using GROMACS 5.1.2 program package. [54] All MD run control parameters were defined with the same parameter in the MD simulations study of α-toc in lipid bilayers in the previous as described above.

Biased umbrella sampling MD simulations

The biased umbrella sampling MD simulations [65] with the Weighed Histogram Analysis Method [66] were performed to investigate the potential of mean force or the free energy profile for α-toc and cholesterol molecule partitioning across the 100% PLPC, 50% 13-tc, 50% 9-tc, 50% 12-al, and 50% 9-al lipid bilayers. Based on the free energy profile could provide the free energy cost for moving an α-toc or a cholesterol molecule into the lipid bilayer, and estimate the free energy barrier for α-toc /cholesterol flip-flop in the lipid bilayers. Furthermore, at the minimum in free energy profile refer to the preferable location of α-toc /cholesterol in the lipid bilayers. This can be directly compare in the unbiased MD simulations and experimental studies. A series of 41 simulation windows were performed to compute a free energy profile for moving an α-toc or cholesterol from the bilayer center to the

water phase. During the umbrella sampling MD simulations, the hydroxyl group of α-toc and cholesterol molecule (see Figure 1) were restrained along in z direction by using a harmonic potential function with a force constant of 3000 kJ/(mol nm^2). All simulations were run under NPT ensemble at the constant temperature of 298 K and a constant pressure at 1 bar. Each simulations were performed at least 50 ns and the last 20 ns was used for analysis.
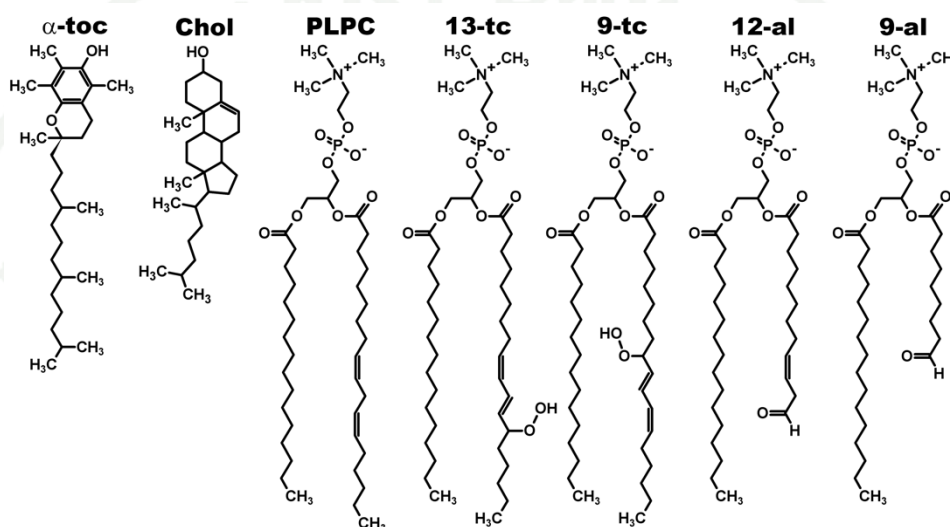
Figure 1 Chemical structure of alpha-tocopherol, cholesterol, and lipid molecules. From left to right: alpha-tocopherol (α-toc), cholesterol (Chol), 1-palmitoyl-2-linoleoyl-sn-glycero-3-phosphatidylcholine (PLPC), 1-palmitoyl-2-(13-hydroperoxy-trans-11,cis-9-octadecadienoyl)-sn-glycero-3-phosphocholine (13-tc), 1-palmitoyl-2-(9-hydroperoxy-trans-10, cis-12-octadecadienoyl)-sn-glycero-3-phosphocholine (9-tc), 1-palmitoyl-2-(12-oxo-cis-9-dodecenoyl)-sn-glycero-3-phosphocholine (12-al) and 1-palmitoyl-2-(9-oxo-nonanoyl)-sn-glycero-3-phosphocholine (9-al).

Table 1. List of simulation systems for the MD simulations of α-tocopherol in the PLPC lipid bilayer and the oxidized PLPC lipid bilayers.

No.	description of the systems	Number of molecule				simulation time (ns)
		PLPC	OXPLs	a-toc	water	
1	100% PLPC	128	0	0	10628	1000
2	100% PLPC + 1.5 % α-toc	128	0	2	10628	1000
3	100% PLPC + 3.0 %α-toc	128	0	4	10628	1000

4	100% PLPC + 5.9 % α-toc	128	0	8	10628	1000
5	50% 13-tc	64	64	0	10628	1000
6	50% 13-tc + 1.5 % α-toc	64	64	2	10628	1000
7	50% 13-tc + 3.0 % α-toc	64	64	4	10628	1000
8	50% 13-tc + 5.9 % α-toc	64	64	8	10628	1000
9	50% 9-tc	64	64	0	10628	1000
10	50% 9-tc + 1.5 % α-toc	64	64	2	10628	1000
11	50% 9-tc + 3.0 % α-toc	64	64	4	10628	1000
12	50% 9-tc + 5.9 % α-toc	64	64	8	10628	1000
13	50% 12-al	64	64	0	10628	1000
14	50% 12-al + 1.5 % α-toc	64	64	2	10628	5000
15	50% 12-al + 3.0 % α-toc	64	64	4	10628	5000
16	50% 12-al + 5.9 % α-toc	64	64	8	10628	5000
17	50% 12-al + 11.1 % α-toc	64	64	16	10628	5000
18	50% 9-al	64	64	0	10628	1000
19	50% 9-al + 1.5 % α-toc	64	64	2	10628	5000
20	50% 9-al + 3.0 % α-toc	64	64	4	10628	5000
21	50% 9-al + 5.9 % α-toc	64	64	8	10628	5000
22	50% 9-al + 11.1 % α-toc	64	64	16	10628	5000

Table 2 List of simulation systems for the MD simulations of cholesterol (Chol) in the PLPC lipid bilayer and the oxidized PLPC lipid bilayers.

No.	description of the systems	Number of molecules in the lipid bilayer			Simulation time (ns)
		PLPC	OXPLs	Cholesterol	
1	100% PLPC without Chol	128	0	0	1000
2	100% PLPC + 1.5 % Chol	128	0	2	3000
3	100% PLPC + 3 % Chol	128	0	4	3000
4	100% PLPC + 6 % Chol	128	0	8	3000
5	100% PLPC + 11 % Chol	128	0	16	3000
6	100% PLPC + 17 % Chol	128	0	26	3000
7	100% PLPC + 20 % Chol	128	0	32	3000
8	100% PLPC + 23 % Chol	128	0	38	3000
9	100% PLPC + 29 % Chol	128	0	52	3000
10	100% PLPC + 33 % Chol	128	0	64	3000
11	100% PLPC + 40 % Chol	128	0	86	3000
12	100% PLPC + 50 % Chol	128	0	128	3000
13	50% 13-tc without Chol	64	64	0	1000
14	50% 13-tc + 1.5 % Chol	64	64	2	3000
15	50% 13-tc + 3 % Chol	64	64	4	3000
16	50% 13-tc + 6 % Chol	64	64	8	3000
17	50% 13-tc + 11 % Chol	64	64	16	3000
18	50% 13-tc + 17 % Chol	64	64	26	3000
19	50% 13-tc + 20 % Chol	64	64	32	3000

20	50% 13-tc + 23 % Chol	64	64	38	3000
21	50% 13-tc + 29 % Chol	64	64	52	3000
22	50% 13-tc + 33 % Chol	64	64	64	3000
23	50% 13-tc + 40 % Chol	64	64	86	3000
24	50% 13-tc + 50 % Chol	64	64	128	3000
25	50% 9-tc without Chol	64	64	0	1000
26	50% 9-tc + 1.5 % Chol	64	64	2	3000
27	50% 9-tc + 3 % Chol	64	64	4	3000
28	50% 9-tc + 6 % Chol	64	64	8	3000
29	50% 9-tc + 11 % Chol	64	64	16	3000
30	50% 9-tc + 17 % Chol	64	64	26	3000
31	50% 9-tc + 20 % Chol	64	64	32	3000
32	50% 9-tc + 23 % Chol	64	64	38	3000
33	50% 9-tc + 29 % Chol	64	64	52	3000
34	50% 9-tc + 33 % Chol	64	64	64	3000
35	50% 9-tc + 40 % Chol	64	64	86	3000
36	50% 9-tc + 50 % Chol	64	64	128	3000
37	50% 12-al without Chol	64	64	0	1000
38	50% 12-al + 1.5 % Chol	64	64	2	1000
39	50% 12-al + 3 % Chol	64	64	4	3000
40	50% 12-al + 6 % Chol	64	64	8	2000
41	50% 12-al + 11 % Chol	64	64	16	3000
42	50% 12-al + 17 % Chol	64	64	26	3000

43	50% 12-al + 20 % Chol	64	64	32	3000
44	50% 12-al + 23 % Chol	64	64	38	3000
45	50% 12-al + 29 % Chol	64	64	52	3000
46	50% 12-al + 33 % Chol	64	64	64	3000
47	50% 12-al + 40 % Chol	64	64	86	3000
48	50% 12-al + 50 % Chol	64	64	128	3000
49	50% 9-al without Chol	64	64	0	1000
50	50% 9-al + 1.5 % Chol	64	64	2	1000
51	50% 9-al + 3 % Chol	64	64	4	1000
52	50% 9-al + 6 % Chol	64	64	8	1000
53	50% 9-al + 11 % Chol	64	64	16	3000
54	50% 9-al + 17 % Chol	64	64	26	3000
55	50% 9-al + 20 % Chol	64	64	32	3000
56	50% 9-al + 23 % Chol	64	64	38	3000
57	50% 9-al + 29 % Chol	64	64	52	3000
58	50% 9-al + 33 % Chol	64	64	64	3000
59	50% 9-al + 40 % Chol	64	64	86	3000
60	50% 9-al + 50 % Chol	64	64	128	3000

Flip-flop rate calculation

To estimate the rate of α-toc/cholesterol flip-flops (k_{flip}) in the lipid bilayers, the additional 50 simulations system of α-toc/cholesterol initially at the bilayer center. The initial configurations for these simulations were taken from the final structures of the umbrella sampling simulation in which the hydroxyl group of the α-toc/choleaterol was set at z=0 nm. The 50 independent simulations of each bilayers were independently run for 50 to 100 ns and the time for the hydroxyl group of the α-toc/cholesterol to return to the equilibrium position (t_d) was recorded. The rate of α-toc/cholesterol flip-flop across a lipid bilayer (k_{flip}) was calculated the following way [36, 67]:

$$k_{flip} = \frac{1}{\left[(1/k_f) + (1/k_d)\right]} \times 1/2$$

, where k_d is the rate of α-toc/cholesterol move from the bilayer center to the equilibrium position and it was calculated by $k_d = t_d^{-1}$. On the others hands, the rate of α-toc/cholesterol move from the equilibrium position to the bilayer center (k_f) was calculated using the equation

$$k_f = k_d \times \exp(-\Delta G_{center}/RT)$$

, where ΔG_{center} is the free energy difference between the equilibrium position and the bilayer center, in this work, ΔG_{center} was approximated equivalent of the free energy barrier ($\Delta G_{barrier}$). The haft time for flip-flop ($t_{1/2}$) was calculated by

$$t_{1/2} = \ln 2/k_{flip}$$

OBJECTIVES

1. To investigate the behavior of alpha-tocopherol and cholesterol in the non-oxidized/oxidized PLPC lipid bilayers

2. To study the effects of alpha-tocopherol and cholesterol on the biophysical properties of non-oxidized/oxidized PLPC lipid bilayers

3. To investigate the effect of alpha-tocopherol and cholesterol on pore formation in the oxidized PLPC lipid bilayers

CONTRIBUTIONS AND OUTCOME OF RESEARCH

Oxidized lipids, products of the lipid peroxidation process extremely influence the change of biophysical properties of cellular membranes. The presence of high concentrations of oxidized lipid especially aldehyde lipids in the lipid membrane caused pore formation and lipid membrane deformation. α-toc is a well-known antioxidant molecule that is essential for defending cellular membranes from free radical attacks and cholesterol show several characteristics that are typically linked with an antioxidant molecule. α-toc and cholesterol have been found in previous research to help prevent pore formation in the oxidized lipid membrane. [13, 68] The action of α-toc and cholesterol within oxidized and non-oxidized lipid bilayers was examined in this study to better understand how these two molecules help to stabilize the oxidized lipid bilayer. To describe the changes in physical properties caused by α-toc and cholesterol, thorough investigations of lipid bilayer properties were carried out. This understanding of how α-toc and cholesterol affect oxidized membranes will likely be useful in the development of novel chemicals for anti-aging cosmetics [69] and cancer-killing applications using cold atmospheric pressure plasma treatment. [17, 70-72]

PUBLICATIONS

1. Does alpha-tocopherol flip-flop help to protect membranes against oxidation?

Phansiri Boonnoy, Mikko Karttunen, and Jirasak Wong-Ekkabut. (2018). *The Journal of Physical Chemistry B*, 122(45), 10362-10370.

2. Role of cholesterol flip-flop in oxidized lipid bilayers

Phansiri Boonnoy, Viwan Jarerattanachat, Mikko Karttunen, and Jirasak Wong-Ekkabut. (2021). *Biophysical Journal*. 120(20), 4525–4535.

Publication 1

Does α-Tocopherol Flip-Flop Help to Protect Membranes Against Oxidation?

Published as part of The Journal of Physical Chemistry virtual special issue "Deciphering Molecular Complexity in Dynamics and Kinetics from the Single Molecule to the Single Cell Level".

Phansiri Boonnoy,[†,‡] Mikko Karttunen,*[,§,∥] and Jirasak Wong-ekkabut*[,†,‡,⊥,#]
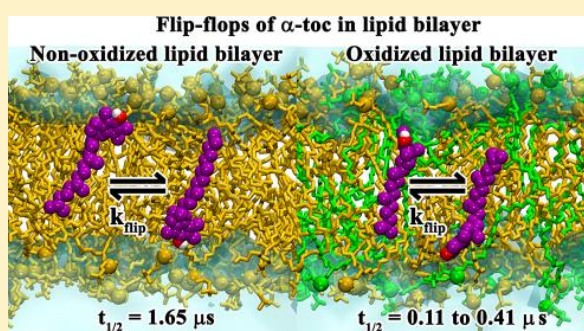
[†]Department of Physics, Faculty of Science, [‡]Computational Biomodelling Laboratory for Agricultural Science and Technology, Faculty of Science, and [#]Specialized Center of Rubber and Polymer Materials for Agriculture and Industry, Faculty of Science, Kasetsart University, Bangkok 10900, Thailand

[§]Department of Chemistry and [∥]Department of Applied Mathematics, Western University, 1151 Richmond Street, London, Ontario N6A 5B7, Canada

[⊥]Thailand Center of Excellence in Physics, Commission on Higher Education, Bangkok 10400, Thailand

Ⓢ *Supporting Information*

ABSTRACT: α-Tocopherols (α-toc) are crucial in protecting biological membranes against oxidation by free radicals. We investigate the behavior of α-toc molecules in lipid bilayers containing oxidized lipids by molecular dynamics (MD) simulations. To verify the approach, the location and orientation of α-toc are first shown to be in agreement with previous experimental results. The simulations further show that α-toc molecules stay inside the lipid bilayer with their hydroxyl groups in contact with the bilayer surface. Interestingly, interbilayer α-toc flip-flop was observed in both oxidized and nonoxidized bilayers with significantly higher frequency in aldehyde lipid bilayer. Free-energy calculations were performed, and estimates of the flip-flop rates across the bilayers were determined. As the main finding, our results show that the presence of oxidized lipids leads to a significant decrease of free-energy barriers and that the flip-flop rates depend on the type of oxidized lipid present. Our results suggest that α-toc molecules could potentially act as high-efficacy scavengers of free radicals to protect membranes from oxidative attack and help stabilize them under oxidative stress.

Flip-flops of α-toc in lipid bilayer
Non-oxidized lipid bilayer | Oxidized lipid bilayer
k_{flip} | k_{flip}
$t_{1/2}$ = 1.65 μs | $t_{1/2}$ = 0.11 to 0.41 μs

■ INTRODUCTION

An imbalance between the production and elimination of oxidizing lipid species in cell membrane can lead to oxidative attack on unsaturated lipids.[1] α-Tocopherol (α-toc; a form of vitamin E) is the most abundant and important lipophilic antioxidant found in cell membranes.[2−4] It is known to act as an essential radical scavenger protecting membranes from oxidation, but several key aspects of the molecular mechanisms of this action remain uncovered. α-toc inhibits lipid peroxidation process by donating a hydrogen atom to a lipid-peroxyl radical and becoming an α-tocopheroxyl radical.[5] Although chemical assessment of α-toc's antioxidant ability has been shown, the mechanisms by which it stabilizes membranes are debated.[3,6−9]

Significant experimental and computational effort has been invested in characterizing the location and interactions of α-toc in model membranes,[8−19] but obtaining precise information has proven to be challenging,[9,16] and the behavior and interaction mechanisms of α-toc molecules inside an oxidized lipid bilayer are being debated. Biophysical studies have, however, demonstrated that the chromanol ring of α-toc is located at the lipid−water interface.[12,13,16] This suggests that membrane surface is the key to α-toc's antioxidant activity. It has also been suggested that α-toc partitions in membrane regions are rich in polyunsaturated lipids, but more studies are needed to confirm this.[8,9]

In addition to the above, molecular dynamics (MD) simulations at elevated temperatures have demonstrated the presence of transmembrane flip-flops.[10,11] It has been shown that the flip-flop rate depends on temperature, the degree of unsaturated lipid chains, and the fluidity of the lipid membrane.[10,11] It has been shown that flip-flops are intimately related to trapping free radicals near the lipid−water interface allowing for the lipid peroxyl radical(s) to be removed.[16] However, thus far there is no information on how α-toc behaves after lipid peroxidation has occurred. In addition, the
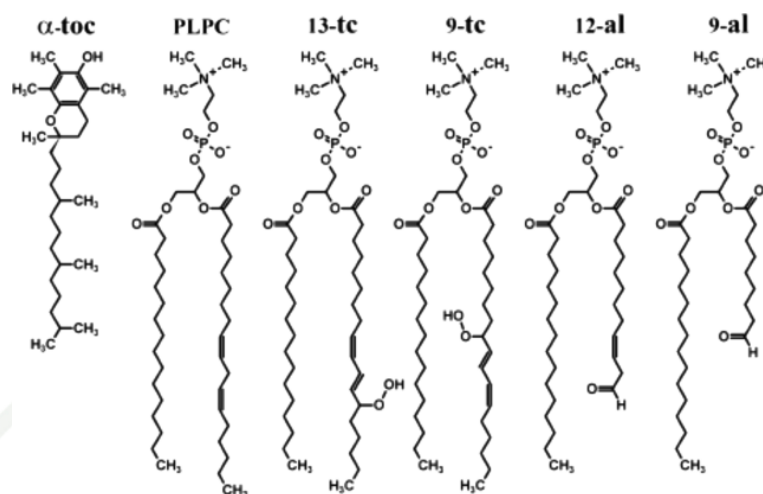
Figure 1. Chemical structures of the α-toc and lipid molecules. (left to right) α-toc, PLPC, 13-tc, 9-tc, 12-al, and 9-al.

functions and molecular insight into α-toc's actions in oxidative cell membrane remain unclear. In our previous MD simulations[18] we have shown that α-toc inhibits pore formation in oxidized lipid bilayers. In particular, α-tocs help to stabilize the bilayer structure by trapping the polar oxidized functional group at the water interface thus reducing water permeability across the bilayer. In addition, transmembrane flip-flop of α-toc were observed in both oxidized and nonoxidized bilayer even at room temperature. However, the energetics of the process need to be elaborated.

In this work, we focus on the dynamics and kinetics of α-toc flip-flop in both pure and oxidized lipid bilayers. The effects of different oxidized functional groups were studied. The free-energy profiles for α-toc desorbing out of the bilayer were calculated, and the flip-flop rates were estimated. The results show that the free-energy barriers become significantly decreased in the presence of oxidized lipids and that the flip-flop rates depend on the type of oxidized lipid present. This study presents new evidence of how α-toc protects oxidized cell membranes.

■ **METHODOLOGY**

We performed MD simulations of oxidized and nonoxidized phospholipid bilayers at various α-toc concentrations. All of the lipid bilayers had 128 lipid molecules (64 per leaflet). A 100% 1-palmitoyl-2-linoleoyl-sn-glycero-3-phosphatidylcholine (PLPC) lipid bilayer was used as a reference to characterize the effects of α-toc on a nonoxidized bilayer. For the oxidized bilayers, we used 1:1 binary mixtures of PLPC and its four main oxidative derivative products, namely, two hydro-peroxides (1-palmitoyl-2-(9-hydroperoxytrans-10, cis-12-octa-decadienoyl)-sn-glycero-3-phosphocholine, 9-tc and 1-palmi-toyl-2-(13-hydroperoxy-trans-11,cis-9-octadecadienoyl)-sn-glycero-3-phosphocholine, 13-tc), and two aldehydes (1-palmitoyl-2-(9-oxo-nonanoyl)-sn-glycero-3-phosphocholine, 9-al and 1-palmitoyl-2-(12-oxo-cis-9-dodecenoyl)-sn-glycero-3-phosphocholine, 12-al). The molecular structures of α-toc and the lipids are shown in Figure 1. We studied bilayers with 0, 2, 4, 8, and 16 α-toc molecules (equivalent to the concentrations of 0%, 1.5%, 3.0%, 5.9%, 11.1%, respectively). All systems were solvated in 10 628 simple point charged (SPC) water.[20] The parameters of both PLPC and the oxidized lipids were taken

from previous studies.[21−23] Detailed descriptions of the topologies and force-field parameters of α-toc are provided in refs 10 and 11. Initially, α-toc molecules were randomly placed in the water phase at ∼4.2 nm in the z-direction from the center of the bilayer. The passive penetration times of the α-toc molecules into the bilayers varied from tens to several hundreds of nanoseconds. At the high concentrations (5.9% and 11.1%) α-toc molecules required much longer times to enter the lipid bilayer (over several microseconds), and in some cases pore formation occurred before complete trans-location of α-toc molecules into the lipid bilayer. To avoid artificial pore formation induced by the initial conditions, the α-toc molecules were randomly inserted at the lipid−water interface at high concentrations. The details of all simulations are provided in Table 1.

Simulation Details. After energy minimization using the steeped descents algorithm, MD simulations were run for 1−5 μs with 2 fs integration time step using the GROMACS 5.1.1 package.[24] All simulations were performed in the constant of particle number, pressure, and temperature (NPT) ensemble. The v-rescale algorithm[25] at 298 K with a time constant of 0.1 ps was used for temperature control, and equilibrium semi-isotropic pressure was set at 1 bar using the Parrinello−Rahman algorithm[26] with a time constant of 4.0 ps and compressibility of 4.5×10^{-5} bar^{-1}. Periodic boundary conditions were applied in all directions, and the neighbor list was updated at every time step. A cutoff of 1.0 nm was applied for the real space part of electrostatic interactions and Lennard-Jones interactions. The particle-mesh Ewald meth-od[27−29] was used to compute the long-range part of electrostatic interactions with a 0.12 nm grid in the reciprocal-space interactions and cubic interpolation of order four. All bond lengths were constrained by the P-LINCS algorithm.[30] The optimized parameters and protocols have been extensively tested and used previously, for example, in refs 18,23, and 31−33. All visualizations were done using Visual Molecular Dynamics (VMD) software.[34]

Free-Energy Calculations. The umbrella sampling technique[35] with the Weighted Histogram Analysis Method[36] (WHAM) was used to calculate the potential of mean force (PMF) for transferring an α-toc through the 100% PLPC, 50% 13-tc, 50% 9-tc, 50% 12-al, and 50% 9-al bilayers. For each

Table 1. List of Systems Studied Here

No.	description of the systems	simulation time (ns)	final structure
1	100% PLPC	1000	bilayer
2	100% PLPC + 2 α-toc (1.5%)	1000	bilayer
3	100% PLPC + 4 α-toc (3.0%)	1000	bilayer
4	100% PLPC + 8 α-toc (5.9%)	1000	bilayer
5	50% 13-tc	1000	bilayer
6	50% 13-tc +2 α-toc (1.5%)	1000	bilayer
7	50% 13-tc +4 α-toc (3.0%)	1000	bilayer
8	50% 13-tc +8 α-toc (5.9%)	1000	bilayer
9	50% 9-tc	1000	bilayer
10	50% 9-tc +2 α-toc (1.5%)	1000	bilayer
11	50% 9-tc +4 α-toc (3.0%)	1000	bilayer
12	50% 9-tc +8 α-toc (5.9%)	1000	bilayer
13	50% 12-al	1000	bilayer with a pore (576 ns)
14	50% 12-al +2 α-toc (1.5%)	1500	bilayer with a pore (1064 ns)
15	50% 12-al +4 α-toc (3.0%)	3000	bilayer with a pore (2802 ns)
16	50% 12-al +8 α-toc (5.9%)	4000	bilayer with a pore (3394 ns)
17	50% 12-al +16 α-toc (11.1%)	5000	bilayer
18	50% 9-al	1000	bilayer with a pore (577 ns)
19	50% 9-al +2 α-toc (1.5%)	1000	bilayer with a pore (391 ns)
20	50% 9-al +4 α-toc (3.0%)	5000	bilayer with a pore (4794 ns)
21	50% 9-al +8 α-toc (5.9%)	2000	bilayer with a pore (1589 ns)
22	50% 9-al +16 α-toc (11.1%)	5000	bilayer

[a]Each 100% PLPC bilayer and 50% hydroperoxide (13-tc, 9-tc) mixture was run for 1 μs. The 50% aldehyde (12-al, 9-al) mixtures were run for 1−5 μs to study the effects of α-toc on pore formation. Pore formation time and when a pore/pores occurred is shown in the brackets in the column marked final structure. Both the absolute number and the percentage of α-toc molecules are given in the column description of the system.

system, a series of 41 simulation windows was run to compute the PMF profile as a function of the distance between α-toc and the bilayer center varying from $z = 0$ nm (bilayer center) to $z = 4.0$ nm (water phase) with 0.1 nm increments. A harmonic potential was applied between the center of mass of the bilayer and the α-toc hydroxyl group with a harmonic force constant of 3000 kJ/(mol nm^2). Each window was run in the NPT ensemble at 298 K for at least 50 ns; the total time of each PMF profile was at least 2.05 μs. The last 20 ns was used for analysis. The statistical uncertainty in umbrella sampling simulations was estimated by the bootstrap analysis method.[37]

■ RESULTS AND DISCUSSION

A series of MD simulations of α-toc molecules in different lipid bilayers was performed to study their dynamics in both oxidized and nonoxidized bilayers. Previous MD simulations[18]

have shown that the presence of ∼6%−11% of α-toc molecules in an aldehyde bilayer helps protect against passive pore formation induced by oxidized lipids.[38] In this work, pore formation was observed in aldehyde bilayers at 5.9% of α-toc, but the time to form a pore extended for over 1−3 μs. We confirmed that 11.1% α-toc in aldehyde bilayers can prevent pore formation and help to stabilize the oxidized bilayer for times exceeding 5 μs (Figure 2A,B). Interestingly, MD simulations also showed that α-toc's orientations and transmembrane flip-flops are different in nonoxidized and oxidized bilayer. This indicates that the interactions of α-toc with the bilayer are different before and after lipid peroxidation. It may also indicate, although it must be tested by experiments, that these differences are important in determining α-toc's antioxidant action. To characterize the flip-flops, we calculated the free-energy profiles for α-toc desorbing out of the bilayer and estimated the rate of α-toc flip-flop. These issues will be discussed below.

The Behavior of α-toc inside the Lipid Bilayers. To investigate where α-toc molecules reside inside the different bilayers, we investigated the time evolution of the positions of α-tocs' hydroxyl groups along the z-axis (Figure 3). The results show the hydroxyl groups prefer to stay at the bilayer-water interface around the carbonyl group (see Figure 1 for the lipid structures) for both oxidized and nonoxidized bilayers, Table S1. This is in agreement with previous MD simulations[18] and experiments.[9]

In nonoxidized membranes, the presence of α-toc molecules in the lipid−water interface region helps to protect the bilayer from approaching free radicals.[5] When oxidized lipids are present, α-toc flip-flop has an important function in helping to reach and scavenge peroxyl radicals within the lipid bilayer.[16] Figure 2C−G shows snapshots of α-toc transmembrane flip-flop. In the next two sections we quantified the process by computing the free energy and the flip-flop rates, but as an indicative rough comparison we followed the molecules in five lipid bilayers containing 5.9% α-toc molecules over 1 μs and found 21, 10, 16, 7, and 4 events for 50% 9-al, 50% 12-al, 50% 13-tc, 30% 9-tc, and 100% PLPC lipid bilayers, respectively. For the aldehyde bilayers containing 11.1% α-toc molecules, we observed 136 flip-flops for the 50% 9-al bilayer and 162 for the 50% 12-al bilayer over 5 μs. This suggests that the faster dynamics of the α-toc molecules may be a key to its antioxidant action and consequent stabilization of the bilayer under oxidative stress.

The orientations of the α-toc molecules were investigated by calculating the angle between the bilayer normal (z-axis) and a vector connecting the last methyl group in the tail to the hydroxyl group in the headgroup (see Figure 1 for the molecular structures). The last 500 ns (before pore creation in aldehyde bilayers) of lipid bilayers with 5.9% α-toc molecules were used for analysis and shown in Figure 4 and Figure S1. The angles range between 0 and 90°: 0° is equal to alignment parallel to the bilayer normal, and 90° corresponds to being perpendicular to the bilayer normal. To check the generality of this approach, we also calculated the orientations of the α-toc molecules by using the vector connecting the weight center of the tail to the hydroxyl group in the headgroup of α-toc molecules. Both methods yield full consistent distributions for the tilt angle as shown in Figure S2. For the PLPC lipid bilayer, most of the α-toc's hydroxyl groups were found to be located slightly underneath the lipids' carbonyl groups within the lipid bilayer (Table S1) in agreement with previous experimental
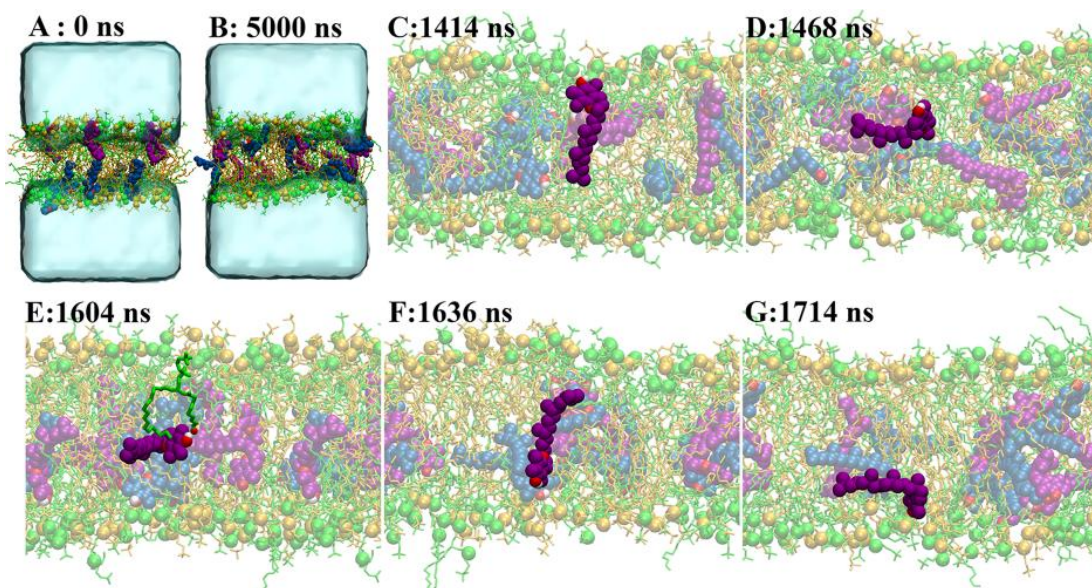
Figure 2. α-toc flip-flop in a 50% 9-al bilayer with 11.1% α-toc molecules present. (A) Initial structure at 0 ns. The 16 α-toc molecules were randomly inserted at the lipid—water interface (eight molecules in each leaflet). PLPC and 9-al lipids are shown as yellow and green lines, respectively, with phosphorus atoms as spheres. α-toc molecules are shown in purple and blue spheres, which represent α-tocs in the upper and lower leaflets, respectively. Water is shown in light blue (only in (A) for clarity). Oxygen and hydrogen atoms of the α-toc molecules are shown in red and white spheres, respectively. (B) The final structure at 5 μs (A) shows that α-tocs have moved (via flip-flop) between the two leaflets. (C–E) The α-toc molecule reorients itself to move toward the bilayer center. Within the aldehyde oxidized bilayer, α-toc's hydroxyl group can form a hydrogen bond with the oxidized lipid tail (E) leading to an increase in the flip-flop rate in the oxidized bilayer. Reorientation of α-toc molecules was observed when they moved to the lower leaflet with the hydroxyl group facing the lipid headgroup and the hydrophobic tail randomly spreading within the bilayer (F, G).

studies.[8,9,19] The tilt angles of the α-toc molecules with respect to the bilayer normal are shown in Figure 4A. Two possible orientations at ∼40 ± 12° and 90 ± 4° to the bilayer normal were observed in PLPC bilayer. In contrast to experiments, the chains of α-toc and saturated 1,2-dimyristoyl-*sn*-glycero-3-phosphocholine (DMPC) and 1,2-dipalmitoyl-*sn*-glycero-3-phosphocholine (DPPC) lipids are oriented with the relative angles of 11 ± 2 and 16 ± 4°, respectively, which may imply to the only parallel orientation to the bilayer normal.[19] However, the α-toc tilt angle is still being debated, since discrepancies can arise from differences in lipid types, lipid phase, and location of α-toc inside the bilayer.[10,17,19] In an analogous manner, differences in tilt angle have been shown to indicate the ability of different sterols to undergo flip-flop.[39] For a general discussion of lipid flip-flops, see articles by Gurtovenko and Vattulainen[40] and Sapay, Bennett, and Tieleman.[41]

For the hydroperoxide lipid bilayer, the polar head groups of the α-toc molecules prefer to stay at the bilayer-water interface in a way similar to what is observed for the PLPC bilayer. The average distances of the carbonyl group from the bilayer center are 1.32 ± 0.01 and 1.37 ± 0.02 nm for 50% 13-tc and 50% 9-tc bilayer, respectively. Meanwhile, the locations of the hydroxyl group of α-toc molecules in 50% 13-tc and 50% 9-tc bilayer are 1.03 ± 0.02 and 1.08 ± 0.04 nm from the bilayer center, respectively. However, all α-toc molecules in the hydroperoxide bilayer prefer to be slightly tilted in parallel to the bilayer (tilted angle is ∼40–60° to the bilayer normal) rather than to lie horizontally in the bilayer (Figure 4B,C). For the aldehyde lipid bilayer, a wide range of orientations was observed caused by a random spread of the α-toc's hydrophobic tail in the bilayer (Figure 4D,E). Interestingly,

it can be seen a flip-flop typically follows (Figure 4D,E) when the α-toc's hydroxyl moves deep inside the bilayer and reorients. The molecular length ($\vec{l}$) of α-toc in lipid bilayer was determined as the distance between the terminal methyl group in the tail and the hydroxyl group in the head (see Figure 1 for molecular structures). The molecular length distribution of α-toc in nonoxidized/oxidized lipid bilayers is shown in Figure 5. The results show an extended structure in both PLPC and oxidized bilayers with the maximum probability densities in molecular length being ∼2.06 ± 0.01 nm (Figure 5). The average molecular lengths were found to be 1.88 ± 0.02, 1.87 ± 0.01, 1.91 ± 0.01, 1.85 ± 0.01, 1.86 ± 0.01 nm in PLPC and 13-tc, 9-tc, 12-al, and 9-al lipid bilayers, respectively. Note the emergence of a shoulder in the case of 5.9% 12-al (solid blue curve). As Figure 4 shows, pore formation is observed in this system. These structures are maintained even when the α-toc molecules move toward the bilayer center and undergo a flip-flop to the opposite side of the bilayer (Figure 4F–J). Note the shortened structure of α-toc when they tilt away from bilayer as seen in Figure S3.

Free Energy Profile of α-toc Molecule in the Bilayer.
Figure 6 shows the PMF profiles for moving an α-toc molecule from the bilayer center to the water phase, and Table 2 lists the equilibrium positions (corresponding to the α-toc hydroxyl group), the free energy of desorption (ΔG_{desorb}) for moving an α-toc from its equilibrium position in bilayer into bulk water, and the free-energy barrier ($\Delta G_{barrier}$) for moving an α-toc from the equilibrium position to the bilayer center. Note that thermal energy is ∼2 kJ mol⁻¹. These results suggest that the
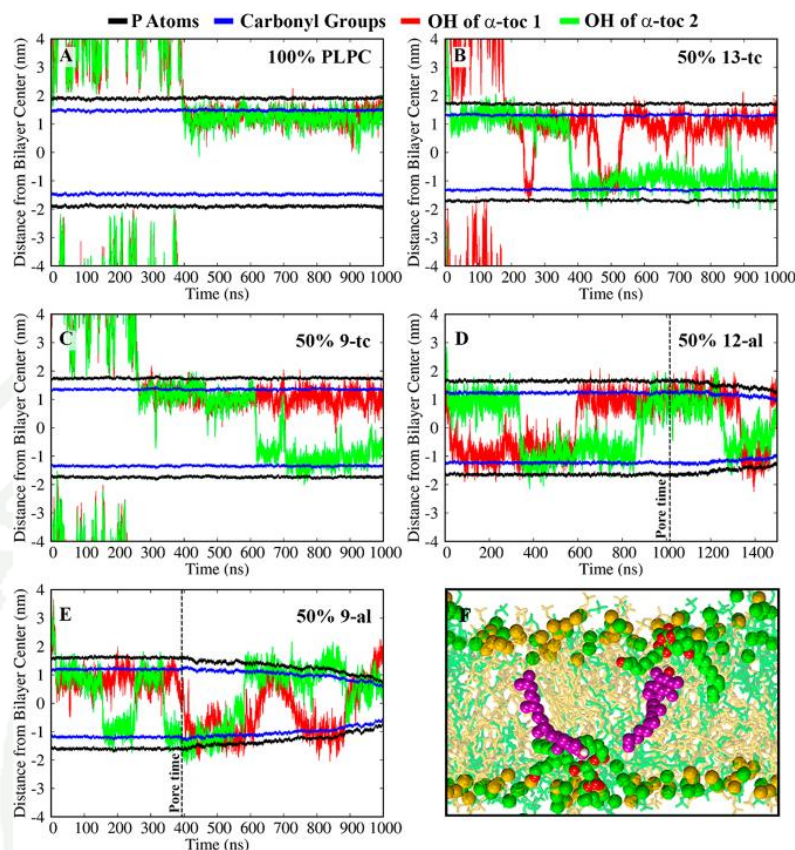
Figure 3. (A−E) Time evolution of the distance of α-toc's hydroxyl group from the bilayer center along the z-axis in nonoxidized and oxidized lipid bilayers containing two α-toc molecules. The dashed vertical lines show the times when pore formation first started to occur. Note that the definition of bilayer center becomes somewhat ambiguous during pore formation. (F) The preferred location of α-toc molecules inside the 50% 9-al bilayer is underneath the lipid carbonyl group. The color code for the lines is given on top of the picture.

probability for an α-toc to undergo flip-flop is higher in oxidized bilayers.

Flip-Flop Rate Calculation. To estimate the rate of α-toc flip-flops (k_{flip}), additional simulations with an α-toc initially at the bilayer center were performed. The initial configurations were taken from the z = 0 nm window in umbrella sampling simulations. Fifty independent simulations of each bilayer were independently run for 50 ns, and the time for the hydroxyl group of the α-toc to return from the bilayer center to the equilibrium position (t_d) was recorded. The rate of α-toc flip-flop across a lipid bilayer (k_{flip}) was calculated following the approach of Bennett et al.[42] using the equation

$$k_{flip} = \frac{1}{[(1/k_f) + (1/k_d)]} \times 1/2$$

where

$$k_f = k_d \times \exp(-\Delta G_{barrier}/RT)$$

and $k_d = t_d^{-1}$ where R and T are the gas constant and temperature, respectively. $\Delta G_{barrier}$ is the free-energy difference between the equilibrium position and the bilayer center. The half time for flip-flop ($t_{1/2}$) was calculated using[43]

$$t_{1/2} = \ln 2/k_{flip}$$

Table 3 shows the results and the parameters. The results show that α-toc molecules undergo rapid flip-flops especially in

the aldehyde bilayers as compared to flip-flops in a pure phospholipid bilayer.

To put the results in Table 3 into context, we compare the α-toc flip-flop rates to those reported in different systems. In pure phospholipid bilayers, previous experimental studies have reported $t_{1/2}$ in a large unilamellar DPPC vesicle in the fluid phase (temperature range of 50−65 °C) to be in range from days to weeks, and no flip-flop was observed in the gel phase over 250 h.[44] Previous free-energy calculations[45] using umbrella sampling technique have suggested that the free-energy barrier for phospholipid flip-flop decreases upon increasing degree of oxidation in 1-palmitoyl-2-oleoyl-glycero-3-phosphocholine (POPC) bilayers, which indicates an increase in the lipid flip-flop rate. However, the flip-flop rates were not explicitly determined, and the free-energy barriers (between bilayer center and equilibrium position) remain relatively high, 65 ± 6 kJ/mol in the case of a 50% hydroperoxide bilayer.[45] Finally, in previous simulations, the phospholipid flip-flop rates in pure DPPC bilayers have been estimated to occur in time scales of 4−30 h.[46]

Next, we compare the α-toc flip-flop rates with those of cholesterol in different bilayers; it has been shown that cholesterol helps to protect membranes against oxidized lipids.[47,48] The flip-flop rates of cholesterol in pure DPPC bilayers range from 1.2 × 10⁴ to 6.6 × 10⁵ s⁻¹.[42] In unsaturated diarachidonyl-phosphocholine (DAPC, 20:4−20:4 phospho-
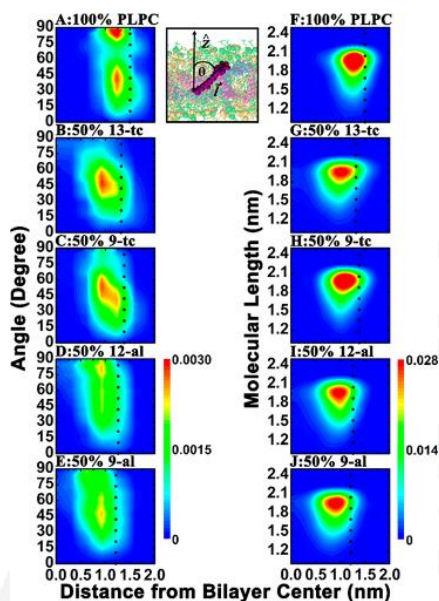
Figure 4. (A−E) Normalized two-dimensional histograms of α-toc's tilt angle in nonoxidized and oxidized bilayers containing 5.9% α-toc molecules. The hydroxyl group in the chromanol ring and the methyl group at the terminal chain represent head and tail of α-toc, respectively. The distance from head to tail of α-toc is defined as the molecular length ($\vec{l}$). (F−J) α-toc's molecular length is plotted as a function of the distance of α-toc's head from the bilayer center. (inset) The tilt angle is defined by the angle between the bilayer normal (z-axis) and the vector connecting the last methyl group in the tail to the hydroxyl group in the head of the α-toc molecule. The tilt angle of 0° represents α-toc oriented in parallel to the bilayer normal (z-axis), and 90° describes the α-toc being perpendicular to the bilayer normal. The dotted lines represent the average positions of the carbonyl groups in lipid chains.
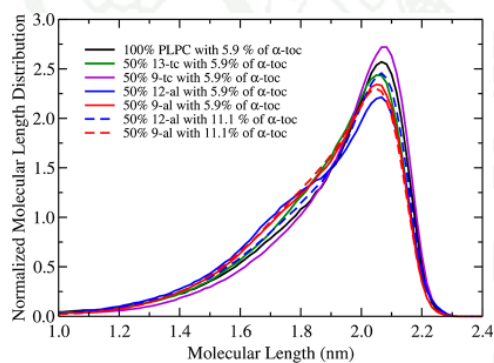

Figure 5. Distribution of α-toc's molecular length ($\vec{l}$) in oxidized and nonoxidized lipid bilayers containing 5.9% and 11.1% of α-toc molecules. The hydroxyl group in the chromanol ring and methyl group at the terminal chain represent head and tail of α-toc, respectively. The distance from head to tail of α-toc is defined the molecular length ($\vec{l}$).

choline (PC)) lipid bilayer, the flip-flop rates (5.2×10^5 to $3.7 \times 10^6 \, s^{-1}$) were observed to be an order of magnitude larger than in fully saturated DPPC lipid bilayers.[42,49] Our calculations show (Table 3) that the α-toc flip-flop rate and
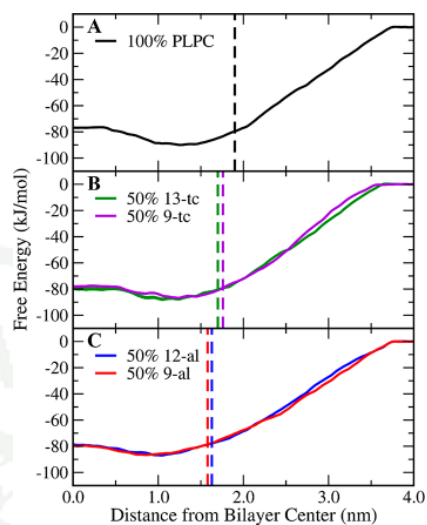

Figure 6. PMF for moving an α-toc from the center of a 100% PLPC bilayer (A), 50% hydroperoxide lipid (B), and a 50% aldehyde lipid (C) to the water phase as a function of distance in the z-direction from the bilayer center. The PMF in bulk water was set to zero. The dashed lines are the average positions of the phosphorus atoms in the lipid headgroup in each bilayer. The free energy of desorption (ΔG_{desorb}) is the difference in free energy between the equilibrium position and bulk water. The free-energy barrier ($\Delta G_{barrier}$) is the maximum free energy for α-toc to move from the equilibrium position to the bilayer center. All free-energy calculations in different lipid bilayers are listed in Table 2. The error in all systems is less than 1 kJ mol^{-1}.

Table 2. Equilibrium Positions Given as the Location of the α-toc Hydroxyl Group from the Bilayer Center[a]

systems	ΔG_{desorb} (kJ/mol)	$\Delta G_{barrier}$ (kJ/mol)	equilibrium position (nm)
100% PLPC	90.0 ± 0.7	13.5 ± 0.5	1.26 ± 0.01
50% 13-tc	87.8 ± 1.0	8.1 ± 0.5	1.10 ± 0.09
50% 9-tc	86.6 ± 0.7	9.2 ± 0.5	1.24 ± 0.02
50% 12-al	87.0 ± 0.7	8.3 ± 0.5	1.04 ± 0.02
50% 9-al	86.6 ± 0.5	7.1 ± 0.2	0.85 ± 0.01

[a]ΔG_{desorb} is the free energy of desorption, that is, the free-energy cost for moving an α-toc from its equilibrium position in bilayer into bulk water, and $\Delta G_{barrier}$ is the free energy for moving an α-toc from its equilibrium position to bilayer center. See also Figure 6.

the flip-flop half time in 100% PLPC bilayer are $4.2 \times 10^5 \, s^{-1}$ and 1.65 μs, respectively. These values are consistent with a previous computational study using 1-stearoyl-2-docosahexaenoylphosphatidylcholine (SDPC, 18:0−22:6PC) and 1-stearoyl-2-oleoylphosphatidylcholine (SOPC, 18:0−18:1PC) bilayers.[16,50] From the binding free-energy calculations of α-toc with polyunsaturated phospholipids, the flip-flop rates have been estimated to be $7.5 \times 10^5 \, s^{-1}$ and $2.5 \times 10^5 \, s^{-1}$ in SDPC and SOPC lipid, respectively.[50] Here, for the oxidized lipid systems the flip-flop rates were found to be (all at 50%): 13-tc: $2.6 \times 10^6 \, s^{-1}$, 9-tc: $1.7 \times 10^6 \, s^{-1}$, 12-al: $5.7 \times 10^6 \, s^{-1}$, and 9-al: $6.4 \times 10^6 \, s^{-1}$. Thus, the flip-flop rates of α-toc in the oxidized bilayers are up to an order of magnitude larger than in the pure PLPC bilayer. This result suggests faster α-toc dynamics in oxidized lipid bilayer, thus providing a simple and robust mechanism to increase interactions with free radicals in membranes with oxidized lipids. We would also like to point

Table 3. Parameters[a] Associated with α-toc Flip-Flop Calculation in Different Lipid Bilayers

systems	t_d (ns)	k_d (s^{-1})	k_f (s^{-1})	k_{flip} (s^{-1})	average t_d (ns)	$\bar{k}_{flip}$ (s^{-1})	$t_{1/2}$ (μs)
100% PLPC	0.3–27.8	3.3×10^9 to 3.6×10^7	1.4×10^7 to 1.6×10^5	7.2×10^6 to 7.7×10^4	5.1 ± 5.8	4.2×10^5	1.65
50% 13-tc	0.1–21.8	1.0×10^{10} to 4.6×10^7	3.8×10^8 to 1.7×10^6	1.8×10^8 to 8.4×10^5	7.1 ± 5.1	2.6×10^6	0.27
50% 9-tc	0.5–27.7	2.0×10^9 to 3.6×10^7	4.9×10^7 to 8.8×10^5	2.4×10^7 to 4.3×10^5	7.1 ± 5.9	1.7×10^6	0.41
50% 12-al	0.1–9.0	1.0×10^{10} to 1.1×10^8	3.5×10^8 to 3.9×10^6	1.7×10^8 to 1.9×10^6	3.0 ± 2.4	5.7×10^6	0.12
50% 9-al	0.4–12.0	2.5×10^9 to 8.3×10^7	1.4×10^8 to 4.8×10^6	6.7×10^7 to 2.2×10^6	4.2 ± 2.8	6.4×10^6	0.11
100% SDPC[b]	8–55	1.3×10^8 to 1.8×10^7	5.7×10^6 to 8.3×10^5	2.7×10^6 to 4.0×10^5		7.5×10^5	0.92
100% SOPC[b]	8–60	1.3×10^8 to 1.7×10^7	2.2×10^6 to 2.9×10^5	1.1×10^6 to 1.4×10^5		2.5×10^5	2.77

[a]Note: t_d is the time for the α-toc's hydroxyl group to move from the bilayer center to the equilibrium position in the bilayer. k_d is the rate for an α-toc to move from the center of bilayer to the equilibrium position; k_d was estimated by $k_d = t_d^{-1}$. k_f is the rate for an α-toc to move from equilibrium to the bilayer center and was calculated by $k_f = k_d \times \exp(-\nabla G_{barrier}/RT)$. The rate of α-toc flip-flop (k_{flip}) was calculated by $k_{flip} = \frac{1}{[(1/k_f) + (1/k_d)]} \times 1/2$. The haft time for α-toc flip-flop ($t_{1/2}$) was calculated by $t_{1/2} = \ln 2/k_{flip}$. [b]Data were taken from a previous study by Leng et al.[50]

out that pore formation in the absence of external fields is a stochastic process, and hence the pore formation times in Table 1 should not be taken as absolute values. Providing a reasonably accurate estimate with small error bars would, however, require a very large number of independent simulations and is beyond the scope of the current study. It is possible to induce pore formation using an electric field, which can be used to overcome the energy barriers as as has been demonstrated by Yusupov et al.[51] The review by Gurtovenko et al.[52] provides a good discussion of flip-flop and pore formation via different mechanisms.

CONCLUSION

We have performed a series of MD simulations of α-toc in different oxidized and nonoxidized lipid bilayers to better understand the role of α-toc in oxidative stress. The presence of ~11% of α-toc was confirmed to stabilize oxidized membranes and prevent water pore formation in a long simulation times over 5 μs. We investigated the locations and conformations of α-toc both in oxidized and nonoxidized bilayers. The results show that α-toc's hydroxyl group favors staying at the bilayer interface for both cases. In addition, α-toc was observed flip-flopping in both oxidized and nonoxidized lipid bilayers. We calculated the free-energy profiles to obtain the free-energy barrier and to estimate the α-toc flip-flop rate in the different bilayers. Importantly, our results show that the free-energy barriers for α-toc flip-flop become significantly suppressed in the presence of oxidized lipids. As a consequence, the flip-flop rate increases with lipid peroxidation by up to an order of magnitude compared to the pure PLPC bilayer. The rate increases in the following order: aldehyde > hydroperoxide > PLPC. This significantly increased flip-flop rate provides a physical mechanism that allows α-toc to scavenge radicals to protect membranes from oxidative attack and to help stabilize membrane under oxidative stress.

Our results indicate that α-toc flip-flop may indeed be essential for membrane protection. To elaborate its role, it would be interesting to investigate its kinetics in multi-component membranes containing polyunsaturated lipids and in the presence of cholesterol. Such studies would help answer questions about synergistic effects of cholesterol and α-toc, possible aggregation behaviors, and the locations, both vertical and lateral, of both oxidized lipids and α-toc. Finally, we would also like to point out that there are several interesting issues related to interactions of oxidized lipids with the lipid matrix including the length of the chains and, in particular, how

oxidized lipids modify the energy barriers for different types of small molecules.[53]

ASSOCIATED CONTENT

Ⓢ Supporting Information

The Supporting Information is available free of charge on the ACS Publications website at DOI: 10.1021/acs.jpcb.8b09064.

Abbreviations of molecular names, distribution of α-toc's tilt angle in nonoxidized/oxidized lipid bilayers containing 5.9% and 11.1% of α-toc molecules, distribution of α-toc's tilt angle with respect to the bilayer normal (z-axis) in nonoxidized and oxidized lipid bilayers, and normalized two-dimensional histogram of α-toc's molecular length as a function of its tilt angle in nonoxidized and oxidized bilayers containing 5.9% α-toc molecules (PDF)

AUTHOR INFORMATION

Corresponding Authors
*E-mail: jirasak.w@ku.ac.th. (J.W.)
*E-mail: mkarttu@uwo.ca. (M.K.)

ORCID Ⓞ
Mikko Karttunen: 0000-0002-8626-3033

Notes
The authors declare no competing financial interest.

REFERENCES

(1) Burton, G. J.; Jauniaux, E. Oxidative stress. *Best Pract. Res. Clin. Obstet. Gynaecol.* **2011**, *25*, 287−299.

(2) Atkinson, J.; Epand, R. F.; Epand, R. M. Tocopherols and tocotrienols in membranes: A critical review. *Free Radical Biol. Med.* **2008**, *44*, 739−764.

(3) Raederstorff, D.; Wyss, A.; Calder, P. C.; Weber, P.; Eggersdorfer, M. Vitamin E function and requirements in relation to PUFA. *Br. J. Nutr.* **2015**, *114*, 1113−1122.

(4) Podda, M.; Weber, C.; Traber, M. G.; Packer, L. Simultaneous determination of tissue tocopherols, tocotrienols, ubiquinols, and ubiquinones. *J. Lipid Res.* **1996**, *37*, 893−901.

(5) Niki, E. Role of vitamin E as a lipid-soluble peroxyl radical scavenger: In vitro and in vivo evidence. *Free Radical Biol. Med.* **2014**, *66*, 3−12.

(6) Burton, G. W.; Joyce, A.; Ingold, K. U. First proof that vitamin E is major lipid-soluble, chain-breaking antioxidant in human blood plasma. *Lancet* **1982**, *320*, 327.

(7) Burton, G. W. Vitamin E: Molecular and biological function. *Proc. Nutr. Soc.* **1994**, *53*, 251−262.

(8) Atkinson, J.; Harroun, T.; Wassall, S. R.; Stillwell, W.; Katsaras, J. The location and behavior of alpha-tocopherol in membranes. *Mol. Nutr. Food Res.* **2010**, *54*, 641−651.

(9) Ausili, A.; de Godos, A. M.; Torrecillas, A.; Aranda, F. J.; Corbalan-Garcia, S.; Gomez-Fernandez, J. C. The vertical location of alpha-tocopherol in phosphatidylcholine membranes is not altered as a function of the degree of unsaturation of the fatty acyl chains. *Phys. Chem. Chem. Phys.* **2017**, *19*, 6731−6742.

(10) Qin, S. S.; Yu, Z. W.; Yu, Y. X. Structural and kinetic properties of alpha-tocopherol in phospholipid bilayers, a molecular dynamics simulation study. *J. Phys. Chem. B* **2009**, *113*, 16537−16546.

(11) Qin, S. S.; Yu, Z. W. Molecular dynamics simulations of alpha-tocopherol in model biomembranes. *Acta Phys.-Chim. Sin.* **2011**, *27*, 213−227.

(12) Marquardt, D.; Williams, J. A.; Kucerka, N.; Atkinson, J.; Wassall, S. R.; Katsaras, J.; Harroun, T. A. Tocopherol activity correlates with its location in a membrane: A new perspective on the antioxidant vitamin E. *J. Am. Chem. Soc.* **2013**, *135*, 7523−7533.

(13) Marquardt, D.; Williams, J. A.; Kinnun, J. J.; Kucerka, N.; Atkinson, J.; Wassall, S. R.; Katsaras, J.; Harroun, T. A. Dimyristoyl phosphatidylcholine: A remarkable exception to α-tocopherol's membrane presence. *J. Am. Chem. Soc.* **2014**, *136*, 203−210.

(14) Marquardt, D.; Kučerka, N.; Katsaras, J.; Harroun, T. A. α-tocopherol's location in membranes is not affected by their composition. *Langmuir* **2015**, *31*, 4464−4472.

(15) Cordeiro, R. M. Reactive oxygen species at phospholipid bilayers: Distribution, mobility and permeation. *Biochim. Biophys. Acta, Biomembr.* **2014**, *1838*, 438−444.

(16) Leng, X. L.; Kinnun, J. J.; Marquardt, D.; Ghefli, M.; Kucerka, N.; Katsaras, J.; Atkinson, J.; Harroun, T. A.; Feller, S. E.; Wassall, S. R. Alpha-tocopherol is well designed to protect polyunsaturated phospholipids: MD simulations. *Biophys. J.* **2015**, *109*, 1608−1618.

(17) Sharma, V. K.; Mamontov, E.; Tyagi, M.; Urban, V. S. Effect of alpha-tocopherol on the microscopic dynamics of dimyristoylphosphatidylcholine membrane. *J. Phys. Chem. B* **2016**, *120*, 154−163.

(18) Boonnoy, P.; Karttunen, M.; Wong-ekkabut, J. Alpha-tocopherol inhibits pore formation in oxidized bilayers. *Phys. Chem. Chem. Phys.* **2017**, *19*, 5699−5704.

(19) Ausili, A.; Torrecillas, A.; de Godos, A. M.; Corbalan-Garcia, S.; Gomez-Fernandez, J. C. Phenolic group of alpha-tocopherol anchors at the lipid-water interface of fully saturated membranes. *Langmuir* **2018**, *34*, 3336−3348.

(20) Berendsen, H. J. C.; Postma, J. P. M.; van Gunsteren, W. F.; Hermans, J. Interaction models for water in relation to protein hydration. In *Intermolecular Forces*; Pullman, B., Ed.; D. Reidel: Dordrecht, The Netherlands, 1981; pp 331−342.

(21) Bachar, M.; Brunelle, P.; Tieleman, D. P.; Rauk, A. Molecular dynamics simulation of a polyunsaturated lipid bilayer susceptible to lipid peroxidation. *J. Phys. Chem. B* **2004**, *108*, 7170−7179.

(22) Wong-ekkabut, J.; Xu, Z.; Triampo, W.; Tang, I. M.; Peter Tieleman, D.; Monticelli, L. Effect of lipid peroxidation on the properties of lipid bilayers: A molecular dynamics study. *Biophys. J.* **2007**, *93*, 4225−4236.

(23) Boonnoy, P.; Jarerattanachat, V.; Karttunen, M.; Wong-ekkabut, J. Bilayer deformation, pores, and micellation induced by oxidized lipids. *J. Phys. Chem. Lett.* **2015**, *6*, 4884−4888.

(24) Abraham, M. J.; Murtola, T.; Schulz, R.; Páll, S.; Smith, J. C.; Hess, B.; Lindahl, E. GROMACS: High performance molecular simulations through multi-level parallelism from laptops to super-computers. *SoftwareX* **2015**, *1*, 19−25.

(25) Bussi, G.; Donadio, D.; Parrinello, M. Canonical sampling through velocity rescaling. *J. Chem. Phys.* **2007**, *126*, 014101.

(26) Parrinello, M.; Rahman, A. Polymorphic transitions in single crystals: A new molecular dynamics method. *J. Appl. Phys.* **1981**, *52*, 7182−7190.

(27) Darden, T.; York, D.; Pedersen, L. Particle mesh Ewald: An N.Log(N) method for Ewald sums in large systems. *J. Chem. Phys.* **1993**, *98*, 10089−10092.

(28) Essmann, U.; Perera, L.; Berkowitz, M. L.; Darden, T.; Lee, H.; Pedersen, L. G. A smooth particle mesh Ewald method. *J. Chem. Phys.* **1995**, *103*, 8577−8593.

(29) Karttunen, M.; Rottler, J.; Vattulainen, I.; Sagui, C. Electrostatics in biomolecular simulations: Where are we now and where are we heading? *Curr. Top. Membr.* **2008**, *60*, 49−89.

(30) Hess. P-LINCS: A parallel linear constraint solver for molecular simulation. *J. Chem. Theory Comput.* **2008**, *4*, 116−122.

(31) Wong-ekkabut, J.; Karttunen, M. Assessment of common simulation protocols for simulations of nanopores, membrane proteins, and channels. *J. Chem. Theory Comput.* **2012**, *8*, 2905−2911.

(32) Wong-ekkabut, J.; Karttunen, M. The good, the bad and the user in soft matter simulations. *Biochim. Biophys. Acta, Biomembr.* **2016**, *1858*, 2529−2538.

(33) Khuntawee, W.; Karttunen, M.; Wong-ekkabut, J. A molecular dynamics study of conformations of beta-cyclodextrin and its eight derivatives in four different solvents. *Phys. Chem. Chem. Phys.* **2017**, *19*, 24219−24229.

(34) Humphrey, W.; Dalke, A.; Schulten, K. VMD: Visual molecular dynamics. *J. Mol. Graphics* **1996**, *14*, 33−8.

(35) Torrie, G. M.; Valleau, J. P. Nonphysical sampling distributions in Monte Carlo free-energy estimation: Umbrella sampling. *J. Comput. Phys.* **1977**, *23*, 187−199.

(36) Kumar, S.; Rosenberg, J. M.; Bouzida, D.; Swendsen, R. H.; Kollman, P. A. The weighted histogram analysis method for free-energy calculations on biomolecules. I. The method. *J. Comput. Chem.* **1992**, *13*, 1011−1021.

(37) Hub, J. S.; Winkler, F. K.; Merrick, M.; de Groot, B. L. Potentials of mean force and permeabilities for carbon dioxide, ammonia, and water flux across a Rhesus protein channel and lipid membranes. *J. Am. Chem. Soc.* **2010**, *132*, 13251−13263.

(38) Howard, A. C.; McNeil, A. K.; McNeil, P. L. Promotion of plasma membrane repair by vitamin E. *Nat. Commun.* **2011**, *2*, 597.

(39) Rog, T.; Stimson, L. M.; Pasenkiewicz-Gierula, M.; Vattulainen, I.; Karttunen, M. Replacing the cholesterol hydroxyl group with the ketone group facilitates sterol flip-flop and promotes membrane fluidity. *J. Phys. Chem. B* **2008**, *112*, 1946−1952.

(40) Gurtovenko, A. A.; Vattulainen, I. Molecular mechanism for lipid flip-flops. *J. Phys. Chem. B* **2007**, *111*, 13554−13559.

(41) Sapay, N.; Bennett, W. F. D.; Tieleman, D. P. Thermodynamics of flip-flop and desorption for a systematic series of phosphatidylcholine lipids. *Soft Matter* **2009**, *5*, 3295−3302.

(42) Bennett, W. F. D.; MacCallum, J. L.; Hinner, M. J.; Marrink, S. J.; Tieleman, D. P. Molecular view of cholesterol flip-flop and chemical potential in different membrane environments. *J. Am. Chem. Soc.* **2009**, *131*, 12714−12720.

(43) Bennett, W. F. D.; Tieleman, D. P. Molecular simulation of rapid translocation of cholesterol, diacylglycerol, and ceramide in model raft and nonraft membranes. *J. Lipid Res.* **2012**, *53*, 421−429.

(44) Marquardt, D.; Heberle, F. A.; Miti, T.; Eicher, B.; London, E.; Katsaras, J.; Pabst, G. H-1 NMR shows slow phospholipid flip-flop in gel and fluid bilayers. *Langmuir* **2017**, *33*, 3731−3741.

(45) Razzokov, J.; Yusupov, M.; Vanuytsel, S.; Neyts, E. C.; Bogaerts, A. Phosphatidylserine induced by oxidation of the plasma

membrane: A better insight by atomic scale modeling. *Plasma Processes Polym.* **2017**, *14*, 1700013.

(46) Bennett, W. F. D.; MacCallum, J. L.; Tieleman, D. P. Thermodynamic analysis of the effect of cholesterol on dipalmitoyl-phosphatidylcholine lipid membranes. *J. Am. Chem. Soc.* **2009**, *131*, 1972−1978.

(47) Khandelia, H.; Loubet, B.; Olżyńska, A.; Jurkiewicz, P.; Hof, M. Pairing of cholesterol with oxidized phospholipid species in lipid bilayers. *Soft Matter* **2014**, *10*, 639−647.

(48) Owen, M. C.; Kulig, W.; Rog, T.; Vattulainen, I.; Strodel, B. Cholesterol protects the oxidized lipid bilayer from water injury: An all-atom molecular dynamics study. *J. Membr. Biol.* **2018**, *251*, 521−534.

(49) Neuvonen, M.; Manna, M.; Mokkila, S.; Javanainen, M.; Rog, T.; Liu, Z.; Bittman, R.; Vattulainen, I.; Ikonen, E. Enzymatic oxidation of cholesterol: Properties and functional effects of cholestenone in cell membranes. *PLoS One* **2014**, *9*, e103743.

(50) Leng, X.; Zhu, F.; Wassall, S. R. Vitamin E has reduced affinity for a polyunsaturated phospholipid: An umbrella sampling molecular dynamics simulations study. *J. Phys. Chem. B* **2018**, *122*, 8351−8358.

(51) Yusupov, M.; Van der Paal, J.; Neyts, E. C.; Bogaerts, A. Synergistic effect of electric field and lipid oxidation on the permeability of cell membranes. *Biochim. Biophys. Acta, Gen. Subj.* **2017**, *1861*, 839−847.

(52) Gurtovenko, A. A.; Anwar, J.; Vattulainen, I. Defect-mediated trafficking across cell membranes: Insights from in silico modeling. *Chem. Rev.* **2010**, *110*, 6077−6103.

(53) Razzokov, J.; Yusupov, M.; Cordeiro, R. M.; Bogaerts, A. Atomic scale understanding of the permeation of plasma species across native and oxidized membranes. *J. Phys. D: Appl. Phys.* **2018**, *51*, 365203.

Does Alpha-Tocopherol Flip-Flop Help to Protect Membranes Against Oxidation?

Phansiri Boonnoy[a,b], Mikko Karttunen[*,c,d] and Jirasak Wong-ekkabut[*,a,b,e,f]

[a] Department of Physics, Faculty of Science, Kasetsart University, Bangkok 10900, Thailand.

[b] Computational Biomodelling Laboratory for Agricultural Science and Technology (CBLAST), Faculty of Science, Kasetsart University, Bangkok 10900, Thailand

[c] Department of Chemistry, Western University, 1151 Richmond Street, London, Ontario N6A 5B7, Canada

[d] Department of Applied Mathematics, Western University, 1151 Richmond Street, London, Ontario N6A 5B7, Canada

[e] Thailand Center of Excellence in Physics (ThEP Center), Commission on Higher Education, Bangkok 10400, Thailand

[f] Specialized Center of Rubber and Polymer Materials for Agriculture and Industry (RPM), Faculty of Science, Kasetsart University, Bangkok 10900, Thailand

[*]Corresponding E-mail: jirasak.w@ku.ac.th and mkarttu@uwo.ca

Abbreviations of molecular names

alpha-tocopherol, α-toc

1-palmitoyl-2-linoleoyl-*sn*-glycero-3-phosphatidylcholine, PLPC

1-palmitoyl-2-(13-hydroperoxy-trans-11,cis-9-octadecadienoyl)-*sn*-glycero-3-phosphocholine lipid, 13-tc

1-palmitoyl-2-(9-hydroperoxytrans-10, cis-12-octadecadienoyl)-*sn*-glycero-3-phosphocholine lipid, 9-tc

1-palmitoyl -2-(12-oxo-cis-9-dodecenoyl)-*sn*-glycero-3-phosphocholine lipid,12-al

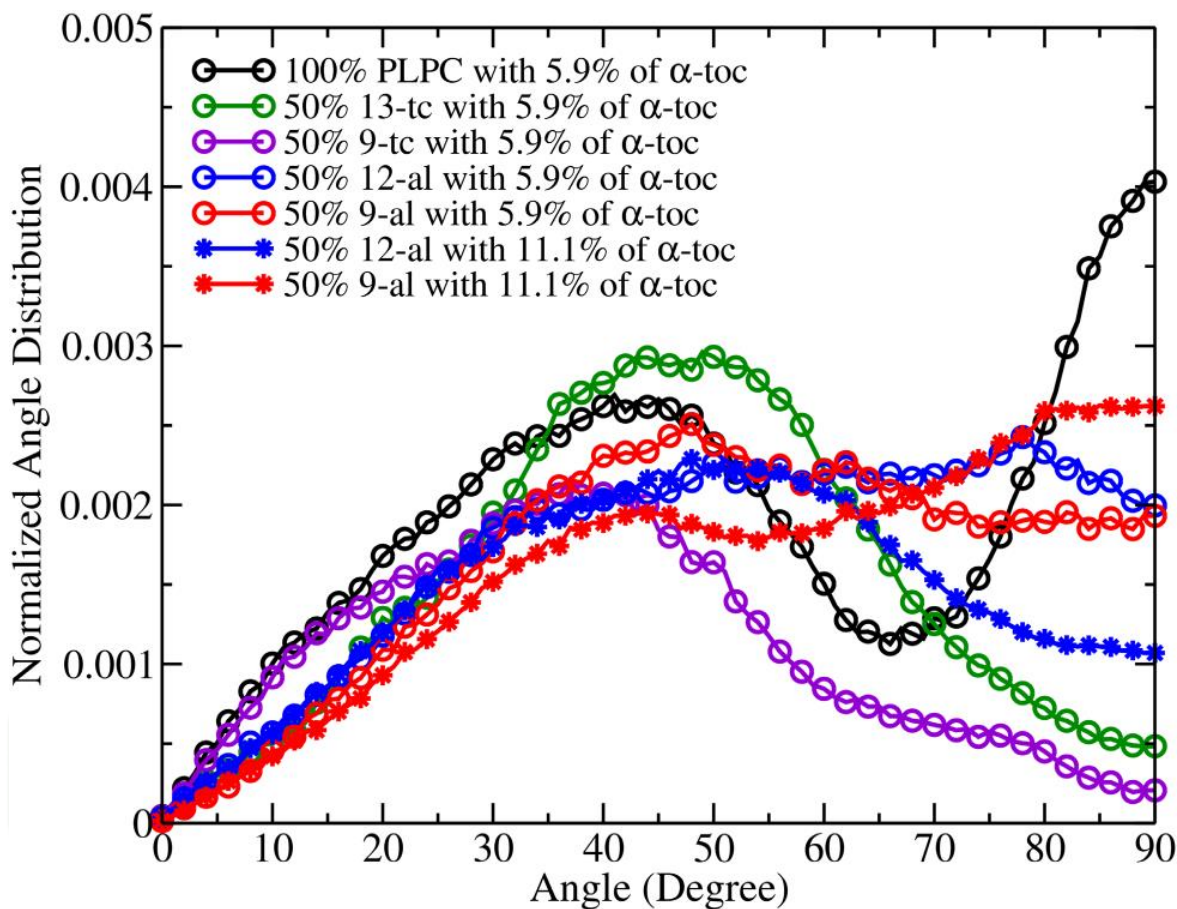1-palmitoyl-2-(9-oxo-nonanoyl)-*sn*-glycero-3-phosphocholine, 9-al

Figure S1. Distribution of α-toc's tilt angle in non-oxidized/oxidized lipid bilayers containing 5.9% and 11.1% of α-toc molecules. The hydroxyl group in chromanol ring and methyl group at the terminal chain (see Figure 1 for the molecular structures) are represented head and tail of α-toc, respectively. The tilted angle is defined by angle between the bilayer normal (*z*-axis) and a vector connecting the last methyl group in the tail to the hydroxyl group in the head group. The tilt angle of 0 degrees represents α-toc oriented in parallel to the bilayer normal (*z*-axis) and 90 degrees describes the α-toc being perpendicular to the bilayer normal.
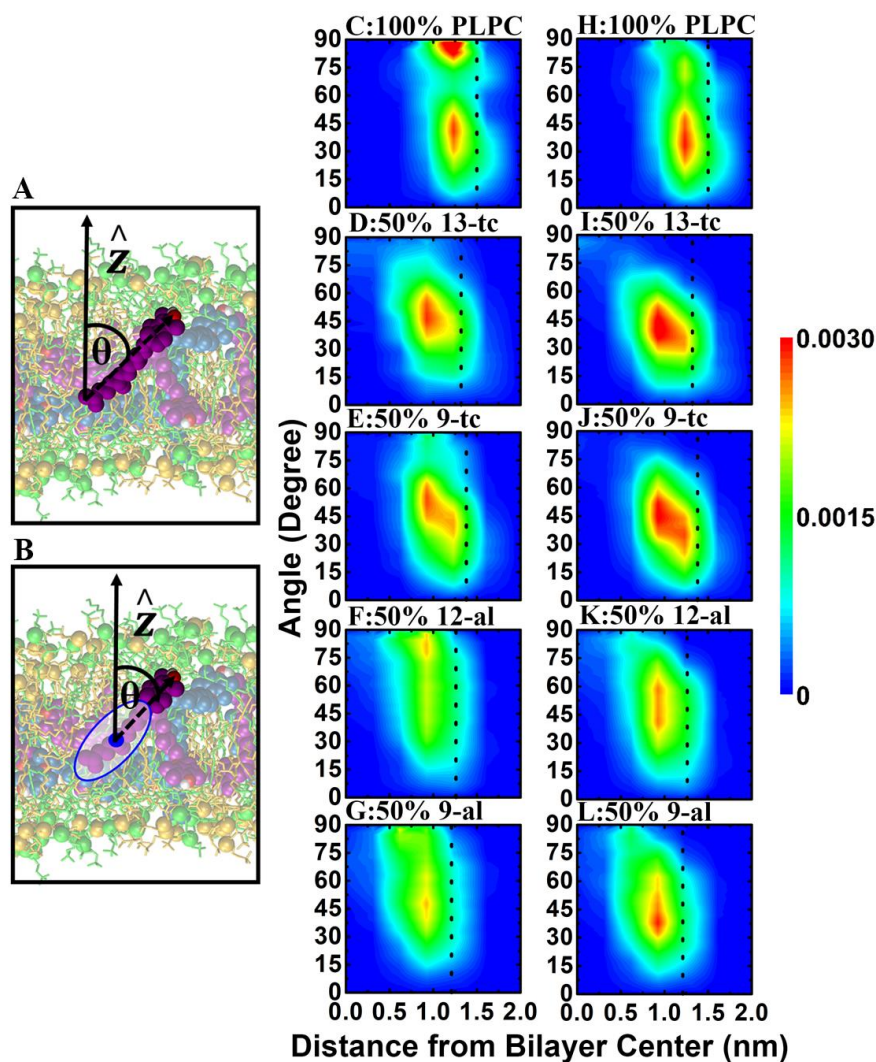
Figure S2. Distribution of α-toc's tilt angle with respect to the bilayer normal (*z*-axis) in non-oxidized and oxidized lipid bilayers. Two different definitions were used to check the generality of the approach. (A): the vector connecting the last methyl group in the tail and the hydroxyl group in the head of the α-toc. (B): the vector connecting the weight center of the tail and the hydroxyl group in the head of the α-toc molecule. (C-G): Distributions of the tilt angle using the definition in (A). (H-L): Distributions using the definition in (B). The dotted lines represent the average positions of the carbonyl groups in lipid chains.
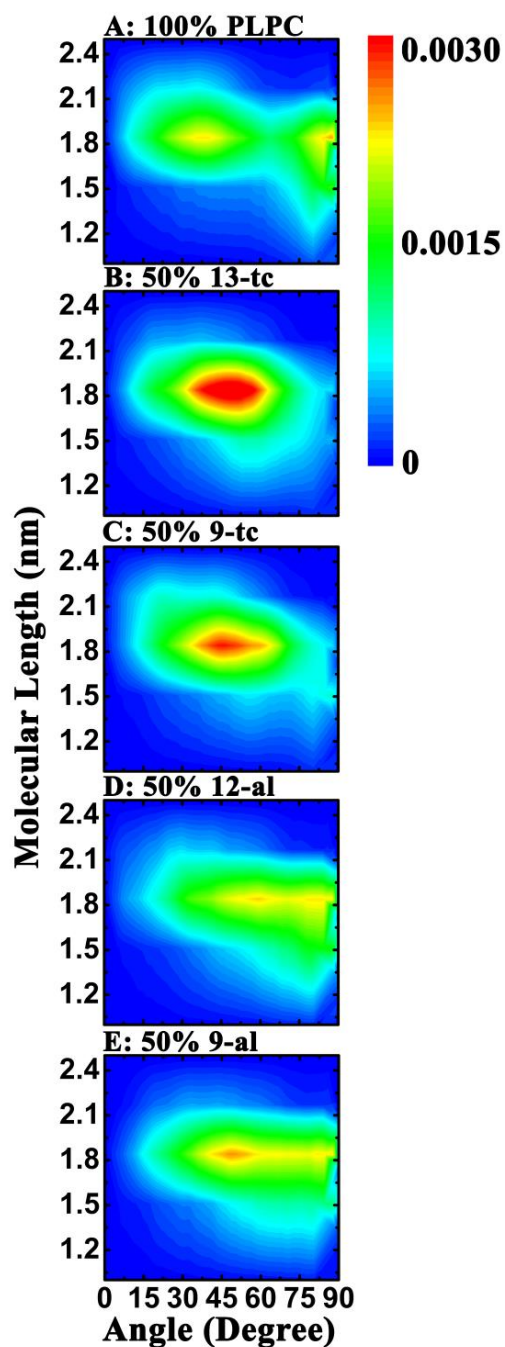
Figure S3. Normalized 2D histogram of α-toc's molecular length as a function of its tilt angle in

non-oxidized and oxidized bilayers containing 5.9% α-toc molecules.

S5

Table S1. The average distances of lipids' phosphorus atoms, lipids' carbonyl groups and α-toc's hydroxyl groups from the bilayer center.

description of the systems	average distances from bilayer center (nm)		
	phosphorus atoms	carbonyl groups	α-toc's hydroxyl groups
100% PLPC	1.90 ± 0.03	1.47 ± 0.03	-
100% PLPC + 2 α-toc (1.5%)	1.90 ± 0.03	1.48 ± 0.03	1.24 ± 0.22
100% PLPC + 4 α-toc (3.0%)	1.91 ± 0.03	1.49 ± 0.03	1.28 ± 0.22
100% PLPC + 8 α-toc (5.9%)	1.93 ± 0.03	1.51 ± 0.03	1.30 ± 0.24
50% 13-tc	1.70 ± 0.03	1.31 ± 0.03	
50% 13-tc + 2 α-toc (1.5%)	1.70 ± 0.03	1.31 ± 0.03	1.01 ± 0.28
50% 13-tc + 4 α-toc (3.0%)	1.73 ± 0.03	1.33 ± 0.03	1.05 ± 0.32
50% 13-tc + 8 α-toc (5.9%)	1.71 ± 0.03	1.33 ± 0.03	1.04 ± 0.32
50% 9-tc	1.73 ± 0.03	1.34 ± 0.03	-
50% 9-tc + 2 α-toc (1.5%)	1.74 ± 0.03	1.35 ± 0.02	1.03 ± 0.26
50% 9-tc + 4 α-toc (3.0%)	1.76 ± 0.03	1.36 ± 0.03	1.11 ± 0.31
50% 9-tc + 8 α-toc (5.9%)	1.78 ± 0.03	1.39 ± 0.03	1.11 ± 0.26
50% 12-al	1.64 ± 0.03	1.22 ± 0.03	
50% 12-al + 2 α-toc (1.5%)	1.65 ± 0.03	1.24 ± 0.03	0.90 ± 0.29
50% 12-al + 4 α-toc (3.0%)	1.66 ± 0.03	1.25 ± 0.03	0.89 ± 0.29
50% 12-al + 8 α-toc (5.9%)	1.68 ± 0.03	1.27 ± 0.03	0.97 ± 0.29
50% 12-al + 16 α-toc (11.1%)	1.73 ± 0.03	1.32 ± 0.03	0.99 ± 0.34
50% 9-al	1.58 ± 0.03	1.16 ± 0.03	-
50% 9-al + 2 α-toc (1.5%)	1.61 ± 0.03	1.20 ± 0.03	0.86 ± 0.29
50% 9-al + 4 α-toc (3.0%)	1.62 ± 0.03	1.20 ± 0.03	0.91 ± 0.29
50% 9-al + 8 α-toc (5.9%)	1.64 ± 0.03	1.22 ± 0.03	0.91 ± 0.28
50% 9-al + 16 α-toc (11.1%)	1.69 ± 0.03	1.28 ± 0.03	0.94 ± 0.29

Publication 2

Article

Biophysical Society

Role of cholesterol flip-flop in oxidized lipid bilayers

Phansiri Boonnoy,[1,2] Viwan Jarerattanachat,[2,3,4] Mikko Karttunen,[5,6,7] and Jirasak Wong-ekkabut[1,2,3,8,*]
[1]Department of Physics and [2]Computational Biomodelling Laboratory for Agricultural Science and Technology, Faculty of Science, Kasetsart University, Bangkok, Thailand; [3]Thailand Center of Excellence in Physics, Ministry of Higher Education, Science, Research and Innovation, Bangkok, Thailand; [4]NSTDA Supercomputer Center, National Electronics and Computer Technology Center, National Science and Technology Development Agency, Khlong Luang, Pathumthani, Thailand; [5]Department of Chemistry, [6]Department of Physics and Astronomy, and [7]The Centre for Advanced Materials Research, The University of Western Ontario, London, Ontario, Canada; and [8]Specialized Center of Rubber and Polymer Materials for Agriculture and Industry, Faculty of Science, Kasetsart University, Bangkok, Thailand

ABSTRACT   We performed a series of molecular dynamics simulations of cholesterol (Chol) in nonoxidized 1-palmitoyl-2-lino-leoyl-*sn*-glycero-3-phosphatidylcholine (PLPC) bilayer and in binary mixtures of PLPC-oxidized-lipid-bilayers with 0–50% Chol concentration and oxidized lipids with hydroperoxide and aldehyde oxidized functional groups. From the 60 unbiased molecular dynamics simulations (total of 161 μs), we found that Chol inhibited pore formation in the aldehyde-containing oxidized lipid bilayers at concentrations greater than 11%. For both pure PLPC bilayer and bilayers with hydroperoxide lipids, no pores were observed at any Chol concentration. Furthermore, increasing cholesterol concentration led to a change of phase state from the liquid-disordered to the liquid-ordered phase. This condensing effect of Chol was observed in all systems. Data analysis shows that the addition of Chol results in an increase in bilayer thickness. Interestingly, we observed Chol flip-flop only in the aldehyde-containing lipid bilayer but neither in the PLPC nor the hydroperoxide bilayers. Umbrella-sampling simulations were performed to calculate the translocation free energies and the Chol flip-flop rates. The results show that Chol's flip-flop rate depends on the lipid bilayer type, and the highest rate are found in aldehyde bilayers. As the main finding, we shown that Chol stabilizes the oxidized lipid bilayer by confining the distribution of the oxidized functional groups.

SIGNIFICANCE   Cholesterol has a fundamental role in regulation of membrane structure and maintaining membrane fluidity. It may protect membranes from oxidative attacks by free radicals. This study uses both unbiased and biased molecular dynamics simulations of cholesterol in oxidized bilayers to compute the free energy barriers, flip-flop rates, and flip-flop half-lives. The free energy barrier indicates that cholesterol has a higher flip-flop rate within aldehyde bilayers than in 1-palmitoyl-2-linoleoyl-*sn*-glycero-3-phosphatidylcholine and hydroperoxide bilayers. The rate for cholesterol flip-flop decreases with increasing cholesterol concentration, and the aldehyde bilayers have the highest rates. Moreover, the results show the role of cholesterol in preventing lipid bilayer pore formation caused by oxidative stress. Our studies will potentially help to design more efficient molecules to protect membranes from oxidative stress.

INTRODUCTION

Lipid peroxidation modifies the basic physical properties, dynamics, and morphology of biological membranes. The presence of oxidized lipids, products from lipid peroxidation, can cause, for example, an increase in water or free radical permeability, increase in lipid membrane area, and a decrease in lipid chain ordering, resulting in a significant increase in membrane fluidity. Peroxidation also promotes the formation of lipid microdomains (1–8), and the presence of oxidized products such as shortened chain lipids with an

aldehyde, carboxylic acid lipids lead to passive pore formation and membrane destruction (2,8–12).

Previous studies have shown that the main causes of pore formation in oxidized bilayers are 1) the presence of high concentration of oxidized lipid with polar moieties such as aldehyde or carboxylic groups at the oxidized lipid chain, and 2) an initial pore formed by those oxidized functional groups that can widely distributed within the bilayer and introduce water into the lipid bilayer (8,10,13,14). Although oxidation is typically seen as detrimental effect, controlled and selective induction of lipid peroxidation in cell membranes has received interest in the context of plasma oncology, a new cancer treatment using cold atmospheric pressure plasma. Cold atmospheric pressure plasma has been shown to be a potential new promising treatment for

Boonnoy et al.

killing tumor cells by inducing massive lipid peroxidation in the cell membrane, resulting in a pore, a collapse of the membrane, and cell death (15–18).

Cholesterol has a fundamental role in regulation of membrane structure and maintaining membrane fluidity. In the context of oxidized lipids, Van der Paal et al. (11) have shown that an increasing cholesterol fraction in aldehyde-containing bilayers can prevent pore formation and bilayer deformation. The hypotheses for how cholesterol protects a bilayer are related to 1) cholesterol's ability to form hydrogen bonds with oxidized phospholipids and consequent decrease in water permeability through the membrane (19), 2) cholesterol-induced increases in bilayer thickness and lipid chain order parameter (11,13,19,20), 3) cholesterol's geometric shape that complements the conical shape of the oxidized lipids and protects the membrane from collapsing (21), and 4) rapid cholesterol flip-flops helping to relax the stress due to the asymmetrical shape of the oxidized membrane leaflet (22). The rate and mechanism of cholesterol flip-flop have been investigated in various model membranes (23–28). However, its rate in oxidized lipid bilayers remains unknown. Interestingly, cholesterol is also considered to be an antioxidant molecule (29,30). Free energy calculations have indicated that cholesterol has a significant effect on the permeation of reactive species across membranes: it increases the free energy barrier for certain reactive nitrogen oxide species and thus hinders their translocation into the lipid bilayer (31). This protects membranes from oxidative attacks by free radicals. Structurally, both cholesterol and the well-known antioxidant molecule α-tocopherol (α-toc; a form of vitamin E) contain a hydrocarbon chain and a ring structure with a hydroxyl group. This suggests that cholesterol may behave similarly to α-toc in oxidized membranes.

We have previously demonstrated that the presence of high concentrations of α-toc could inhibit pore formation in oxidized lipid bilayers: α-tocs trapped the aldehyde groups at the membrane-water interface, resulting in a decreased water permeability and decreased probability for pore creation (14). In addition, α-tocs have been found to potentially flip-flop more in oxidized lipid bilayer as compared with nonoxidized lipid bilayer. This behavior is also important in how α-toc stabilizes membranes under oxidative stress (14,32). In an independent study, Schumann-Gillett and O'Mara (13) have shown that the presence of cholesterol disturbs the orientation of the oxidized sn-2 chain of 1-palmitoyl-2-(9′-oxo-valeroyl)-sn-glycero-3-phosphocholine by pushing the aldehyde functional group to move forward to the membrane-water interface. Because of the limited simulation time and low concentrations of oxidized lipids, they observed neither pore formation induced by oxidized lipids nor cholesterol flip-flops in 500-ns molecular dynamics (MD) simulations, thus leaving the question about the physical mechanism of how cholesterol inhibits pore formation in oxidized lipid bilayers unresolved. Their observations do, however, suggest that α-toc and cholesterol may, at least qualitatively, use a similar mechanism for preventing pore formation in oxidized lipid bilayers.

It is also well known that increasing the fraction of cholesterol in a membrane induces a lipid phase transition from the liquid-disordered (L_d) to the liquid-ordered (L_o) phase in nonoxidized lipid bilayers (33–36) associated with lipid raft microdomains in membranes (33,36–41). These have been implicated in cell signaling and membrane trafficking (42,43). Previous studies have focused on the effect of cholesterol on nonoxidized bilayers (36,39,41,44), but how cholesterol induces ordered phase in oxidized phospholipid bilayers remains unknown.

The aims of this work are to investigate the behavior of cholesterol flip-flop and the effect of lipid phase transition induced by cholesterol in both nonoxidized and oxidized lipid bilayers. We performed a series of systematic MD simulations by varying the cholesterol concentration (0–50%) in pure 1-palmitoyl-2-linoleoyl-sn-glycero-3-phosphatidyl-choline (PLPC) bilayers and in binary mixtures of PLPC and its four main oxidative products. Free energy barriers for a cholesterol translocating in lipid bilayers and cholesterol flip-flop rates were estimated to understand cholesterol flip-flop in the different systems.

MATERIALS AND METHODS

Unbiased MD simulations

To investigate the behavior of cholesterol in the PLPC and oxidized-PLPC lipid bilayers, a series of MD simulations of cholesterol in PLPC bilayers and binary mixtures with 1:1 ratio of PLPC/PLPC's oxidation products were performed. The four main oxidation products of PLPC, namely 1-palmitoyl-2-(13-hydroperoxy-trans-11,cis-9-octadecadienoyl)-sn-glycero-3-phosphocholine (13-tc), 1-palmitoyl-2-(9-hydroperoxy-trans-10, cis-12-octadecadienoyl)-sn-glycero-3-phosphocholine (9-tc), 1-palmitoyl-2-(12-oxo-cis-9-dodecenoyl)-sn-glycero-3-phosphocholine (12-al), and 1-palmitoyl-2-(9-oxo-nonanoyl)-sn-glycero-3-phosphocholine (9-al), were used. Chemical structures of cholesterol and lipids are shown in Fig. 1. The structures and force field parameters of 1) PLPC and oxidized lipids were taken from previous studies (1,3,10,32,45), and 2) cholesterol from Höltje et al. (46). All systems were generated using the MemGen program (47). Full descriptions of the simulation systems are shown in Table S1.

After energy minimization with the steepest descents algorithm, MD simulations were run for 1–3 μs with an integration time step of 2 fs by using the GROMACS 5.1.2 program package (48). All simulations were performed under the constant of the number of atoms, pressure, and temperature (NPT) ensemble. The temperature was set to 298 K by the velocity-rescaling algorithm (49) with a time constant of 0.1 ps. Semi-isotropic pressure was applied using the Parrinello-Rahman algorithm (50) with a time constant of 4.0 ps and compressibility of 4.5×10^{-5} bar^{-1} to keep a constant pressure at 1 bar. All bond lengths were constrained by the parallel linear constraint solver (P-LINCS) algorithm (51). Periodic boundary conditions were applied in all three dimensions, and the neighbor list was updated at every integration time step (52). A cutoff value of 1.0 nm was used for the real space part of van der Waals and electrostatic interactions. The particle-mesh Ewald method (53–55) was applied to compute the long-rang electrostatic interactions with a 0.12-nm grid in the reciprocal-space interaction and cubic interpolation of order 4. The last 500 ns were used for data analysis. For the bilayers with a pore, the last 50 ns before pore formation were used for analysis. Statistical errors were estimated based on standard deviation. The
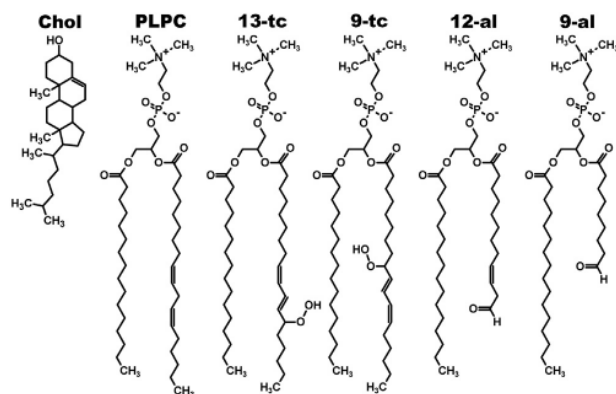
FIGURE 1 Chemical structures of cholesterol, PLPC, and its four main oxidative products, hydroperoxide (*13-tc* and *9-tc*), and aldehyde lipids (*12-al* and *9-al*).

simulation protocol has been previously validated and used to study several biomolecular interactions such as lipid-lipid interactions, carbon-nanoparticle-matrix interactions, membrane transport, and protein-DNA-drug interactions, including drug delivery systems (56–62). Visual Molecular Dynamics (63) was used for visualizations.

Umbrella-sampling MD simulations

Biased umbrella-sampling MD simulations (64) with the Weighted Histogram Analysis Method (65) were performed to investigate the potential of mean force (free energy profile) for a cholesterol molecule partitioning across the 100% PLPC, 50% 13-tc, 50% 9-tc, 50% 12-al, and 50% 9-al lipid bilayers. The free energy profile allows for estimation of the free energy barrier for cholesterol flip-flop. A series of 26 simulation windows with varying positions of cholesterol were performed to compute the free energy profiles. Cholesterol was moved from the bilayer center (at z = 0 nm) to the lipid-water interface (at z = 2.5 nm) with 0.1-nm increments per window. During the umbrella-sampling MD simulations, cholesterol's hydroxyl group (see Fig. 1) was restrained in the z-direction using a harmonic potential function with a force constant of 3000 kJ/(mol nm^2). All simulations were run under the NPT ensemble at the temperature of 298 K and pressure of 1 bar. MD simulations were performed for at least 100 ns, and the last 50 ns was used for analysis. The last 50 ns from umbrella-sampling simulation was divided into 10 intervals. The averages were calculated for the potential of mean force profiles, and statistical errors of free energy were estimated using standard error (66).

Calculation of cholesterol flip-flop rate

To calculate the flip-flop rate (k_{flip}), we performed additional 250 unbiased MD simulations of cholesterol in 100% PLPC, 50% 13-tc, 50% 9-tc, 50% 12-al, and 50% 9-al lipid bilayers. The initial configurations of each system

were taken from the structures at 100 ns of the umbrella-sampling MD simulations in which the cholesterol's hydroxyl group was located at the bilayer center. After removing the harmonic restraint, the 50 independent unbiased MD simulations of each lipid bilayer were independently run for 50–300 ns. We measured the time for the hydroxyl group of cholesterol to move from the bilayer center to the equilibrium position (t_d) and calculated the rate for cholesterol flip-flop (k_{flip}) using (24,26)

$$k_{flip} = \frac{1}{\left[(1/k_f) + (1/k_d) \right]} \times 1/2, \quad (1)$$

where $k_d = 1/t_d$ is the rate at which cholesterol moves from the bilayer center to the equilibrium position. The rate for cholesterol to move from the equilibrium position to the bilayer center (k_f) was calculated using

$$k_f = k_d \times \exp(-\Delta G_{barrier}/RT), \quad (2)$$

where $\Delta G_{barrier}$ is the energy barrier for cholesterol flip-flop. R and T are the gas constant and temperature, respectively. The half-life for cholesterol flip-flop ($t_{1/2}$) is then given as

$$t_{1/2} = \ln 2 / k_{flip}. \quad (3)$$

RESULT AND DISCUSSION

Summary of the membrane structures is shown in Table 1, and Figs. S1–S5 show snapshots of the systems. Without cholesterol, no pore formation was observed in 100% PLPC and 50% hydroperoxide-containing oxidized bilayers (50% 13-tc and 50% 9-tc), whereas stable pores were observed in the 50% aldehyde-containing oxidized bilayers (50% 12-al and 50% 9-al). These results agree well with previous MD simulation studies that have shown that aldehyde lipids at high concentrations (>50%) are capable of inducing pore formation (2,10,11,14,32).

The presence of cholesterol appears to inhibit pore formation in the 50% aldehyde-containing oxidized bilayers: although pores were observed at low cholesterol concentrations (1.5–6%), pore formation did not occur at higher concentrations (>11%) during the 3-μs simulations. Recent computational simulation studies (11,19) have suggested that at least 16 and 30% cholesterol is required to inhibit pore formation in pure aldehyde and mixtures of aldehyde/carboxylic oxidized bilayers, respectively; the concentration of cholesterol necessary to inhibit pore formation in an oxidized membrane depends on the lipid composition.

TABLE 1 Simulated systems and membrane structures

System	Cholesterol concentration											
	0%	1.5%	3%	6%	11%	17%	20%	23%	29%	33%	40%	50%
100% PLPC	✕	✕	✕	✕	✕	✕	✕	✕	✕	✕	✕	✕
50% 13-tc	✕	✕	✕	✕	✕	✕	✕	✕	✕	✕	✕	✕
50% 9-tc	✕	✕	✕	✕	✕	✕	✕	✕	✕	✕	✕	✕
50% 12-al	pore	pore	pore	pore	✔	✔	✕	✕	✕	✕	✕	✕
50% 9-al	pore	pore	pore	pore	✔	✔	✔	✔	✕	✕	✕	✕

The cross mark (✕) indicates that no cholesterol flip-flops were observed. The check mark (✔) indicates that flip-flops were observed. The phase states of bilayers were reported in Table S1.
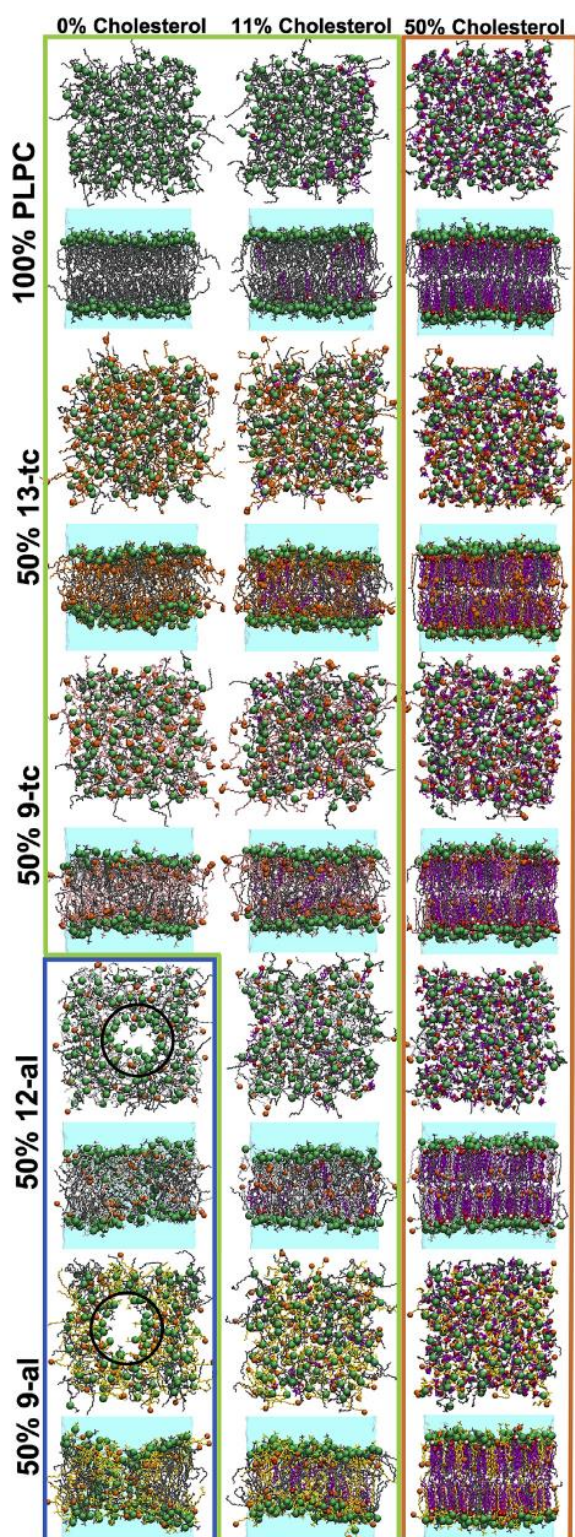
Boonnoy et al.

FIGURE 2 Top- and side-view snapshots of the lipid bilayers: at 0% cholesterol, the 100% PLPC bilayer and the 50% hydroperoxide bilayers are in the L_d phase. The 50% aldehyde-containing oxidized bilayers are in the L_d phase and have a pore. The open black circle indicates a water pore in bilayer. At 11 and 50% cholesterol, the lipid bilayers are in the L_d and L_o phases, respectively.

Visualizations of trajectories showed rapid flip-flops of cholesterol between leaflets only for the 50% aldehyde bilayers (50% 12-al and 50% 9-al) at cholesterol concentrations 11–23%. Furthermore, increasing cholesterol concentration led to a phase state change from an L_d phase to an L_o phase as shown in Fig. 2 and Table S1. This was observed for all bilayers. The L_o phase appeared at higher cholesterol concentrations in the presence of oxidized lipids.

Effects of cholesterol on the density distribution of the oxidized *sn*-2 chain in the bilayer

We analyzed the mass density of the oxidized functional groups along the z-direction (bilayer normal) using distance from the bilayer center. The bilayer center is defined as the center of mass of the lipid bilayer. The mass density profiles are symmetrized of the upper and lower leaflets and are shown in Fig. 3.

Mass density profiles of the hydroperoxide group in 50% 13-tc and 50% 9-tc bilayers

In the absence of cholesterol, the preferential location of the hydroperoxide group in the 50% 13-tc and 50% 9-tc is near the lipid-water interface. This is consistent with previous experimental and computational studies (6,10,67,68). When increasing cholesterol concentration, the peak of the density distribution shifts slightly toward the lipid-water interface as the bilayer thickness increases (Fig. 3, A and B).

The above behavior changes at a certain cholesterol concentration (29% for 13-tc and 40% for 9-tc). The addition of cholesterol induces a reduction in the density of the hydroperoxide functional groups at the lipid-water interface, whereas their density at the bilayer center becomes larger. At 40 and 50% cholesterol concentrations, qualitative differences between the 50% 13-tc and 50% 9-tc bilayers were observed. In the 50% 13-tc bilayer, there are two peaks with the maximum occurring near the bilayer center and the second peak near the lipid-water interface (Fig. 3 A). In contrast, in the 50% 9-tc bilayer, however, the distribution of hydroperoxide group consists of three peaks: 1) at about the lipid-water interface, 2) below the carbonyl group, and 3) at ~0.5 nm from the bilayer center (Fig. 3 B).

Mass density profiles of the aldehyde group in 50% 12-al and 50% 9-al bilayers

Up to cholesterol concentrations of 23% in 12-al and 29% in 9-al, the aldehyde group of the oxidized *sn*-2 chain had a

---

Blue, green and orange boxes represent the bilayers in L_d phase with a pore, L_d phase, and L_o phase, respectively. The light blue surface represents the water region. Phosphorus atoms in lipid headgroups are shown as green spheres. The lipid chains of PLPC, 13-tc, 9-tc, 12-al, 9-al, and cholesterol are shown in gray, orange, pink, white, yellow, and purple (chains), respectively. The oxidized functional groups are displayed as orange spheres. Cholesterols' hydroxyl groups are shown in red and white spheres representing oxygen and hydrogen atoms, respectively. To see the figure in color, go online.
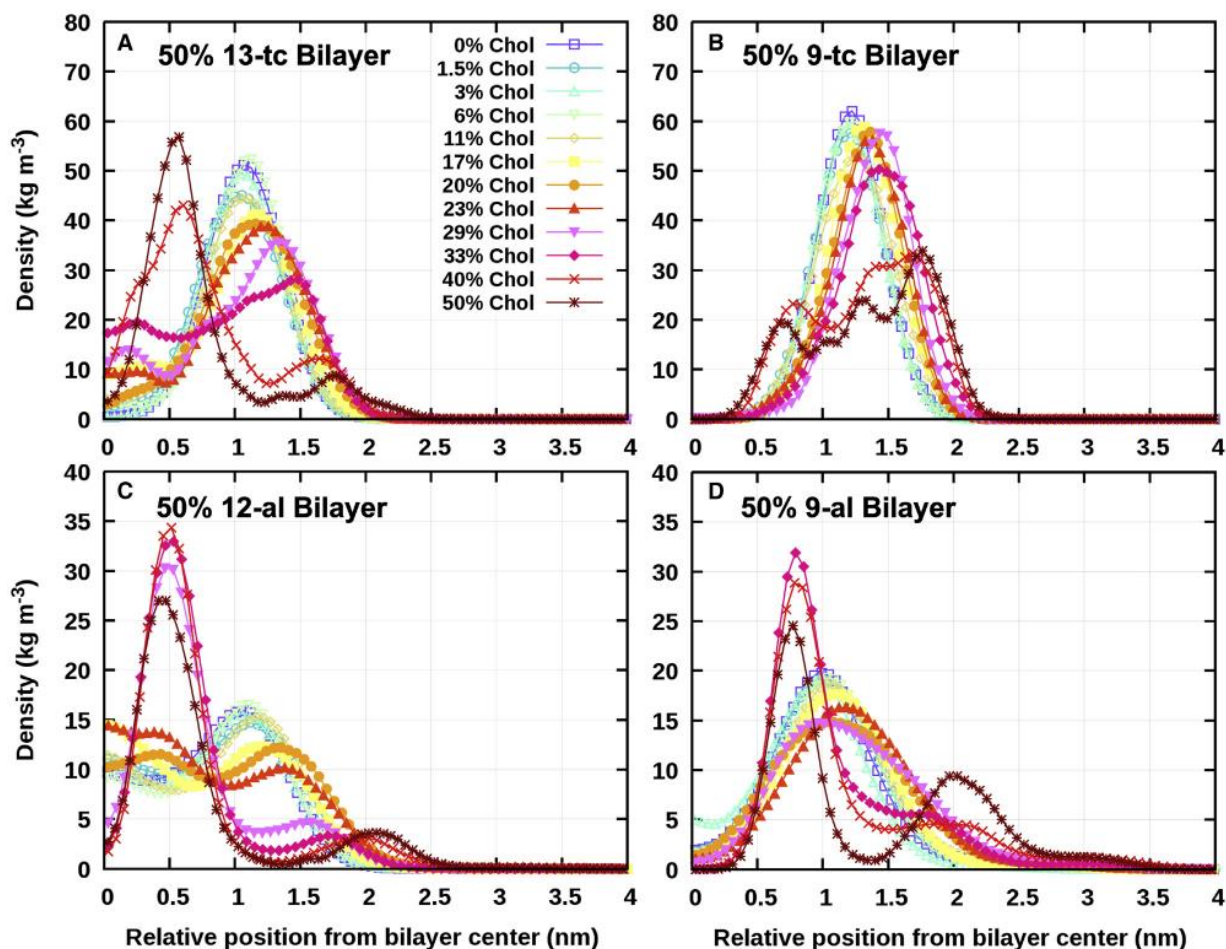
FIGURE 3 Density distributions of the oxidized functional groups (see Fig. 1 for structures) along the z axis with respect to the distance from the bilayer center at different cholesterol concentrations. The mass density profiles are symmetrized. Shown are the hydroperoxide functional group in the case of 13-tc (A) and 9-tc (B) and aldehyde functional group in the case of 12-al (C) and 9-al (D). To see the figure in color, go online.

wide distribution across the bilayer (Fig. 3, C and D). Upon addition of cholesterol, however, the maximum at the lipid-water interface decreases, whereas the density at the bilayer center increases. Above these concentrations, the bilayer is in the L_o phase, and the density maximum shifts from the lipid-water interface to the bilayer interior ($\sim$0.8 nm from the bilayer center), but broad peak at the lipid-water interface is still observed. As discussed in our previous MD simulation study (10), the orientation and broad distribution of aldehyde within the oxidized bilayer are the main mechanisms of how aldehyde lipids increase water permeability and induce pore formation.

Further addition of cholesterol leads to a qualitative change in the distribution. This behavior directly affects the aldehyde lipids' ability to induce pore formation (10) and appears to be the same as how α-toc inhibits pore formation in aldehyde bilayers (14). In addition, the increase in the amplitude of the peak near the bilayer center indicates that the sn-2 chain points toward the bilayer center. Our previous MD simula-

tions have demonstrated that the distribution of oxidized lipid chains determines the lipid shape and plays an essential role in self-assembly: 12-al and 9-al lipid taking the shape of truncated cones usually self-aggregate to induce a pore in the lipid bilayer, and they form micellar structure, whereas PLPC, 13-tc, and 9-tc lipids taking cylindrical shapes typically form bilayers (10,69). These imply that at high cholesterol concentrations, aldehyde lipids undergo a significant geometrical change from a truncated cone to a cylindrical shape, helping to prevent pore formation and making the lipid bilayer structure more stable.

Cholesterol flip-flop rate

It has been previously suggested (22) that rapid cholesterol flip-flops may protect membranes by balancing the area and relaxing differential-density stress in a symmetrical oxidized lipid membrane. We observed spontaneous cholesterol flip-flops in the 50% 12-al bilayer containing 11 and

Boonnoy et al.

17% of cholesterol and in the 50% 9-al bilayers containing 11, 17, 20, and 23% of cholesterol. In these cases, one to three cholesterol molecules flipped between the two leaflets, and each of those molecules underwent a single flip-flop only. For the 100% PLPC and 50% hydroperoxide (13-tc and 9-tc) bilayers, no cholesterol flip-flops were observed during 3 μs. To the best of our knowledge, cholesterol flip-flop rates in oxidized lipid bilayers have not yet been elaborated. To do that, we first performed umbrella-sampling MD simulations to calculate the free energy barriers and then calculated the cholesterol flip-flop rates in the different oxidized lipid bilayers.

Free energy profiles

The free energy profiles for moving a cholesterol molecule from the bilayer center to the lipid-water interface are shown in Fig. 4, and the associated thermodynamic properties are listed in Table 2. In the profiles, the position of the minimal free energy represents the equilibrium position of the hydroxyl group of cholesterol molecule with respect to the distance from bilayer center. The free energy barrier ($\Delta G_{barrier}$) is the maximum in free energy inside the bilayer for moving a cholesterol from the equilibrium position to the bilayer center. The free energy profiles were calculated using the Weighted Histogram Analysis Method tool in the GROMACS package.
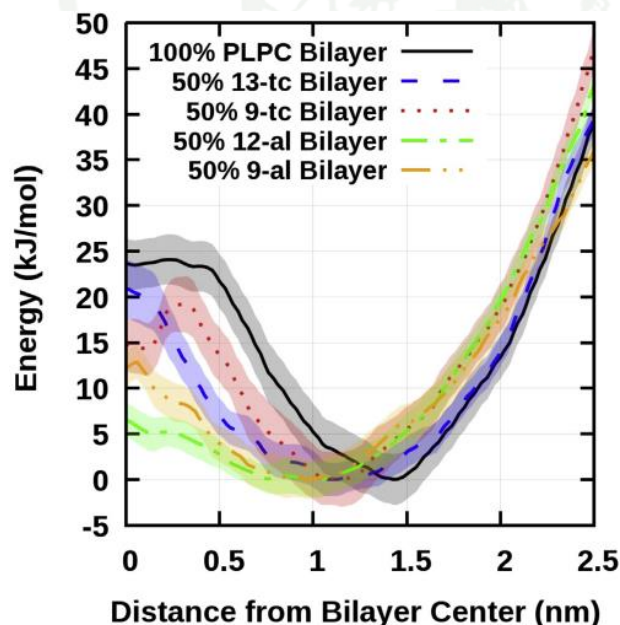

FIGURE 4 Free energy profiles of cholesterol molecule flip-flop across the 100% PLPC and 50% oxidized-PLPC bilayers. The free energy was set equal to zero at the equilibrium position of the hydroxyl group of cholesterol in the bilayer. Error bars were estimated using the standard error as described in Umbrella-sampling MD simulations. Fig. S6 shows the free energy profiles with the errors computed by the commonly used bootstrap method (70). To see the figure in color, go online.

TABLE 2 Thermodynamic properties for moving a cholesterol molecule across the 100% PLPC and 50% oxidized-PLPC bilayers

System	$\Delta G_{barrier}$ (kJ/mol)	Equilibrium position (nm)
100% PLPC	24.09 ± 3.83	1.40 ± 0.02
50% 13-tc	21.40 ± 3.62	1.12 ± 0.05
50% 9-tc	19.15 ± 4.26	1.12 ± 0.03
50% 12-al	6.85 ± 2.61	0.89 ± 0.06
50% 9-al	12.86 ± 2.80	0.99 ± 0.03

$\Delta G_{barrier}$ is the free energy for moving a cholesterol molecule from its equilibrium position to the bilayer center. Equilibrium position is measured with respect to the distance from the bilayer center.

In 100% PLPC bilayer, the equilibrium position of cholesterols' hydroxyl groups was found to be 1.40 ± 0.02 nm from the bilayer center. This position is related to the location of the lipids' carbonyl groups. The average distance of the carbonyl group from the bilayer center is 1.48 ± 0.03 nm. The result implies that the hydroxyl group of cholesterol prefers to stay at the lipid-water interface close to the carbonyl group in the 100% PLPC bilayer. In the 50% oxidized lipid bilayers, the equilibrium positions of cholesterols' hydroxyl groups were observed to be deeper inside the bilayer than in the pure PLPC bilayer at the distances of 1.12 ± 0.05, 1.12 ± 0.03, 0.89 ± 0.06, and 0.99 ± 0.03 nm from bilayer center for 50% 13-tc, 50% 9-tc, 50% 12-al, and 50% 9-al, respectively. This results from the decrease of bilayer thickness in the presence of oxidized lipids. In addition, the location of the cholesterol hydroxyl group remains in the bilayer interior under the lipid carbonyl groups. The average distances of the lipid carbonyl groups from the bilayer center are 1.31 ± 0.03, 1.34 ± 0.03, 1.23 ± 0.03, and 1.18 ± 0.16 nm for 50% 13-tc, 50% 9-tc, 50% 12-al, and 50% 9-al, respectively.

The free energy barrier ($\Delta G_{barrier}$) for cholesterol flip-flop between leaflets in 100% PLPC bilayer is ~24.09 ± 3.83 kJ mol^{-1}. For a comparison, in 1-palmitoyl-2-oleoyl-sn-glycero-3-phosphocholine bilayer, $\Delta G_{barrier}$ has been reported to be ~23–29 kJ mol^{-1} (24–26) and ~21.5–27 kJ mol^{-1} in 1,2-dipalmitoyl-sn-glycero-3-phosphocholine (DPPC) bilayer (24,25,71). The slight differences in $\Delta G_{barrier}$ might depend on the type of lipid as well as temperature (24,72). Compared with 100% PLPC, in 50% hydroperoxide bilayers, the free energy barrier decreases only slightly: in 50% 13-tc, the barrier was determined to be 21.40 ± 3.62 kJ mol^{-1} and in 50% 9-tc $\Delta G_{barrier}$ = 19.15 ± 4.26 kJ mol^{-1}. In the cases of 50% aldehyde lipids, the changes are more dramatic: $\Delta G_{barrier}$ = 6.85 ± 2.61 kJ mol^{-1} for 50% 12-al and $\Delta G_{barrier}$ = 12.86 ± 2.80 kJ mol^{-1} for 50% 9-al. These results suggest that the probability for cholesterol flip-flop within the aldehyde-containing oxidized bilayer is higher than the hydroperoxide-containing oxidized bilayer and the nonoxidized-PLPC bilayer consistent with the data of cholesterol flip-flop in the lipid bilayer from the unbiased MD simulations (Table 1).

We have compared the results of t_d and the reorientation time in the unbiased simulations of 50% 9-al bilayer containing 11% (Fig. S7 A) and 17% (Fig. S7 B) cholesterol. However, only one cholesterol flip-flop event was observed in each system, and thus, these results should be considered as very much qualitative rather than quantitative. The results indicate that the reorientation timescale is very rapid compared with t_d.

The thermodynamic and kinetic properties for cholesterol flip-flop are shown in Table 3. To obtain the statistical significance in $\overline{k}_{flip}$, the standard deviations for the average rates of cholesterol flip-flop ($\overline{k}_{flip}$) were calculated, and the results are shown in Table 3. In addition, to compare the differences in $\overline{k}_{flip}$ among lipid types, the p-values of k_{flip} were calculated using the t-test (see Table S2). The results indicate that the average rate of cholesterol flip-flop ($\overline{k}_{flip}$) in 50% oxidized lipid bilayers is higher than in the PLPC bilayer. In the 100% PLPC bilayer, $\overline{k}_{flip}$ is approximately $(3.0 \pm 2.5) \times 10^3$ s^{-1}. In the 50% hydroperoxide-containing oxidized bilayers, $\overline{k}_{flip}$ were found to be $(3.4 \pm 3.8) \times 10^3$ s^{-1} for 50% 13-tc bilayer and $(3.3 \pm 3.4) \times 10^4$ s^{-1} for 50% 9-tc bilayer. Although no significant increase in $\overline{k}_{flip}$ was observed in the 50% 13-tc bilayer as compared with the 100% PLPC bilayer, an increase by an order of magnitude was observed in the 50% 9-tc bilayer. This implies that the position of the hydroperoxide group in the oxidized lipid chain may influence cholesterol flip-flop in the oxidized bilayer. In the 50% aldehyde-containing oxidized bilayer, $\overline{k}_{flip}$ had a rate higher by one to three orders of magnitude compared with the 100% PLPC and the hydroperoxide-containing oxidized bilayer. The values for $\overline{k}_{flip}$ were found to be $(3.2 \pm 3.7) \times 10^6$ s^{-1} for 50% 12-al bilayer and $(4.5 \pm 4.8) \times 10^5$ s^{-1} for 50% 9-al bilayer. The results suggest that the cholesterol flip-flop rate depends on the bilayer type, and the highest flip-flop rate is found in the aldehyde-containing oxidized bilayer.

Using MD simulations, Bennett et al. (24) found that the cholesterol flip-flop rate in the long-chain 1,2-diarachidonoyl-sn-glycero-3-phosphatidylcholine (20:4-20:4 phosphatidylcholine) bilayer was an order of magnitude higher than in the DPPC (16:0-16:0 phosphatidylcholine) bilayer and suggests faster cholesterol flip-flop in less-ordered membranes with polyunsaturated 1,2-diarachidonoyl-sn-glycero-3-phosphatidylcholine lipids. They also reported that k_{flip} of cholesterol decreased when cholesterol concentration increased from 0 to 40% in a DPPC bilayer. An increase in cholesterol concentration from 0 to 40% in a DPPC bilayer could lead to a lipid phase transition from L_d to the L_o (73,74). The above implies that adding cholesterol in the DPPC bilayer results in an increase in membrane packing and a consequent decrease in cholesterol flip-flop. In addition, Gu et al. (28) have reported that a decrease in temperature from 310 to 290 K results in an increase in lipid chain packing in a ternary DPPC-1,2-dioleoyl-sn-glycero-3-phosphocholine-cholesterol-mixture. This was shown to lead to a significant decrease by approximately an order of magnitude in cholesterol flip-flop events. The observed decrease in the flip-flop rate is fully consistent with the well-known condensing effect of cholesterol (72,75).

Effects of cholesterol on the physical properties of oxidized-PLPC bilayers

The analyses of mass density profiles show that the hydroxyl groups of cholesterol (i.e., cholesterol headgroup) are at the lipid-water interface and that the cholesterols' terminal methyl groups (i.e., cholesterol tail) extend toward the bilayer center (see Figs. S8–S12).

The average distance from the bilayer center to 1) the hydroxyl groups of cholesterol, 2) lipids' phosphorus atoms, and 3) lipids' carbonyl groups were calculated to investigate their relative positions in the bilayer. The results in Fig. 5 and Table S3 show that the hydroxyl group of cholesterol prefers to be located below the lipid carbonyl groups, when the bilayer is in the L_d phase. It is consistent with the equilibrium position of cholesterols' hydroxyl groups from the free energy calculation (Fig. 4). Upon increasing cholesterol concentration, the cholesterol headgroup moves closer to the lipid-water interface, with the hydroxyl group of cholesterol interacting with the lipid headgroup. The average bilayer thickness (Fig. 6) was obtained as the distance between the phosphorus atoms. For all lipid bilayers, the addition of cholesterol leads to an increase in bilayer thickness.

TABLE 3 Cholesterol flip-flop in the different lipid bilayers

System	t_d (ns)	Average t_d (ns)	k_d (s^{-1})	k_f (s^{-1})	$\overline{k}_{flip}$ (s^{-1})	$t_{1/2}$ (s)
100% PLPC	2.5–56.1	16.4 ± 11.2	4.0×10^8 to 1.8×10^7	2.4×10^4 to 1.1×10^3	$(3.0 \pm 2.5) \times 10^3$	$(3.8 \pm 2.6) \times 10^{-4}$
50% 13-tc	4.0–215.4	48.8 ± 34.5	2.5×10^8 to 4.6×10^6	4.5×10^4 to 8.3×10^2	$(3.4 \pm 3.8) \times 10^3$	$(3.8 \pm 2.7) \times 10^{-4}$
50% 9-tc	1.1–41.2	11.4 ± 8.0	9.5×10^8 to 2.4×10^7	4.2×10^5 to 1.1×10^4	$(3.3 \pm 3.4) \times 10^4$	$(3.6 \pm 2.5) \times 10^{-5}$
50% 12-al	1.5–53.1	16.3 ± 10.6	6.8×10^8 to 1.9×10^7	4.3×10^7 to 1.2×10^6	$(3.2 \pm 3.7) \times 10^6$	$(3.8 \pm 2.5) \times 10^{-7}$
50% 9-al	1.2–39.1	7.0 ± 6.2	8.5×10^8 to 2.6×10^7	4.8×10^6 to 1.4×10^5	$(4.5 \pm 4.8) \times 10^5$	$(1.7 \pm 1.5) \times 10^{-6}$

The value of t_d is the time for the hydroxyl group of cholesterol move from the bilayer center to the equilibrium position. The value of k_d is the rate for the hydroxyl group of cholesterol to move from the bilayer center to the equilibrium position; k_d was calculated by $k_d = 1/t_d$. The rate for cholesterol to move from the equilibrium position to the bilayer center (k_f) was calculated by Eq. 2. The rate of cholesterol flip-flops (k_{flip}) was calculated by Eq. 1, and the average rate for cholesterol flip-flop ($\overline{k}_{flip}$) was estimated. The half-life for cholesterol flip-flop ($t_{1/2}$) was calculated by Eq. 3. The errors were estimated using standard deviation.
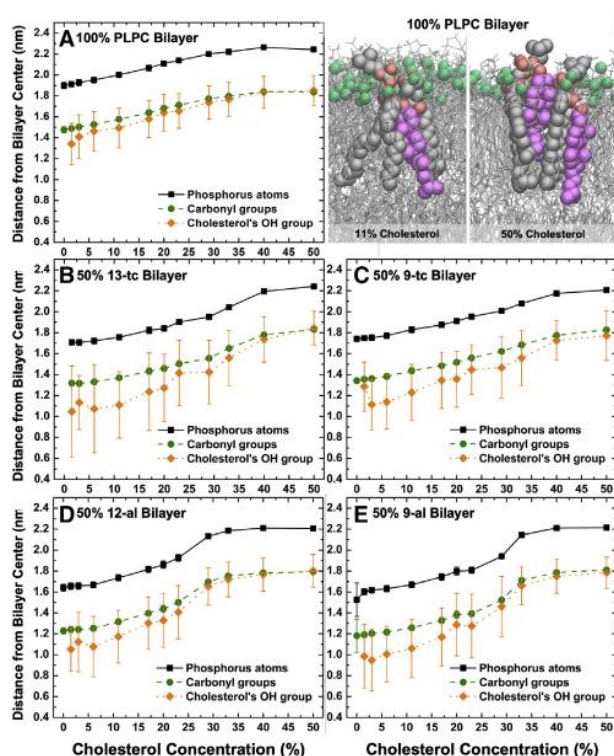
FIGURE 5 Average distance of the lipid phosphorus atoms, carbonyl groups, and cholesterol's hydroxyl group from the bilayer center for 100% PLPC (*A*), 50% 13-tc (*B*), 50% 9-tc (*C*), 50% 12-al (*D*), and 50% 9-al (*E*) bilayer. The snapshot shows an example of the location of cholesterol in the 100% PLPC bilayer at 11 and 50% of cholesterol. Cholesterol is shown in magenta. Phosphorus atoms in the lipid headgroups are displayed as green spheres and PLPC molecules as gray lines. The red and white spheres are oxygen and hydrogen atoms, respectively. To see the figure in color, go online.
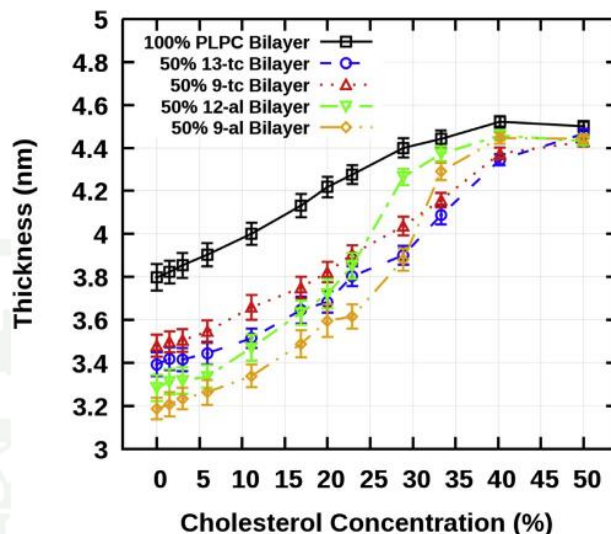

FIGURE 6 Average bilayer thickness of the 100% nonoxidized-PLPC bilayer and 50% oxidized lipid bilayer as a function of cholesterol concentration. The errors were estimated using standard deviation. To see the figure in color, go online.

At 0% cholesterol concentration, the 100% PLPC bilayer is thicker compared with the 50% oxidized lipid bilayer. Note that all the lipid bilayers at 0% cholesterol are in the L_d phase. For all lipid bilayers, the addition of 1.5–6% cholesterol concentration did not significantly increase thickness. However, increasing cholesterol concentration over 11% led to a significant increase in bilayer thickness compared with the bilayer without cholesterol. At 50% cholesterol concentration, the L_o phase was observed in all lipid bilayers, and no difference in the thicknesses between 100% PLPC bilayer and 50% oxidized lipid bilayer was observed.

To gain understanding of the effect of cholesterol on the elastic properties, we computed the area compressibility modulus (K_A) in all lipid bilayers. K_A was calculated from the fluctuations in the area per lipid using (76)

$$K_A = \frac{k_B T \langle A_L \rangle}{N (\sigma_A)^2}, \qquad (4)$$

where k_B and T are the Boltzmann constant and temperature, respectively. $\langle A_L \rangle$ is the average area per lipid, $(\sigma_A)^2$ is the variance of the area per lipid, and N is the number of lipids per leaflet. The average K_A as a function of cholesterol concentration in the 100% PLPC and 50% oxidized lipid bilayers is shown in Fig. S13. The results showed that in the L_d phase, the addition of cholesterol did not significantly change the area compressibility modulus. However, when the lipid phase state changes from L_d to the L_o phase, a rapid increase in K_A is clearly observed in all bilayers.

CONCLUSIONS

We performed 161-μs unbiased MD simulations as well as umbrella-sampling simulations to understand the role of cholesterol in preventing lipid bilayer pore formation caused by oxidative stress. As model systems, we used pure PLPC and 50% binary mixtures of PLPC-oxidized-lipids and varied cholesterol concentration. Without cholesterol, no pore formation was observed for 100% PLPC and 50% PLPC-hydroperoxide-bilayers, whereas a stable pore was observed in the 50% PLPC-aldehyde-bilayers. We found that adding over 11% cholesterol concentrations can prevent pores in aldehyde bilayers. First, we investigated the effect of cholesterol on oxidized chain distribution in the lipid bilayer. The results show that cholesterol restricts the distribution and changes the orientation of the oxidized lipid functional group in the bilayer. This had a direct influence on pore formation in the aldehyde lipid bilayers in which cholesterols confine the distribution of the aldehyde groups, resulting in a decreased probability for pore creation compared with systems without cholesterol (10). It is consistent with the mechanism of how α-tocs inhibited pores in oxidized lipid bilayers in our previous study (14).

Next, we studied cholesterol flip-flop within the bilayer. In the 100% PLPC and 50% hydroperoxide bilayer, no flip-flop events were observed during 3 μs. However, there were one to three flip-flop events within the aldehyde bilayer. To understand the flip-flop behavior in the different bilayers, we performed 130 biased umbrella-sampling MD simulations to calculate the free energy barrier and performed extended unbiased MD simulations to estimate the rate for cholesterol flip-flop. The free energy barrier indicates that flip-flops are more favorable within the aldehyde bilayer as compared with the PLPC and hydroperoxide bilayers. The rate for cholesterol flip-flop decreases with increasing cholesterol concentration, the highest rate being in the aldehyde bilayer. Systematic analyses were carried out to describe the changes caused by varying concentrations of cholesterol in oxidized lipid bilayers. We found that cholesterols induce tighter lipid packing, resulting in inhibition of membrane damage. This work improves our understanding toward the interplay between cholesterols and oxidized lipids and can potentially be applied for improving cold plasma treatments of tumors (17,77).

SUPPORTING MATERIAL

Supporting material can be found online at https://doi.org/10.1016/j.bpj.2021.08.036.

REFERENCES

1. Wong-Ekkabut, J., Z. Xu, …, L. Monticelli. 2007. Effect of lipid peroxidation on the properties of lipid bilayers: a molecular dynamics study. *Biophys. J.* 93:4225–4236.

2. Lis, M., A. Wizert, …, L. Cwiklik. 2011. The effect of lipid oxidation on the water permeability of phospholipids bilayers. *Phys. Chem. Chem. Phys.* 13:17555–17563.

3. Jarerattanachat, V., M. Karttunen, and J. Wong-Ekkabut. 2013. Molecular dynamics study of oxidized lipid bilayers in NaCl solution. *J. Phys. Chem. B.* 117:8490–8501.

4. Weber, G., T. Charitat, …, A. P. Schroder. 2014. Lipid oxidation induces structural changes in biomimetic membranes. *Soft Matter.* 10:4241–4247.

5. Runas, K. A., and N. Malmstadt. 2015. Low levels of lipid oxidation radically increase the passive permeability of lipid bilayers. *Soft Matter.* 11:499–505.

6. Guo, Y., V. A. Baulin, and F. Thalmann. 2016. Peroxidised phospholipid bilayers: insight from coarse-grained molecular dynamics simulations. *Soft Matter.* 12:263–271.

7. Tsubone, T. M., M. S. Baptista, and R. Itri. 2019. Understanding membrane remodelling initiated by photosensitized lipid oxidation. *Biophys. Chem.* 254:106263.

8. Tsubone, T. M., H. C. Junqueira, …, R. Itri. 2019. Contrasting roles of oxidized lipids in modulating membrane microdomains. *Biochim. Biophys. Acta Biomembr.* 1861:660–669.

9. Cwiklik, L., and P. Jungwirth. 2010. Massive oxidation of phospholipid membranes leads to pore creation and bilayer disintegration. *Chem. Phys. Lett.* 486:99–103.

10. Boonnoy, P., V. Jarerattanachat, …, J. Wong-Ekkabut. 2015. Bilayer deformation, pores, and micellation induced by oxidized lipids. *J. Phys. Chem. Lett.* 6:4884–4888.

11. Van der Paal, J., E. C. Neyts, …, A. Bogaerts. 2016. Effect of lipid peroxidation on membrane permeability of cancer and normal cells subjected to oxidative stress. *Chem. Sci.* 7:489–498.

12. Bacellar, I. O. L., M. C. Oliveira, …, M. S. Baptista. 2018. Photosensitized membrane permeabilization requires contact-dependent reactions between photosensitizer and lipids. *J. Am. Chem. Soc.* 140:9606–9615.

13. Schumann-Gillett, A., and M. L. O'Mara. 2019. The effects of oxidised phospholipids and cholesterol on the biophysical properties of POPC bilayers. *Biochim. Biophys. Acta Biomembr.* 1861:210–219.

14. Boonnoy, P., M. Karttunen, and J. Wong-Ekkabut. 2017. Alpha-tocopherol inhibits pore formation in oxidized bilayers. *Phys. Chem. Chem. Phys.* 19:5699–5704.

15. Wang, T. Y., M. D. J. Libardo, …, J. P. Pellois. 2017. Membrane oxidation in cell delivery and cell killing applications. *ACS Chem. Biol.* 12:1170–1182.

16. Libardo, M. D. J., T. Y. Wang, …, A. M. Angeles-Boza. 2017. How does membrane oxidation affect cell delivery and cell killing? *Trends Biotechnol.* 35:686–690.

17. Keidar, M. 2015. Plasma for cancer treatment. *Plasma Sources Sci. Technol.* 24:033001.

18. Agmon, E., J. Solon, …, B. R. Stockwell. 2018. Modeling the effects of lipid peroxidation during ferroptosis on membrane properties. *Sci. Rep.* 8:5155.

19. Owen, M. C., W. Kulig, …, B. Strodel. 2018. Cholesterol protects the oxidized lipid bilayer from water injury: an all-atom molecular dynamics study. *J. Membr. Biol.* 251:521–534.

20. Kulig, W., A. Olżyńska, …, P. Jungwirth. 2015. Cholesterol under oxidative stress-how lipid membranes sense oxidation as cholesterol is being replaced by oxysterols. *Free Radic. Biol. Med.* 84:30–41.

21. Khandelia, H., B. Loubet, …, M. Hof. 2014. Pairing of cholesterol with oxidized phospholipid species in lipid bilayers. *Soft Matter.* 10:639–647.

22. Kerdous, R., J. Heuvingh, and S. Bonneau. 2011. Photo-dynamic induction of oxidative stress within cholesterol-containing membranes: shape transitions and permeabilization. *Biochim. Biophys. Acta.* 1808:2965–2972.

23. Sheetz, M. P., and S. J. Singer. 1974. Biological membranes as bilayer couples. A molecular mechanism of drug-erythrocyte interactions. *Proc. Natl. Acad. Sci. USA.* 71:4457–4461.

24. Bennett, W. F., J. L. MacCallum, …, D. P. Tieleman. 2009. Molecular view of cholesterol flip-flop and chemical potential in different membrane environments. *J. Am. Chem. Soc.* 131:12714–12720.

25. Jo, S., H. Rui, …, W. Im. 2010. Cholesterol flip-flop: insights from free energy simulation studies. *J. Phys. Chem. B.* 114:13342–13348.

26. Bennett, W. F. D., and D. P. Tieleman. 2012. Molecular simulation of rapid translocation of cholesterol, diacylglycerol, and ceramide in model raft and nonraft membranes. *J. Lipid Res.* 53:421–429.

27. Thallmair, S., H. I. Ingólfsson, and S. J. Marrink. 2018. Cholesterol flip-flop impacts domain registration in plasma membrane models. *J. Phys. Chem. Lett.* 9:5527–5533.

Boonnoy et al.

28. Gu, R. X., S. Baoukina, and D. P. Tieleman. 2019. Cholesterol flip-flop in heterogeneous membranes. *J. Chem. Theory Comput.* 15:2064–2070.

29. Smith, L. L. 1991. Another cholesterol hypothesis: cholesterol as antioxidant. *Free Radic. Biol. Med.* 11:47–61.

30. Parasassi, T., A. M. Giusti, …, E. Gratton. 1995. Cholesterol protects the phospholipid bilayer from oxidative damage. *Free Radic. Biol. Med.* 19:511–516.

31. Van der Paal, J., C. Verheyen, …, A. Bogaerts. 2017. Hampering effect of cholesterol on the permeation of reactive oxygen species through phospholipids bilayer: possible explanation for plasma cancer selectivity. *Sci. Rep.* 7:39526.

32. Boonnoy, P., M. Karttunen, and J. Wong-Ekkabut. 2018. Does α-tocopherol flip-flop help to protect membranes against oxidation? *J. Phys. Chem. B.* 122:10362–10370.

33. de Almeida, R. F., J. Borst, …, A. J. Visser. 2007. Complexity of lipid domains and rafts in giant unilamellar vesicles revealed by combining imaging and microscopic and macroscopic time-resolved fluorescence. *Biophys. J.* 93:539–553.

34. Mills, T. T., G. E. Toombes, …, J. F. Nagle. 2008. Order parameters and areas in fluid-phase oriented lipid membranes using wide angle x-ray scattering. *Biophys. J.* 95:669–681.

35. Alwarawrah, M., J. Dai, and J. Huang. 2010. A molecular view of the cholesterol condensing effect in DOPC lipid bilayers. *J. Phys. Chem. B.* 114:7516–7523.

36. Leeb, F., and L. Maibaum. 2018. Spatially resolving the condensing effect of cholesterol in lipid bilayers. *Biophys. J.* 115:2179–2188.

37. Vist, M. R., and J. H. Davis. 1990. Phase equilibria of cholesterol/dipalmitoylphosphatidylcholine mixtures: 2H nuclear magnetic resonance and differential scanning calorimetry. *Biochemistry.* 29:451–464.

38. Waheed, Q., R. Tjörnhammar, and O. Edholm. 2012. Phase transitions in coarse-grained lipid bilayers containing cholesterol by molecular dynamics simulations. *Biophys. J.* 103:2125–2133.

39. Wang, Y., P. Gkeka, …, Z. Cournia. 2016. DPPC-cholesterol phase diagram using coarse-grained molecular dynamics simulations. *Biochim. Biophys. Acta.* 1858:2846–2857.

40. Lee, S., D. W. Jeong, and M. C. Choi. 2017. Vertical order of DPPC multilayer enhanced by cholesterol-induced ripple-to-liquid ordered (LO) phase transition: synchrotron x-ray reflectivity study. *Curr. Appl. Phys.* 17:392–397.

41. Bennett, W. F. D., J. E. Shea, and D. P. Tieleman. 2018. Phospholipid chain interactions with cholesterol drive domain formation in lipid membranes. *Biophys. J.* 114:2595–2605.

42. Munro, S. 2003. Lipid rafts: elusive or illusive? *Cell.* 115:377–388.

43. Simons, K., and E. Ikonen. 1997. Functional rafts in cell membranes. *Nature.* 387:569–572.

44. de Meyer, F., and B. Smit. 2009. Effect of cholesterol on the structure of a phospholipid bilayer. *Proc. Natl. Acad. Sci. USA.* 106:3654–3658.

45. Bachar, M., P. Brunelle, …, A. Rauk. 2004. Molecular dynamics simulation of a polyunsaturated lipid bilayer susceptible to lipid peroxidation. *J. Phys. Chem. B.* 108:7170–7179.

46. Höltje, M., T. Förster, …, H. D. Höltje. 2001. Molecular dynamics simulations of stratum corneum lipid models: fatty acids and cholesterol. *Biochim. Biophys. Acta.* 1511:156–167.

47. Knight, C. J., and J. S. Hub. 2015. MemGen: a general web server for the setup of lipid membrane simulation systems. *Bioinformatics.* 31:2897–2899.

48. Abraham, M. J., T. Murtola, …, E. Lindahl. 2015. GROMACS: high performance molecular simulations through multi-level parallelism from laptops to supercomputers. *SoftwareX.* 1–2:19–25.

49. Bussi, G., D. Donadio, and M. Parrinello. 2007. Canonical sampling through velocity rescaling. *J. Chem. Phys.* 126:014101.

50. Parrinello, M., and A. Rahman. 1981. Polymorphic transitions in single crystals: a new molecular dynamics method. *J. Appl. Phys.* 52:7182–7190.

51. Hess, B. 2008. P-LINCS: a parallel linear constraint solver for molecular simulation. *J. Chem. Theory Comput.* 4:116–122.

52. Wong-Ekkabut, J., and M. Karttunen. 2016. The good, the bad and the user in soft matter simulations. *Biochim. Biophys. Acta.* 1858:2529–2538.

53. Darden, T., D. York, and L. Pedersen. 1993. Particle mesh Ewald: an N· log (N) method for Ewald sums in large systems. *J. Chem. Phys.* 98:10089–10092.

54. Essmann, U., L. Perera, …, L. G. Pedersen. 1995. A smooth particle mesh Ewald method. *J. Chem. Phys.* 103:8577–8593.

55. Karttunen, M., J. Rottler, …, C. Sagui. 2008. Electrostatics in biomolecular simulations: where are we now and where are we heading? *Curr. Top. Membr.* 60:49–89.

56. Wong-Ekkabut, J., and M. Karttunen. 2016. Molecular dynamics simulation of water permeation through the alpha-hemolysin channel. *J. Biol. Phys.* 42:133–146.

57. Kongsema, M., S. Wongkhieo, …, J. Wong-Ekkabut. 2019. Molecular mechanism of Forkhead box M1 inhibition by thiostrepton in breast cancer cells. *Oncol. Rep.* 42:953–962.

58. Enkavi, G., M. Javanainen, …, I. Vattulainen. 2019. Multiscale simulations of biological membranes: the challenge to understand biological phenomena in a living substance. *Chem. Rev.* 119:5607–5774.

59. Nalakarn, P., P. Boonnoy, …, J. Wong-Ekkabut. 2019. Dependence of fullerene aggregation on lipid saturation due to a balance between entropy and enthalpy. *Sci. Rep.* 9:1037.

60. Khuntawee, W., T. Sutthibutpong, …, J. Wong-Ekkabut. 2019. Molecular dynamics study of natural rubber-fullerene composites: connecting microscopic properties to macroscopic behavior. *Phys. Chem. Chem. Phys.* 21:19403–19413.

61. Nisoh, N., V. Jarerattanachat, …, J. Wong-Ekkabut. 2020. Formation of aggregates, icosahedral structures and percolation clusters of fullerenes in lipids bilayers: the key role of lipid saturation. *Biochim. Biophys. Acta Biomembr.* 1862:183328.

62. Khuntawee, W., R. Amornloetwattana, …, J. Wong-ekkabut. 2021. In silico and in vitro design of cordycepin encapsulation in liposomes for colon cancer treatment. *RSC Adv.* 11:8475–8484.

63. Humphrey, W., A. Dalke, and K. Schulten. 1996. VMD: visual molecular dynamics. *J. Mol. Graph.* 14:33–38.

64. Torrie, G. M., and J. P. Valleau. 1977. Nonphysical sampling distributions in Monte Carlo free-energy estimation: umbrella sampling. *J. Comput. Phys.* 23:187–199.

65. Kumar, S., J. M. Rosenberg, …, P. A. Kollman. 1992. The weighted histogram analysis method for free-energy calculations on biomolecules. I. The method. *J. Comput. Chem.* 13:1011–1021.

66. Watkins, J. C. 2016. An Introduction to the Science of Statistics: From Theory to Implementation, Preliminary Edition: The University of Arizona, Arizona, math.arizona.edu/~jwatkins/statbook.pdf.

67. Garrec, J., A. Monari, …, M. Tarek. 2014. Lipid peroxidation in membranes: the peroxyl radical does not "float". *J. Phys. Chem. Lett.* 5:1653–1658.

68. Rosa, R., F. Spinozzi, and R. Itri. 2018. Hydroperoxide and carboxyl groups preferential location in oxidized biomembranes experimentally determined by small angle x-ray scattering: Implications in membrane structure. *Biochim. Biophys. Acta Biomembr.* 1860:2299–2307.

69. Israelachvili, J. N., D. J. Mitchell, and B. W. Ninham. 1976. Theory of self-assembly of hydrocarbon amphiphiles into micelles and bilayers. *J. Chem. Soc. Faraday Trans. II.* 72:1525–1568.

70. Hub, J. S., F. K. Winkler, …, B. L. de Groot. 2010. Potentials of mean force and permeabilities for carbon dioxide, ammonia, and water flux across a Rhesus protein channel and lipid membranes. *J. Am. Chem. Soc.* 132:13251–13263.

71. Choubey, A., R. K. Kalia, …, P. Vashishta. 2013. Cholesterol translocation in a phospholipid membrane. *Biophys. J.* 104:2429–2436.

72. Ermilova, I., and A. P. Lyubartsev. 2018. Cholesterol in phospholipid bilayers: positions and orientations inside membranes with different unsaturation degrees. *Soft Matter.* 15:78–93.

73. Sankaram, M. B., and T. E. Thompson. 1991. Cholesterol-induced fluid-phase immiscibility in membranes. *Proc. Natl. Acad. Sci. USA.* 88:8686–8690.

74. de Almeida, R. F., and E. Joly. 2014. Crystallization around solid-like nanosized docks can explain the specificity, diversity, and stability of membrane microdomains. *Front Plant Sci.* 5:72.

75. Róg, T., M. Pasenkiewicz-Gierula, …, M. Karttunen. 2009. Ordering effects of cholesterol and its analogues. *Biochim. Biophys. Acta.* 1788:97–121.

76. Marrink, S. J., A. H. De Vries, and A. E. Mark. 2004. Coarse grained model for semiquantitative lipid simulations. *J. Phys. Chem. B.* 108:750–760.

77. Yan, D., J. H. Sherman, and M. Keidar. 2017. Cold atmospheric plasma, a novel promising anti-cancer treatment modality. *Oncotarget.* 8:15977–15995.
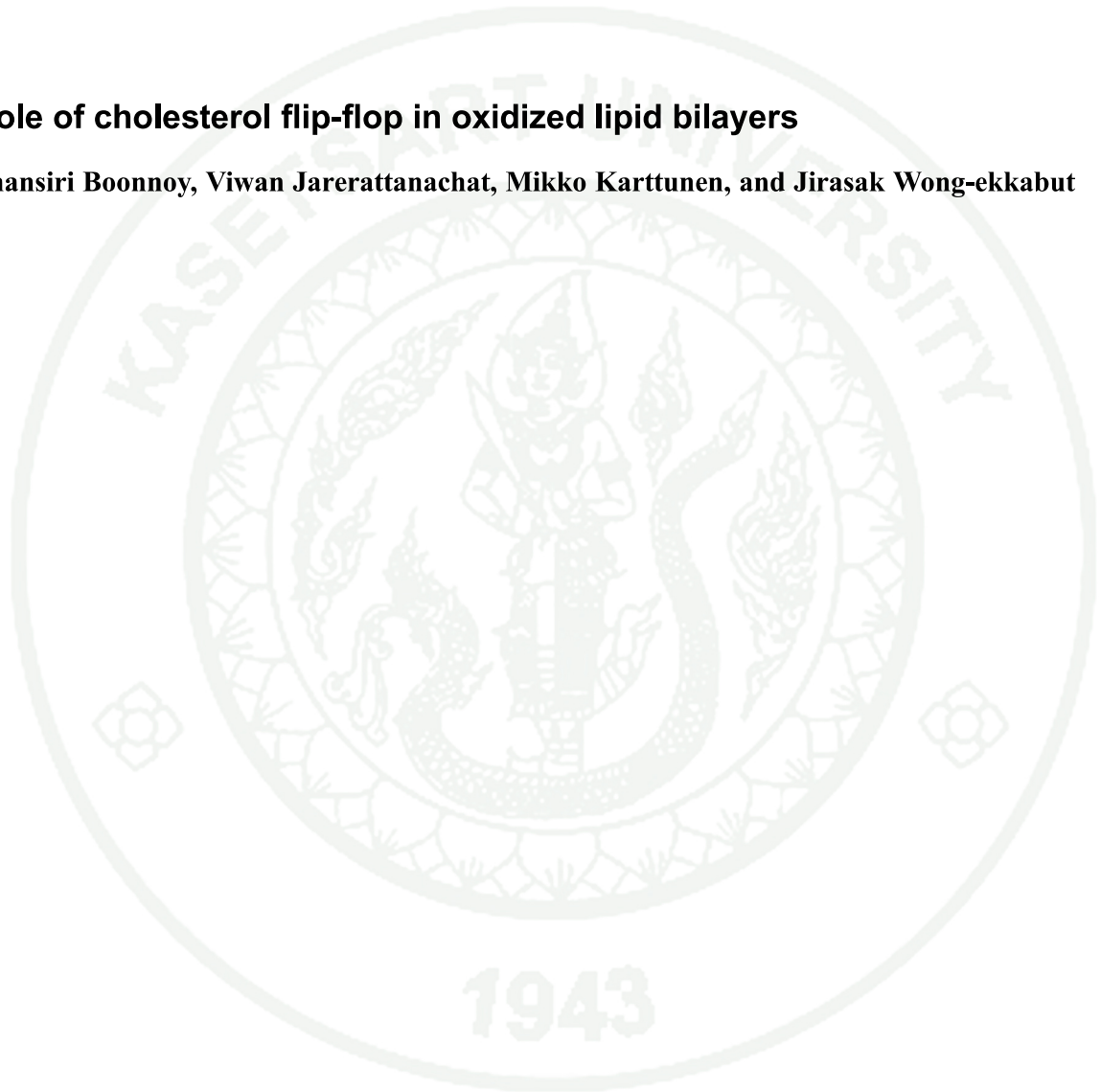
Supplemental information

Role of cholesterol flip-flop in oxidized lipid bilayers

Phansiri Boonnoy, Viwan Jarerattanachat, Mikko Karttunen, and Jirasak Wong-ekkabut

Supporting Information

Role of cholesterol flip-flop in oxidized lipid bilayers

Phansiri Boonnoy[a,b], Viwan Jarerattanachat [b,c,d], Mikko Karttunen[e,f,g] and Jirasak Wong-ekkabut[*,a,b,c,h]

[a] Department of Physics, Faculty of Science, Kasetsart University, Bangkok 10900, Thailand

[b] Computational Biomodelling Laboratory for Agricultural Science and Technology (CBLAST), Faculty of Science, Kasetsart University, Bangkok 10900, Thailand

[c] Thailand Center of Excellence in Physics (ThEP Center), Ministry of Higher Education, Science, Research and Innovation, Bangkok 10400, Thailand

[d] NSTDA supercomputer Center (ThaiSC), National Electronics and Computer Technology Center (NECTEC), National Science and Technology Development Agency (NSTDA), Khlong Luang, Pathumthani 12120, Thailand

[e] Department of Chemistry, The University of Western Ontario, 1151 Richmond Street, London, Ontario N6A 3K7, Canada

[f] Department of Physics and Astronomy, The University of Western Ontario, 1151 Richmond Street, London, Ontario N6A 3K7, Canada

[g] The Centre for Advanced Materials Research (CAMBR), The University of Western Ontario, 1151 Richmond Street, London, Ontario N6A 5B7, Canada

[h] Specialized Center of Rubber and Polymer Materials for Agriculture and Industry (RPM), Faculty of Science, Kasetsart University, Bangkok 10900, Thailand

[*]Corresponding E-mail: jirasak.w@ku.ac.th

Table S1. List of simulated systems. All systems were solvated in 10,560 simple point charge (SPC) water molecules (1). The time in brackets shows the moment of time when a pore was observed a pore. The symbol ***** denotes the systems in which cholesterol flip-flops were observed.

| No.	Systems	Number of molecules in the lipid bilayer			Simulation time (ns)	Final structure
		#PLPC	#OXPLs	#Cholesterol		
1	100% PLPC without Chol	128	0	0	1000	Bilayer in liquid-disorder phase
2	100% PLPC + 1.5 % Chol	128	0	2	3000	Bilayer in liquid-disorder phase
3	100% PLPC + 3 % Chol	128	0	4	3000	Bilayer in liquid-disorder phase
4	100% PLPC + 6 % Chol	128	0	8	3000	Bilayer in liquid-disorder phase
5	100% PLPC + 11 % Chol	128	0	16	3000	Bilayer in liquid-disorder phase
6	100% PLPC + 17 % Chol	128	0	26	3000	Bilayer in liquid-disorder phase
7	100% PLPC + 20 % Chol	128	0	32	3000	Bilayer in liquid-disorder phase
8	100% PLPC + 23 % Chol	128	0	38	3000	Bilayer in liquid-order phase
9	100% PLPC + 29 % Chol	128	0	52	3000	Bilayer in liquid-order phase
10	100% PLPC + 33 % Chol	128	0	64	3000	Bilayer in liquid-order phase
11	100% PLPC + 40 % Chol	128	0	86	3000	Bilayer in liquid-order phase
12	100% PLPC + 50 % Chol	128	0	128	3000	Bilayer in liquid-order phase
13	50% 13-tc without Chol	64	64	0	1000	Bilayer in liquid-disorder phase
14	50% 13-tc + 1.5 % Chol	64	64	2	3000	Bilayer in liquid-disorder phase
15	50% 13-tc + 3 % Chol	64	64	4	3000	Bilayer in liquid-disorder phase
16	50% 13-tc + 6 % Chol	64	64	8	3000	Bilayer in liquid-disorder phase
17	50% 13-tc + 11 % Chol	64	64	16	3000	Bilayer in liquid-disorder phase
18	50% 13-tc + 17 % Chol	64	64	26	3000	Bilayer in liquid-disorder phase
19	50% 13-tc + 20 % Chol	64	64	32	3000	Bilayer in liquid-disorder phase
20	50% 13-tc + 23 % Chol	64	64	38	3000	Bilayer in liquid-disorder phase
21	50% 13-tc + 29 % Chol	64	64	52	3000	Bilayer in liquid-disorder phase
22	50% 13-tc + 33 % Chol	64	64	64	3000	Bilayer in liquid-order phase
23	50% 13-tc + 40 % Chol	64	64	86	3000	Bilayer in liquid-order phase
24	50% 13-tc + 50 % Chol	64	64	128	3000	Bilayer in liquid-order phase
25	50% 9-tc without Chol	64	64	0	1000	Bilayer in liquid-disorder phase
26	50% 9-tc + 1.5 % Chol	64	64	2	3000	Bilayer in liquid-disorder phase
27	50% 9-tc + 3 % Chol	64	64	4	3000	Bilayer in liquid-disorder phase
28	50% 9-tc + 6 % Chol	64	64	8	3000	Bilayer in liquid-disorder phase
29	50% 9-tc + 11 % Chol	64	64	16	3000	Bilayer in liquid-disorder phase
30	50% 9-tc + 17 % Chol	64	64	26	3000	Bilayer in liquid-disorder phase
31	50% 9-tc + 20 % Chol	64	64	32	3000	Bilayer in liquid-disorder phase
32	50% 9-tc + 23 % Chol	64	64	38	3000	Bilayer in liquid-disorder phase
33	50% 9-tc + 29 % Chol	64	64	52	3000	Bilayer in liquid-order phase
34	50% 9-tc + 33 % Chol	64	64	64	3000	Bilayer in liquid-order phase
35	50% 9-tc + 40 % Chol	64	64	86	3000	Bilayer in liquid-order phase
36	50% 9-tc + 50 % Chol	64	64	128	3000	Bilayer in liquid-order phase
37	50% 12-al without Chol	64	64	0	1000	Bilayer with a pore at 905 ns
38	50% 12-al + 1.5 % Chol	64	64	2	1000	Bilayer with a pore at 787 ns
39	50% 12-al + 3 % Chol	64	64	4	3000	Bilayer with a pore at 2020 ns
40	50% 12-al + 6 % Chol	64	64	8	2000	Bilayer with a pore at 1831 ns
*41	50% 12-al + 11 % Chol	64	64	16	3000	Bilayer in liquid-disorder phase
*42	50% 12-al + 17 % Chol	64	64	26	3000	Bilayer in liquid-disorder phase
43	50% 12-al + 20 % Chol	64	64	32	3000	Bilayer in liquid-disorder phase
44	50% 12-al + 23 % Chol	64	64	38	3000	Bilayer in liquid-disorder phase
45	50% 12-al + 29 % Chol	64	64	52	3000	Bilayer in liquid-order phase
46	50% 12-al + 33 % Chol	64	64	64	3000	Bilayer in liquid-order phase
47	50% 12-al + 40 % Chol	64	64	86	3000	Bilayer in liquid-order phase
48	50% 12-al + 50 % Chol	64	64	128	3000	Bilayer in liquid-order phase
49	50% 9-al without Chol	64	64	0	1000	Bilayer with a pore at 134 ns
50	50% 9-al + 1.5 % Chol	64	64	2	1000	Bilayer with a pore at 441 ns
51	50% 9-al + 3 % Chol	64	64	4	1000	Bilayer with a pore at 100 ns
52	50% 9-al + 6 % Chol	64	64	8	1000	Bilayer with a pore at 351 ns
*53	50% 9-al + 11 % Chol	64	64	16	3000	Bilayer in liquid-disorder phase
*54	50% 9-al + 17 % Chol	64	64	26	3000	Bilayer in liquid-disorder phase
*55	50% 9-al + 20 % Chol	64	64	32	3000	Bilayer in liquid-disorder phase
*56	50% 9-al + 23 % Chol	64	64	38	3000	Bilayer in liquid-disorder phase
57	50% 9-al + 29 % Chol	64	64	52	3000	Bilayer in liquid-disorder phase
58	50% 9-al + 33 % Chol	64	64	64	3000	Bilayer in liquid-order phase
59	50% 9-al + 40 % Chol	64	64	86	3000	Bilayer in liquid-order phase
60	50% 9-al + 50 % Chol	64	64	128	3000	Bilayer in liquid-order phase
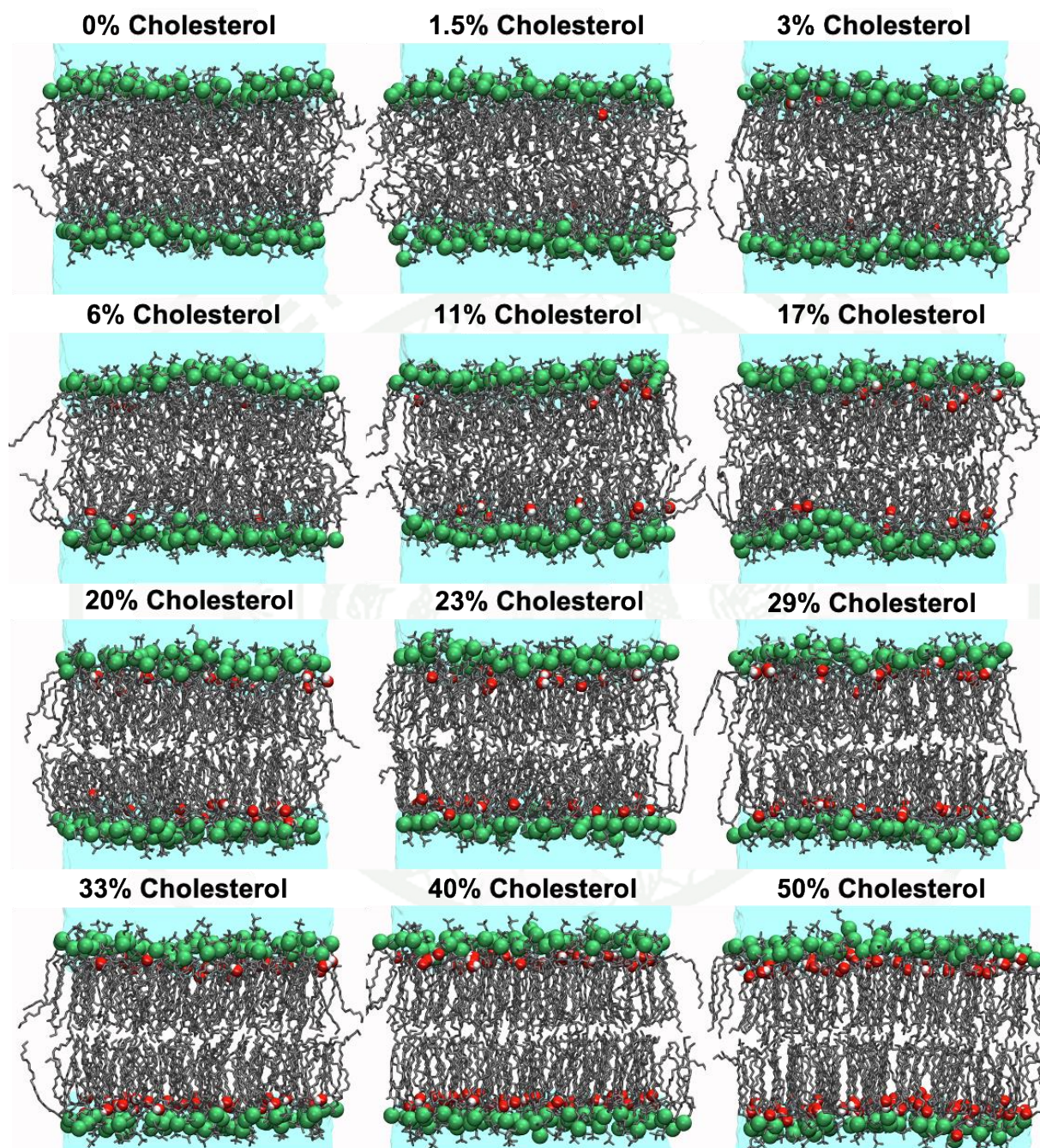
Figure S1. Snapshots of the 100% PLPC bilayer at different cholesterol concentrations. The light blue surface represent water. Phosphorus atoms in lipid head groups are shown as green spheres. The gray line represents the hydrocarbon tails of the PLPC molecules. The red and white spheres are oxygen and hydrogen atoms in cholesterols' hydroxyl groups, respectively.
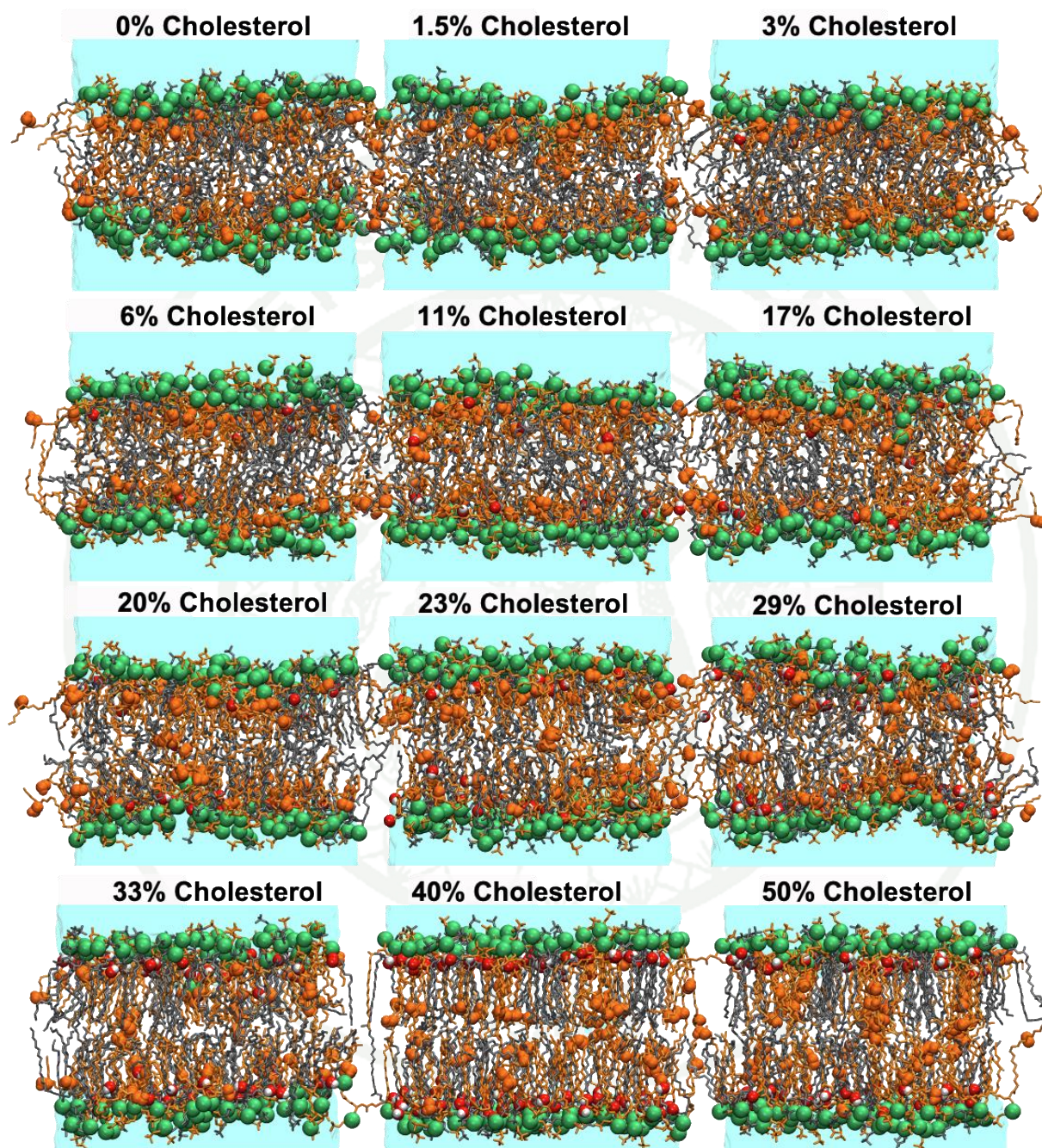
Figure S2. Snapshots of the 50% 13-tc bilayer at different cholesterol concentrations. The light blue surface represent water. Phosphorus atoms in lipid head groups are shown as green spheres. The gray and orange lines are PLPC and 13-tc molecules, respectively. The red and white spheres are oxygen and hydrogen atoms in cholesterols' hydroxyl groups. The orange sphere represents the oxidized functional group of hydroperoxide in 13-tc lipid.
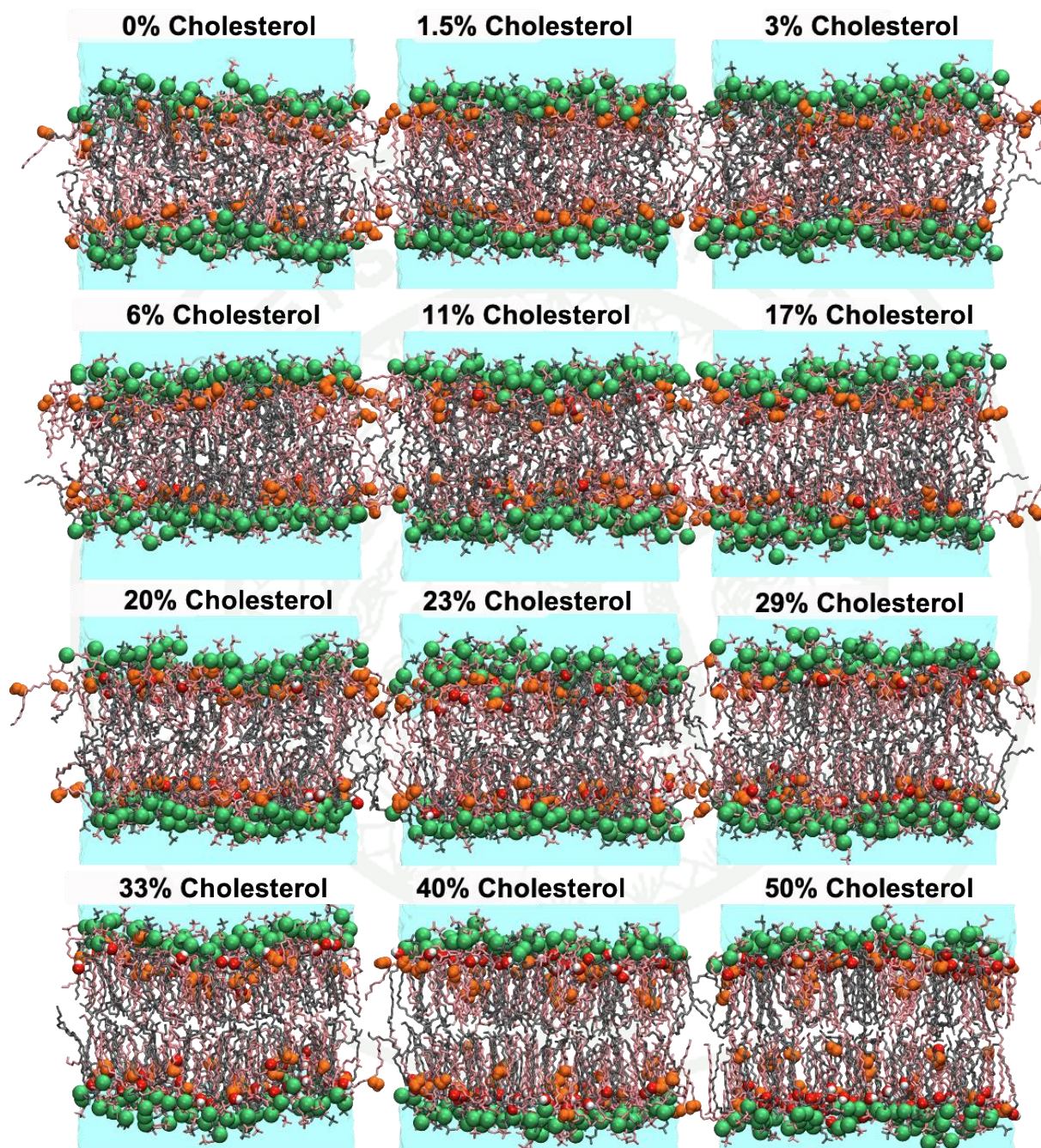
Figure S3. Snapshots of the 50% 9-tc bilayer at different cholesterol concentrations. The light blue surface represent water. Phosphorus atoms in lipid head groups are shown as green spheres. The gray and pink line are PLPC and 9-tc molecules, respectively. The red and white spheres are oxygen and hydrogen atoms in cholesterols' hydroxyl groups, respectively. The orange sphere represents the oxidized functional group of hydroperoxide in 9-tc lipid.
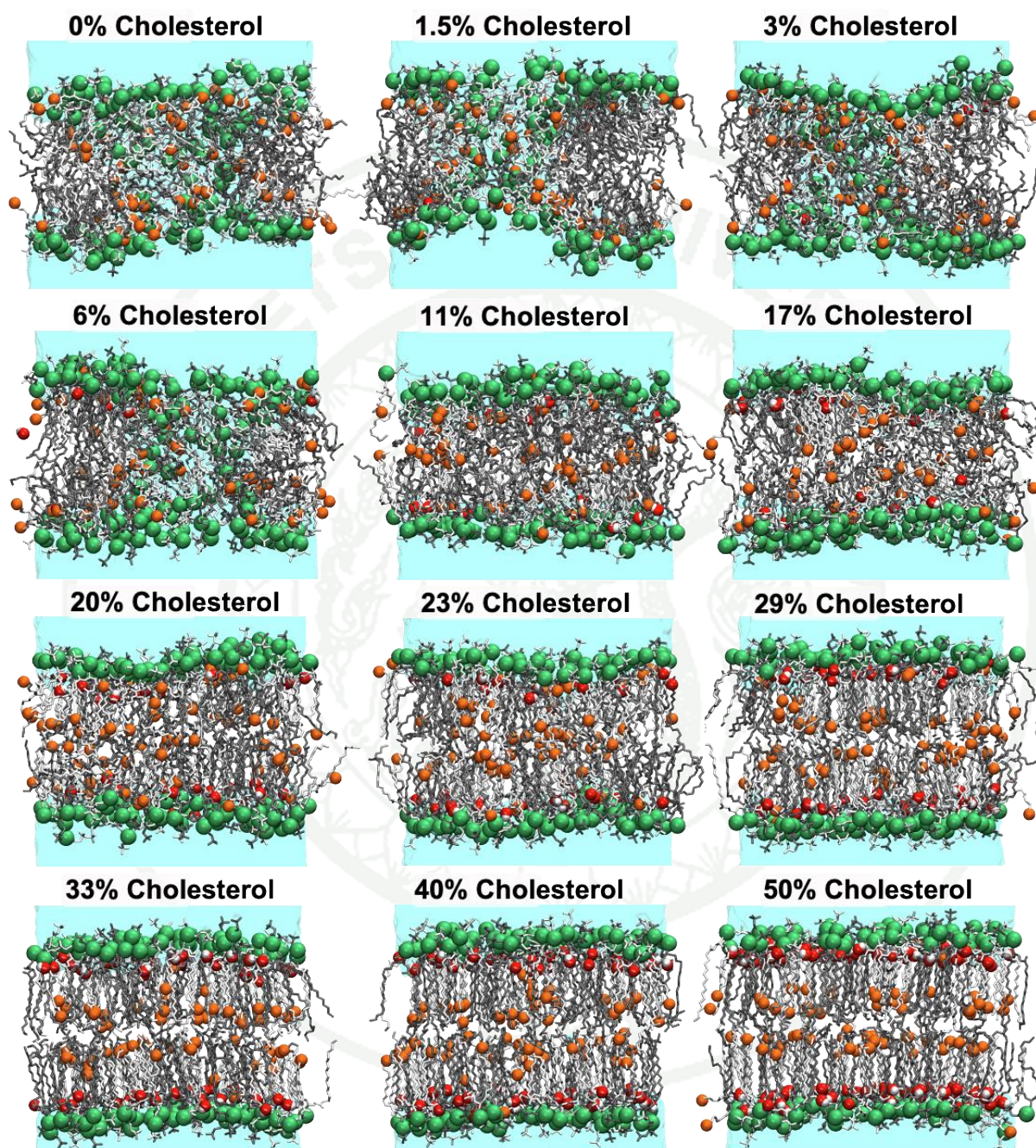
Figure S4. Snapshots of the 50% 12-al bilayer at different cholesterol concentrations. Water pore was observed in the systems with low concentration of 0% - 6% of cholesterol. The light blue surface represent water. Phosphorus atoms in lipid head groups are shown as green spheres. The gray and white line are PLPC and 12-al molecules, respectively. The red and white spheres are oxygen and hydrogen atoms in cholesterols' hydroxyl groups, respectively. The orange sphere represents the oxidized functional group of aldehydes in 12-al lipid.
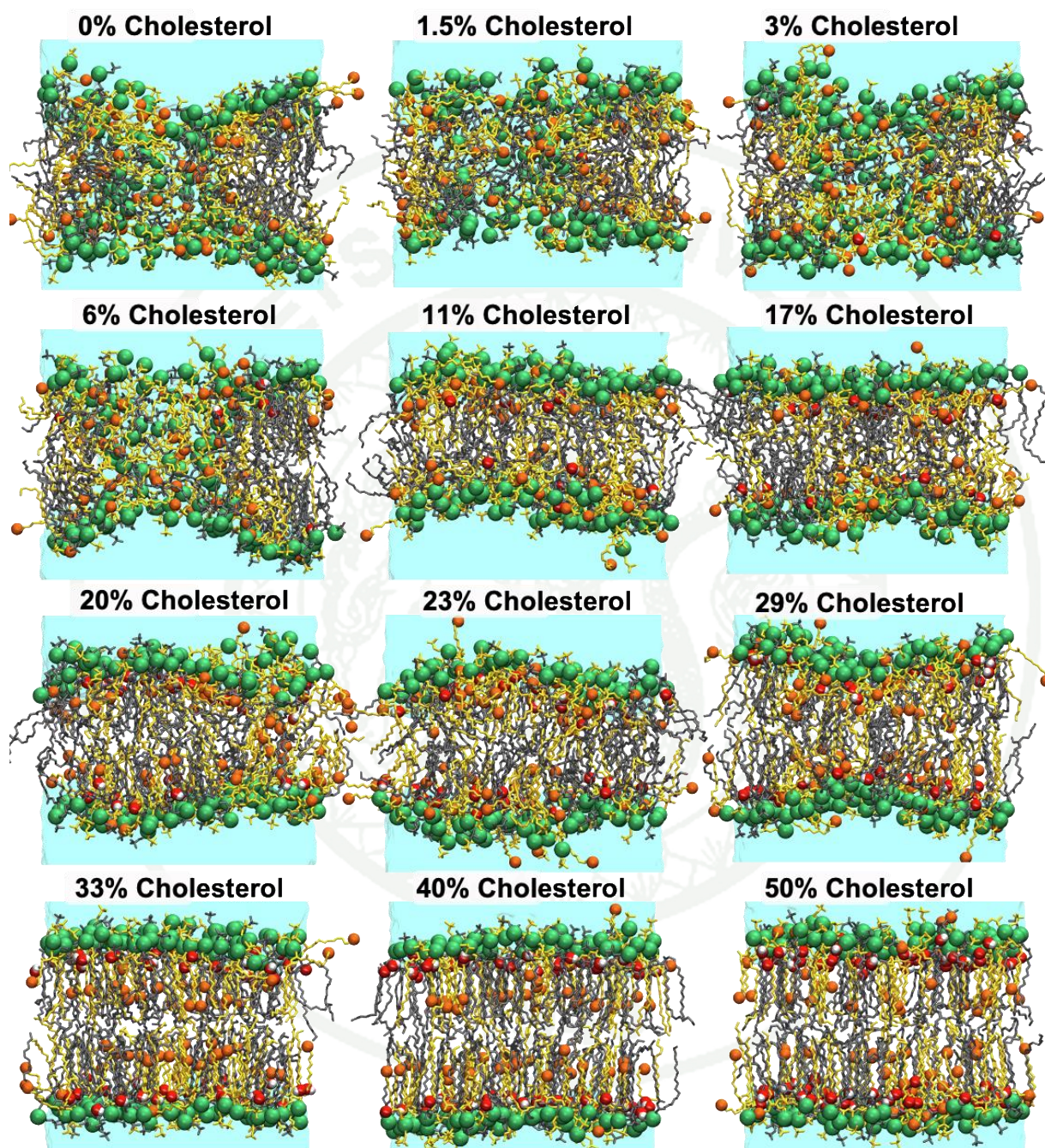
Figure S5. Snapshots of the 50% 9-al bilayer at different cholesterol concentrations. Water pore was observed in the systems with low concentration of 0% - 6% of cholesterol. The light blue surface represent water. Phosphorus atoms in lipid head groups are shown as spheres. The gray and yellow line are PLPC and 9-al molecules, respectively. The red and white spheres are oxygen and hydrogen atom in cholesterol's hydroxyl group, respectively. The orange sphere represents the oxidized functional group of aldehydes in 9-al lipid.
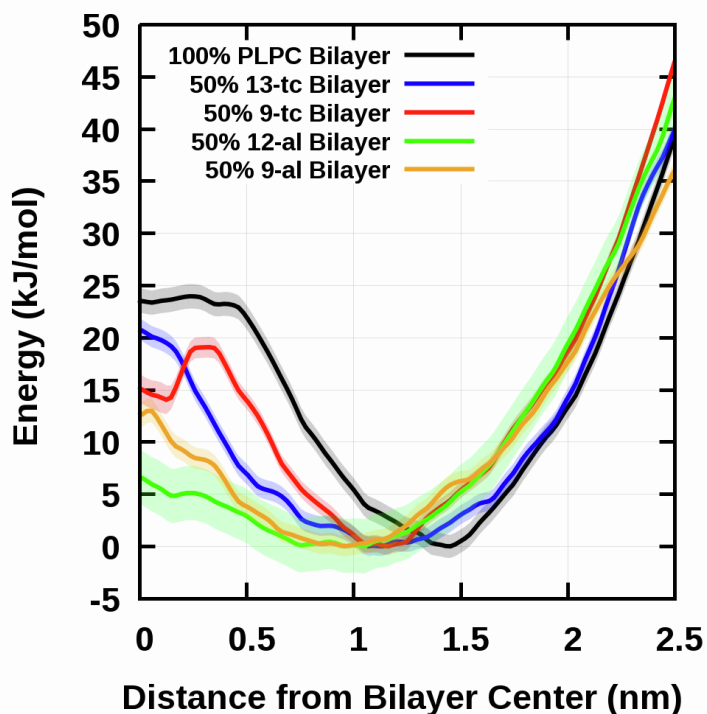
Figure S6. Free energy profiles of cholesterol molecule flip-flop across the 100% PLPC and 50% oxidized PLPC bilayers calculated using WHAM tool in the GROMACS package. Error bars were estimated using the bootstrap method (2) and appear underestimated as compared to those computed using standard error (Fig. 4 in the main text).
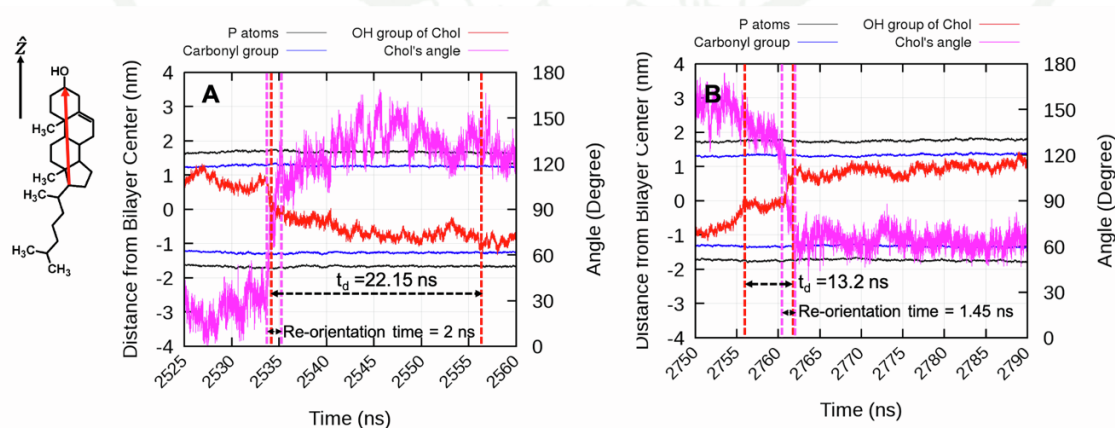

Figure S7. t_d and the re-orientation time in the unbiased simulations of 50% 9-al bilayer containing 11% (A) and 17% (B) cholesterol. The re-orientation timescale is much shorter than t_d.

Table S2. The p-values of k_{flip} were calculated from the t-test. ($p < 0.05$ was considered as statistically significant).

System	100% PLPC	50% 13-tc	50% 9-tc	50% 12-al	50% 9-al
100% PLPC	1.0	0.5	1.8×10^{-8}	3.7×10^{-8}	2.3×10^{-15}
50% 13-tc	-	1.0	2.9×10^{-8}	3.8×10^{-8}	2.3×10^{-15}
50% 9-tc	-	-	1.0	4.8×10^{-8}	2.2×10^{-14}
50% 12-al	-	-	-	1.0	7.5×10^{-6}
50% 9-al	-	-	-	-	1.0

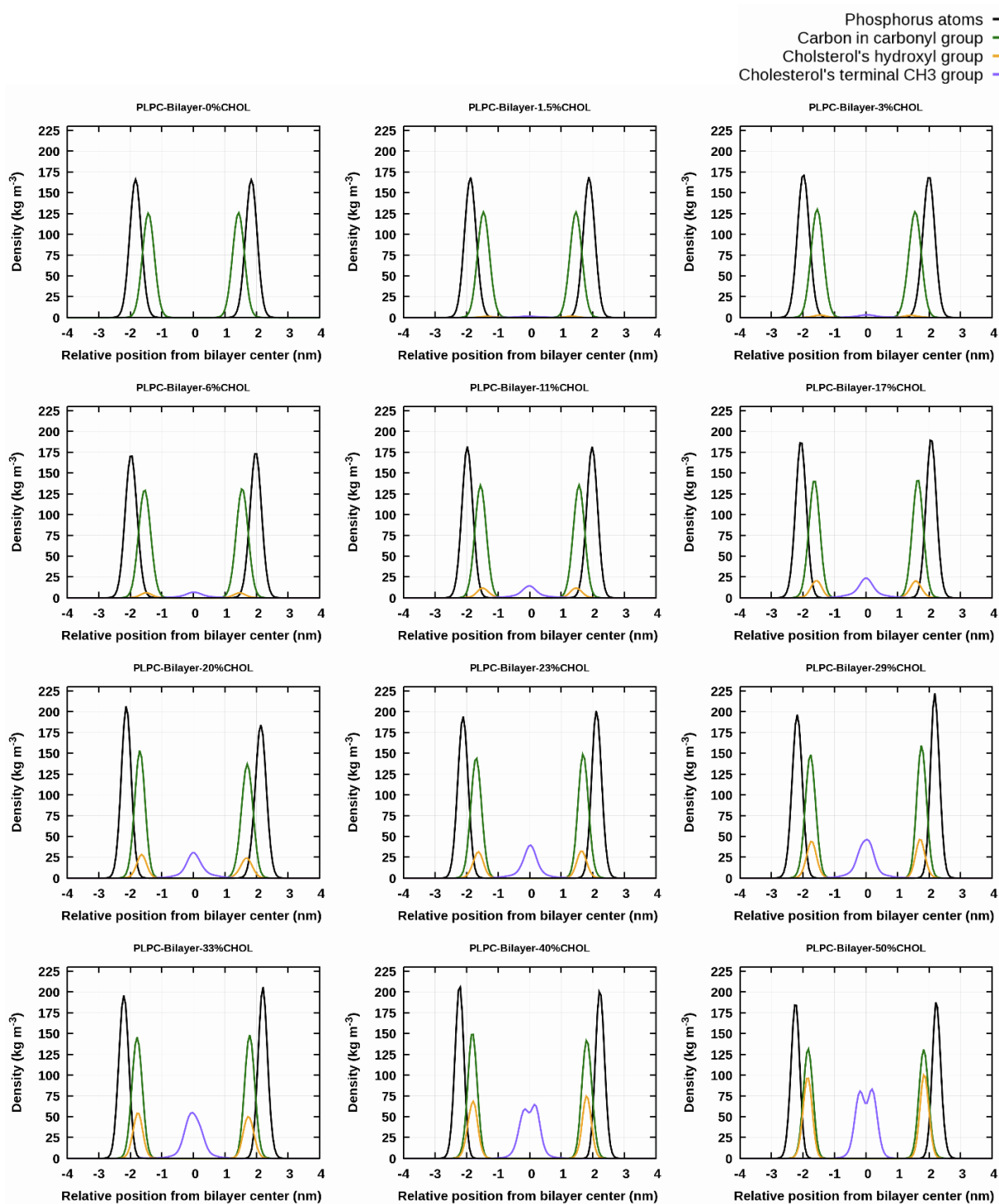**Figure S8**. Mass density profiles for i) lipid's phosphorus atoms, ii) lipid's carbonyl groups, iii) cholesterol's hydroxyl group, and iv) cholesterol's terminal methyl group in 100 % PLPC lipid bilayer with different cholesterol concentrations.

Figure S9. Mass density profiles of the 13-tc systems. The legend at the top right hand corner shows the components and the figure titles indicate the systems.

Figure S10. Mass density profiles of the 9-tc systems. The legend at the top right hand corner shows the components and the figure titles indicate the systems.

Figure S11. Mass density profiles of the 12-al systems. The legend at the top right hand corner shows the components and the figure titles indicate the systems.
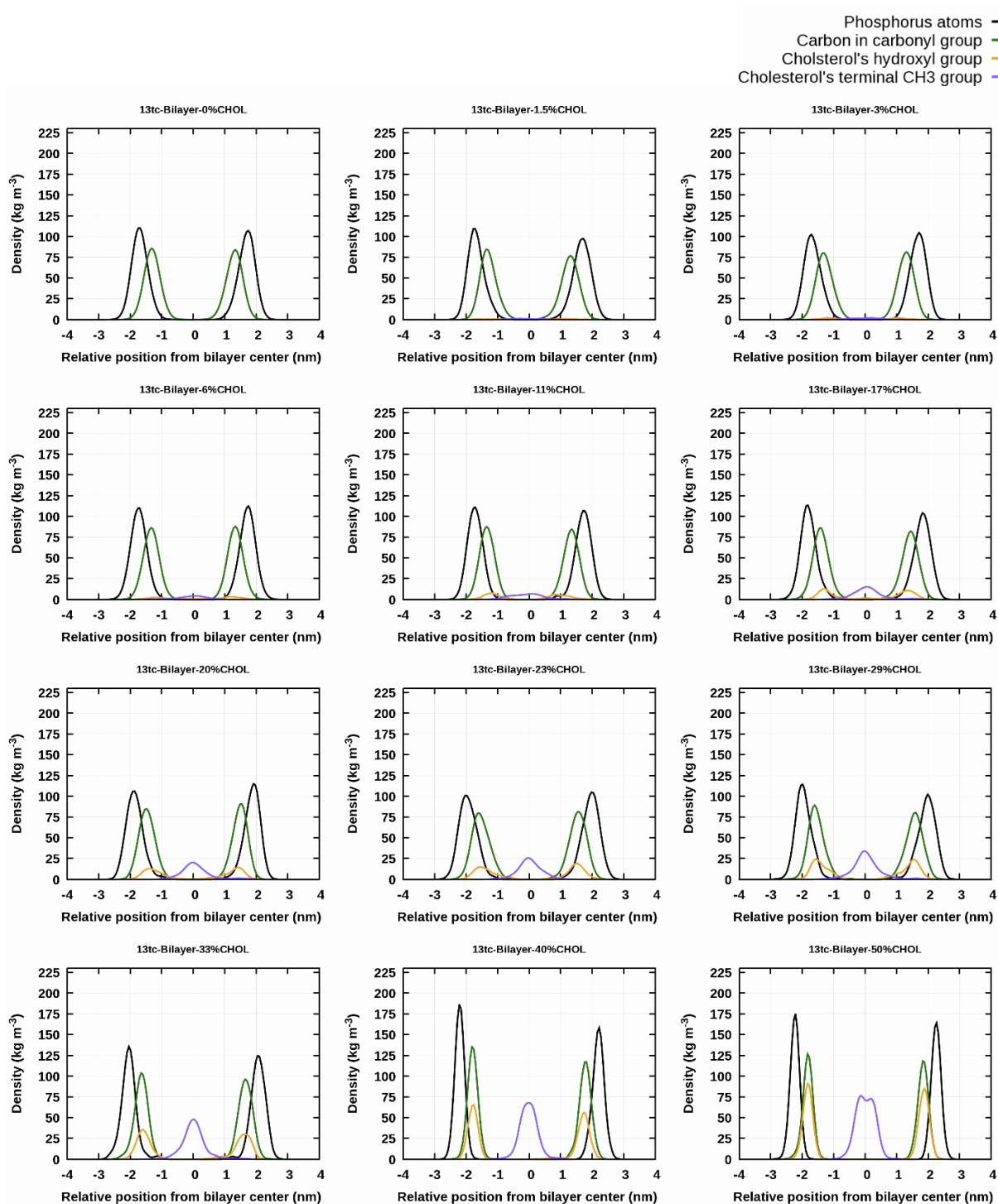
Figure S12. Mass density profiles of the 9-al systems. The legend at the top right hand corner shows the components and the figure titles indicate the systems.

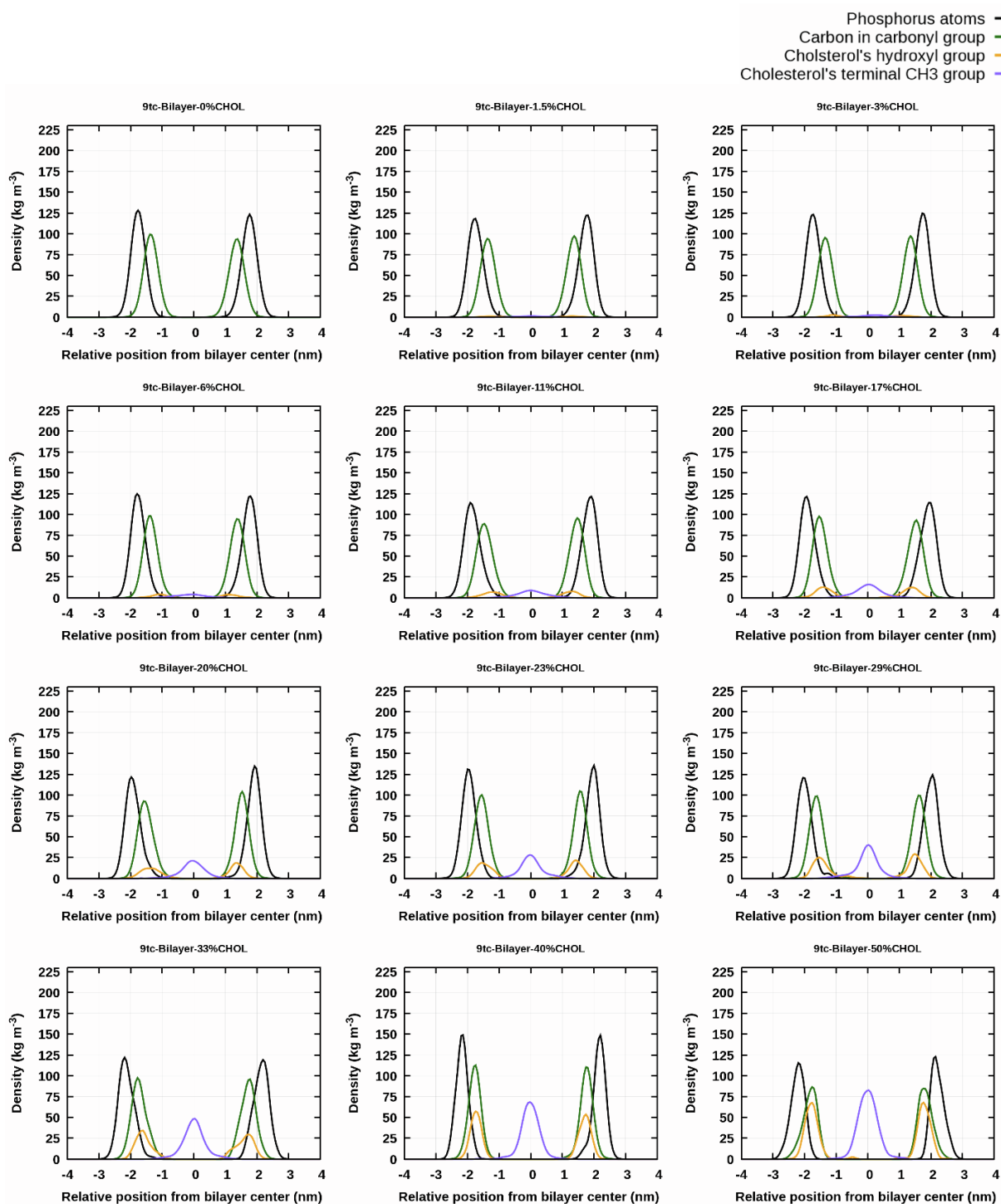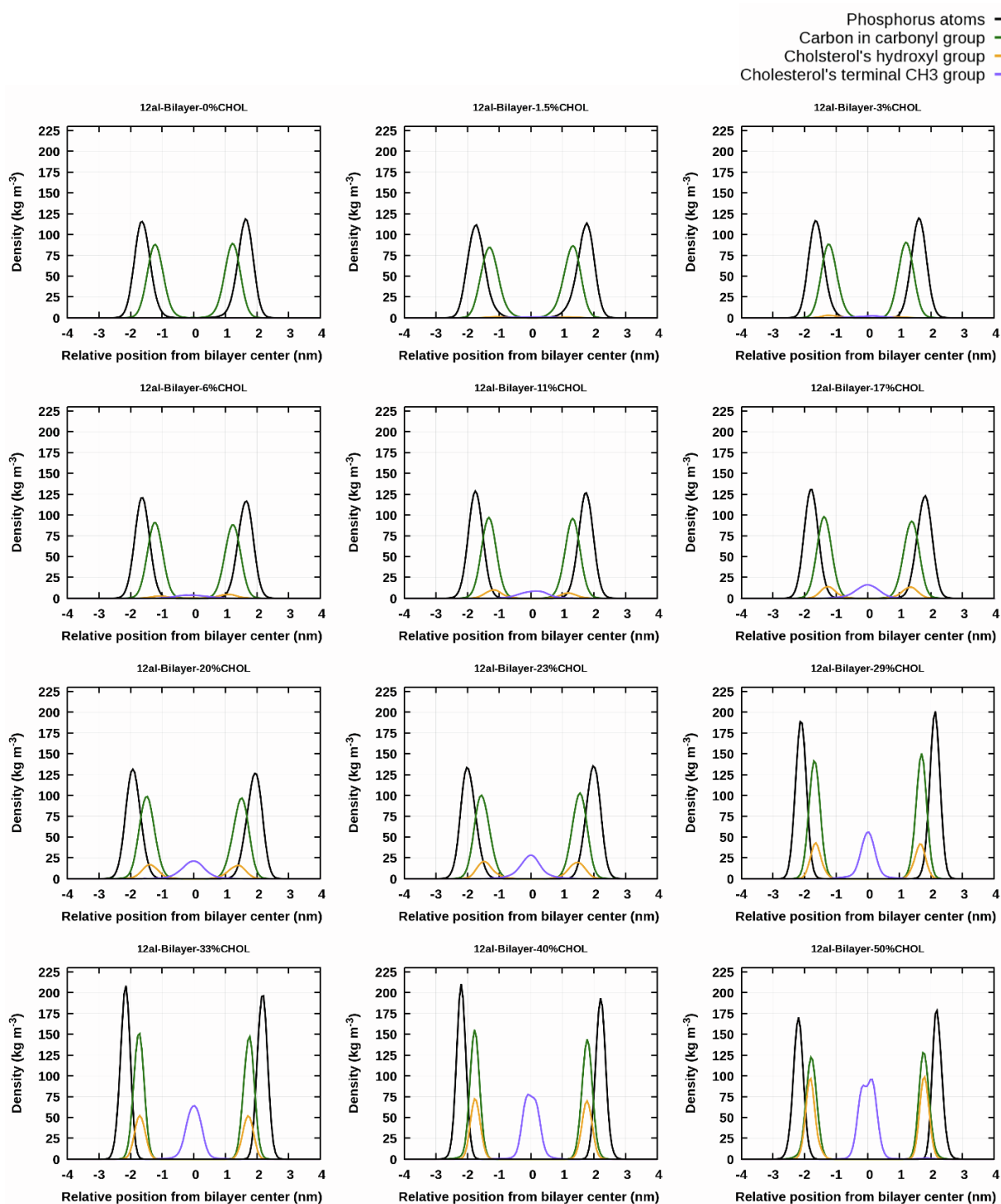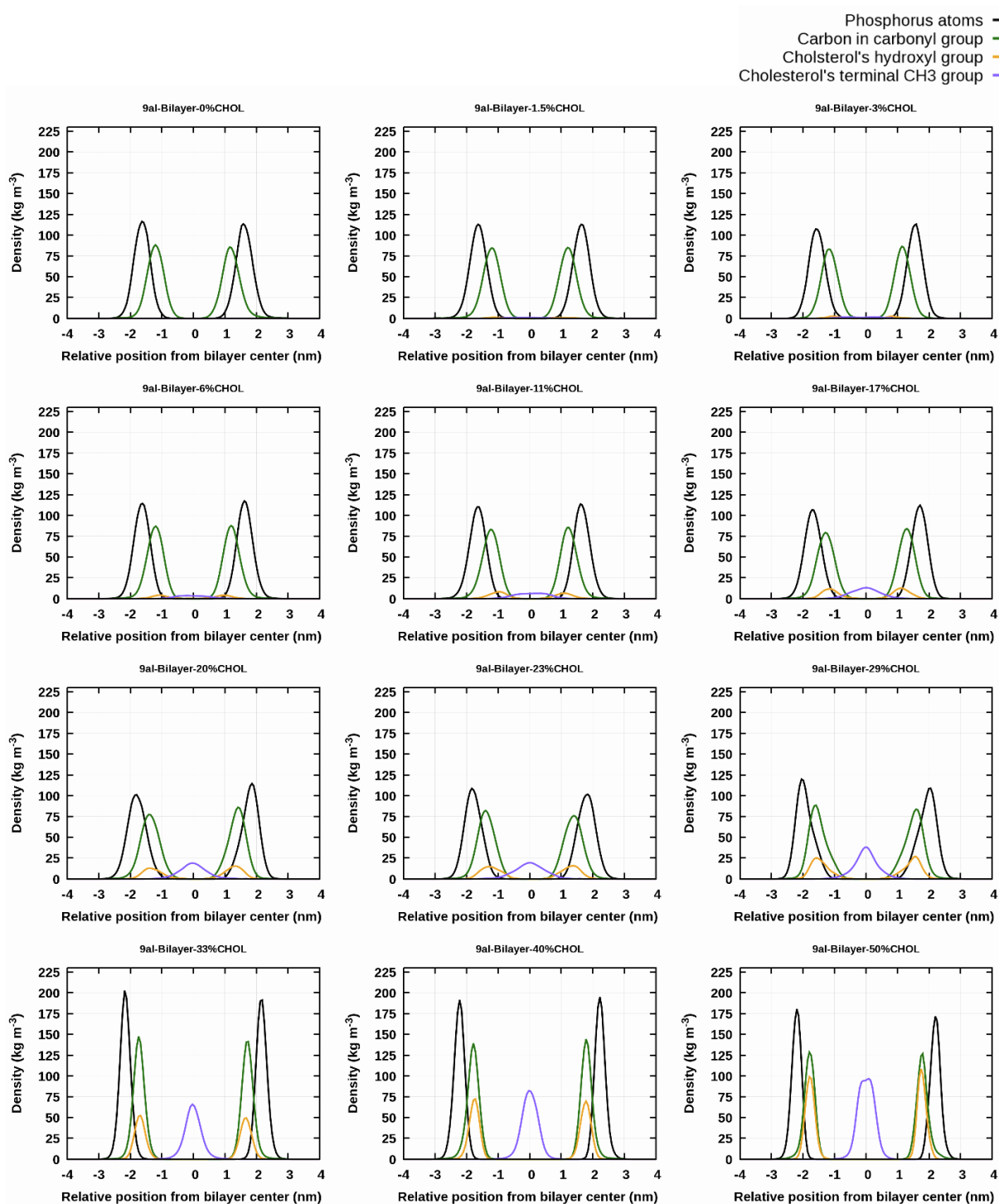**Table S3.** Average distances of different atoms and groups from the bilayer center.

System	Distance from the bilayer center (nm)		
	Phosphorus atom	Carbonyl group	Chol's OH group
100% PLPC without Chol	1.90 ± 0.03	1.48 ± 0.03	-
100% PLPC + 1.5 % Chol	1.91 ± 0.03	1.49 ± 0.03	1.34 ± 0.20
100% PLPC + 3 % Chol	1.93 ± 0.03	1.50 ± 0.03	1.41 ± 0.21
100% PLPC + 6 % Chol	1.95 ± 0.03	1.53 ± 0.03	1.46 ± 0.19
100% PLPC + 11 % Chol	2.00 ± 0.03	1.58 ± 0.02	1.49 ± 0.19
100% PLPC + 17 % Chol	2.07 ± 0.03	1.64 ± 0.03	1.58 ± 0.18
100% PLPC + 20 % Chol	2.11 ± 0.02	1.68 ± 0.02	1.64 ± 0.18
100% PLPC + 23 % Chol	2.14 ± 0.02	1.71 ± 0.02	1.65 ± 0.17
100% PLPC + 29 % Chol	2.20 ± 0.02	1.77 ± 0.02	1.74 ± 0.16
100% PLPC + 33 % Chol	2.22 ± 0.02	1.80 ± 0.02	1.77 ± 0.16
100% PLPC + 40 % Chol	2.26 ± 0.01	1.84 ± 0.01	1.83 ± 0.15
100% PLPC + 50 % Chol	2.24 ± 0.01	1.83 ± 0.01	1.85 ± 0.14
50% 13-tc without Chol	1.70 ± 0.03	1.31 ± 0.03	-
50% 13-tc + 1.5 % Chol	1.71 ± 0.03	1.32 ± 0.03	1.05 ± 0.44
50% 13-tc + 3 % Chol	1.71 ± 0.03	1.32 ± 0.03	1.13 ± 0.26
50% 13-tc + 6 % Chol	1.72 ± 0.03	1.33 ± 0.02	1.07 ± 0.42
50% 13-tc + 11 % Chol	1.76 ± 0.02	1.37 ± 0.02	1.11 ± 0.32
50% 13-tc + 17 % Chol	1.82 ± 0.03	1.43 ± 0.03	1.24 ± 0.37
50% 13-tc + 20 % Chol	1.84 ± 0.03	1.46 ± 0.03	1.27 ± 0.32
50% 13-tc + 23 % Chol	1.90 ± 0.02	1.50 ± 0.02	1.41 ± 0.31
50% 13-tc + 29 % Chol	1.95 ± 0.02	1.56 ± 0.02	1.42 ± 0.30
50% 13-tc + 33 % Chol	2.04 ± 0.02	1.65 ± 0.02	1.56 ± 0.26
50% 13-tc + 40 % Chol	2.19 ± 0.02	1.78 ± 0.01	1.74 ± 0.22
50% 13-tc + 50 % Chol	2.24 ± 0.01	1.83 ± 0.01	1.84 ± 0.16
50% 9-tc without Chol	1.74 ± 0.03	1.34 ± 0.02	-
50% 9-tc + 1.5 % Chol	1.75 ± 0.02	1.36 ± 0.02	1.29 ± 0.23
50% 9-tc + 3 % Chol	1.75 ± 0.03	1.36 ± 0.03	1.11 ± 0.24
50% 9-tc + 6 % Chol	1.77 ± 0.03	1.38 ± 0.02	1.14 ± 0.26
50% 9-tc + 11 % Chol	1.83 ± 0.03	1.44 ± 0.03	1.23 ± 0.27
50% 9-tc + 17 % Chol	1.87 ± 0.03	1.49 ± 0.02	1.35 ± 0.27
50% 9-tc + 20 % Chol	1.91 ± 0.03	1.52 ± 0.02	1.36 ± 0.27
50% 9-tc + 23 % Chol	1.95 ± 0.02	1.56 ± 0.02	1.45 ± 0.24
50% 9-tc + 29 % Chol	2.01 ± 0.02	1.62 ± 0.02	1.47 ± 0.29
50% 9-tc + 33 % Chol	2.08 ± 0.02	1.68 ± 0.02	1.56 ± 0.26
50% 9-tc + 40 % Chol	2.17 ± 0.02	1.78 ± 0.02	1.73 ± 0.19
50% 9-tc + 50 % Chol	2.21 ± 0.01	1.83 ± 0.01	1.77 ± 0.24
50% 12-al without Chol	1.64 ± 0.03	1.23 ± 0.03	-
50% 12-al + 1.5 % Chol	1.66 ± 0.03	1.24 ± 0.03	1.05 ± 0.21
50% 12-al + 3 % Chol	1.66 ± 0.03	1.24 ± 0.03	1.12 ± 0.29
50% 12-al + 6 % Chol	1.67 ± 0.03	1.25 ± 0.03	1.08 ± 0.29
50% 12-al + 11 % Chol	1.73 ± 0.03	1.32 ± 0.03	1.17 ± 0.25
50% 12-al + 17 % Chol	1.82 ± 0.03	1.40 ± 0.03	1.30 ± 0.25
50% 12-al + 20 % Chol	1.86 ± 0.03	1.44 ± 0.03	1.33 ± 0.26
50% 12-al + 23 % Chol	1.93 ± 0.03	1.50 ± 0.03	1.41 ± 0.25
50% 12-al + 29 % Chol	2.13 ± 0.02	1.70 ± 0.02	1.65 ± 0.18
50% 12-al + 33 % Chol	2.19 ± 0.02	1.75 ± 0.02	1.72 ± 0.17
50% 12-al + 40 % Chol	2.21 ± 0.02	1.78 ± 0.01	1.77 ± 0.16
50% 12-al + 50 % Chol	2.21 ± 0.01	1.79 ± 0.01	1.80 ± 0.16
50% 9-al without Chol	1.53 ± 0.16	1.18 ± 0.16	-
50% 9-al + 1.5 % Chol	1.60 ± 0.03	1.19 ± 0.03	0.99 ± 0.30
50% 9-al + 3 % Chol	1.62 ± 0.03	1.20 ± 0.02	0.95 ± 0.29
50% 9-al + 6 % Chol	1.63 ± 0.03	1.22 ± 0.03	1.01 ± 0.27
50% 9-al + 11 % Chol	1.67 ± 0.03	1.26 ± 0.03	1.06 ± 0.28
50% 9-al + 17 % Chol	1.74 ± 0.03	1.33 ± 0.03	1.17 ± 0.28
50% 9-al + 20 % Chol	1.80 ± 0.04	1.38 ± 0.04	1.29 ± 0.30
50% 9-al + 23 % Chol	1.81 ± 0.03	1.39 ± 0.03	1.27 ± 0.31
50% 9-al + 29 % Chol	1.94 ± 0.03	1.52 ± 0.02	1.46 ± 0.29
50% 9-al + 33 % Chol	2.14 ± 0.02	1.71 ± 0.02	1.66 ± 0.18
50% 9-al + 40 % Chol	2.21 ± 0.02	1.79 ± 0.01	1.75 ± 0.16
50% 9-al + 50 % Chol	2.21 ± 0.01	1.81 ± 0.01	1.78 ± 0.15
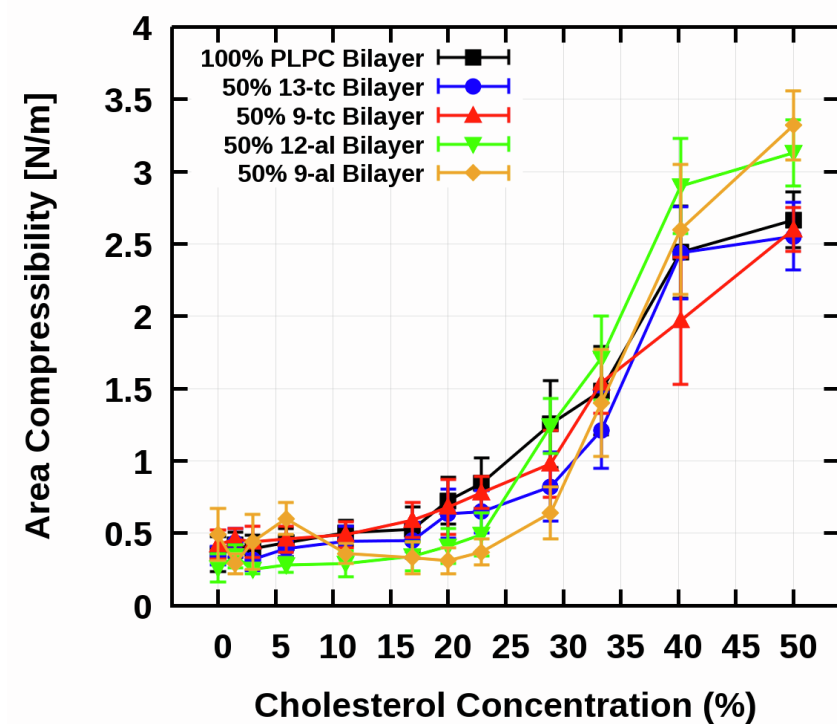
Figure S13. The area compressibility modulus (K_A) as a function of cholesterol concentration in the 100% PLPC and 50% oxidized lipid bilayers.

Supporting References

1. Berendsen, H. J., J. P. Postma, W. F. van Gunsteren, and J. Hermans. 1981. Interaction models for water in relation to protein hydration. In Intermolecular forces. Springer, pp. 331-342.

2. Hub, J. S., F. K. Winkler, M. Merrick, and B. L. de Groot. 2010. Potentials of mean force and permeabilities for carbon dioxide, ammonia, and water flux across a Rhesus protein channel and lipid membranes. J. Am. Chem. Soc. 132: 13251-13263.

CONCLUSIONS

Lipid peroxidation produces oxidized lipid, which is the consequence of free radical oxidative attack on unsaturated fatty acids in lipid chains. The presence of oxidized lipids in the lipid membrane has an impact on their dynamic and physical properties, particularly oxidized lipids with a shortened tail and a polar group such as aldehyde or carboxylic group, which can promote induced pore formation in the oxidized lipid membrane. Previous experimental and computational researchs have confirmed this. [5-12] Cholesterol and α-toc are well-known as an efficient antioxidant molecules that protect cellular membranes from free radical damage. In this work, to investigate the impact of cholesterol and α-toc in model membranes under oxidative stress, a series of microseconds-long MD simulations of α-toc and cholesterol in non-oxidized PLPC and 50% oxidized-PLPC lipid bilayers were performed. Pure PLPC lipid bilayer was used a model membrane under normal condition. The 50% oxidized-PLPC mixed bilayers, the combination between PLPC and its lipid peroxidation product with the oxidized functional groups of hydroperoxide and aldehyde were employed as a model membrane under oxidative stress. Without cholesterol and α-toc, no pore formation was observed in pure PLPC lipid bilayer and the hydroperoxide-containing oxidized bilayers. In contrast, a stable pore was found in the aldehyde-containing oxidized bilayers. These is agreement with the previous studies. [10, 13, 68] In this study, it was discovered that the presence of cholesterol or α-toc helped restrict pore formation in the aldehyde-containing oxidized bilayer. Although either 1.5 to 6% cholesterol or α-toc were added to the bilayer, pore creation was observed. However, adding either cholesterol or α-toc in concentrations greater than 11% could inhibit pores in the bilayers. Using MD simulations help to understand insight on the atomic scale of how cholesterol and α-toc stabilize oxidized membrane. By following the mechanism of pore formation in the aldehyde-containing oxidized bilayer . [10] The aldehyde oxidized functional group can widely distribute between the lipid-water interface and the interior of the lipid bilayer. It pulled water molecules into the bilayer resulting in an increase in water permeability and causing a pore formation in the lipid bilayer. This work showed that the presence of cholesterol and α-toc restricts the distribution and

changes the orientation of the oxidized lipid functional group in the bilayer. This behavior directly affected the mechanism of how the aldehyde functional group induces pore formation in the oxidized lipid bilayer. Next, the behavior of α-toc /cholesterol flip-flop within the bilayer have been investigated. α-toc flip-flops in a non-oxidized membrane, preventing free radicals from damaging unsaturated phospholipid molecules, as suggested in previous studies.[42] In the context of cholesterol, the activity of cholesterol flip-flop helps to stabilize oxidized membrane by balancing the area and relaxing differential-density stress in an asymmetrical oxidized lipid membrane. [43] Here, for all concentrations of α-toc, α-toc flip-flop was seen both in non-oxidized PLPC and 50% oxidized PLPC bilayers. Interestingly, the number of α-toc flip-flop events in the oxidized membrane was found to be higher than in the non-oxidized PLPC membrane. In this case study of cholesterol , however, the flip-flops of cholesterol were only found in the 50% aldehyde-containing oxidized bilayers at 11-23% of cholesterol concentrations. There is no cholesterol flip-flop event in the non-oxidized PLPC bilayer and in the 50% hydroperoxide-containing oxidized bilayers at any cholesterol concentrations, even a lengthy simulation time over 3 microseconds. The findings of the free energy calculations indicated that the presence of oxidized lipids lowers the free-energy barriers for α-toc and cholesterol flip-flop within the lipid bilayer, with the rate of flip-flop varying depending on the kind of oxidized lipid present. The rate for α-toc and cholesterol flip-flop increases in the following order: aldehyde-containing oxidized bilayers > hydroperoxide-containing oxidized bilayers > non-oxidized PLPC bilayer. The rapid flip-flop rate of α-toc in oxidized lipid bilayers, particularly in aldehyde-containing oxidized bilayers, suggests that α-toc provides a physical mechanism that allows itself to scavenge free radicals and protects membranes from oxidative attack while also assisting in membrane stabilization under oxidative stress. In non-oxidized PLPC bilayer and in oxidized-PLPC lipid bilayers, cholesterol has a slower flip-flop rate than α-toc. However, the findings demonstrate that cholesterol prefers to stay near the lipid molecule's carbonyl groups at the lipid-water interface and stabilizes the oxidized lipid bilayer by limiting the distribution of oxidized functional groups resulting in a decreased probability of pore creation. Additionally, increasing cholesterol concentration resulted in a phase transition from liquid-disordered to liquid-ordered.

This condensing effect of cholesterol was found in non-oxidized PLPC bilayer and in oxidized-PLPC lipid bilayers. This finding suggests that cholesterol influences oxidized lipid chain ordering, which has a direct effect on pore formation in aldehyde lipid bilayers.

RECOMMENDATION AND FUTURE WORK

The main finding of this study was that chol/α-toc has a higher potential to flip in oxidized lipid bilayers than in non-oxidized lipid bilayers. It's interesting to investigate the dynamic force that pushes chol/α-toc flip-flops within the oxidized lipid bilayer in order to better understand their behavior in the membrane under oxidative stress. Additional study will focus on the interaction between lipid components and cholesterol α-toc during their flip-flop trajectory within the bilayer. The influence of membrane curvature, membrane lipid surface tension, as well as membrane thickness fluctuation, and membrane area fluctuation induced by the presence of oxidized lipid will also be investigated.

As more information on the interactions of oxidized lipids, α-toc, and cholesterol becomes available, there are several interesting issues related to the interactions of these molecules. Interestingly, it can potentially be applied for derverloping of cancer killing by using cold plasma treatments. Cold plasma is an ionized gas produced by the disintegration of noble gas or ambient air by the application of an electric or electromagnetic field. Reactive nitrogen- oxygen species (RNOS) produced in the plasma that can interact with unsaturated phospholipids in the cell membrane, causing massive lipid peroxidation, pore creation, membrane collapse, and cell death. In recent years, cold plasmas have been demonstrated to induce cell death in cancer cells. [17, 70-72] However, it is important to understand the detailed information about the key role factors of how plasma selectively kills a cancer cell while allowing healthy cells unharmed. There are interesting topics related to this. For example, 1) An investigation into the differences in lipid membrane compositions between cancer cells and healthy cells, as well as their impact on the therapy of plasma-killing cells. 2) The influence of a variety of RONS species on cell membrane oxidation. How does RONS penetrate and interact with the lipids membrane of cancer cells and healthy cells? 3) The effect of RONS on cell membrane with varying lipid types, lipid's unsaturation degree, cholesterol content, and antioxidant level in the cell membrane. These investigations will support the growth of knowledge and the design of more effective methods for destroying cancer cells in medicine using plasma.

LITERATURE CITED

1. Engelman, D.M., *Membranes are more mosaic than fluid.* Nature, 2005. **438**(7068): p. 578-580.

2. Burton, G.J., et al., *Oxidative stress.* 2011. **25**(3): p. 287-299.

3. Gaschler, M.M. and B.R. Stockwell, *Lipid peroxidation in cell death.* Biochemical and biophysical research communications, 2017. **482**(3): p. 419-425.

4. Jurkiewicz, P., et al., *Biophysics of lipid bilayers containing oxidatively modified phospholipids: insights from fluorescence and EPR experiments and from MD simulations.* Biochimica et Biophysica Acta (BBA)-Biomembranes, 2012. **1818**(10): p. 2388-2402.

5. Wong-Ekkabut, J., et al., *Effect of lipid peroxidation on the properties of lipid bilayers: a molecular dynamics study.* Biophysical journal, 2007. **93**(12): p. 4225-4236.

6. Cwiklik, L. and P. Jungwirth, *Massive oxidation of phospholipid membranes leads to pore creation and bilayer disintegration.* Chemical Physics Letters, 2010. **486**(4-6): p. 99-103.

7. Lis, M., et al., *The effect of lipid oxidation on the water permeability of phospholipids bilayers.* 2011. **13**(39): p. 17555-17563.

8. Jarerattanachat, V., M. Karttunen, and J.J.T.J.o.P.C.B. Wong-ekkabut, *Molecular dynamics study of oxidized lipid bilayers in NaCl solution.* 2013. **117**(28): p. 8490-8501.

9. Weber, G., et al., *Lipid oxidation induces structural changes in biomimetic membranes.* 2014. **10**(24): p. 4241-4247.

10. Boonnoy, P., et al., *Bilayer deformation, pores, and micellation induced by oxidized lipids.* The journal of physical chemistry letters, 2015. **6**(24): p. 4884-4888.

11. Runas, K.A. and N. Malmstadt, *Low levels of lipid oxidation radically increase the passive permeability of lipid bilayers.* Soft Matter, 2015. **11**(3): p. 499-505.

12. Bacellar, I.O., et al., *Permeability of DOPC bilayers under photoinduced oxidation: Sensitivity to photosensitizer.* 2018. **1860**(11): p. 2366-2373.

13. Van der Paal, J., et al., *Effect of lipid peroxidation on membrane permeability of cancer and normal cells subjected to oxidative stress.* 2016. **7**(1): p. 489-498.

14. Bacellar, I.O., et al., *Photosensitized membrane permeabilization requires contact-dependent reactions between photosensitizer and lipids.* Journal of the American Chemical Society, 2018. **140**(30): p. 9606-9615.

15. Owen, M.C., et al., *Cholesterol protects the oxidized lipid bilayer from water injury: an all-atom molecular dynamics study.* The Journal of membrane biology, 2018. **251**(3): p. 521-534.

16. Tsubone, T.M., et al., *Contrasting roles of oxidized lipids in modulating membrane microdomains.* 2019. **1861**(3): p. 660-669.

17. Wang, T.-Y., et al., *Membrane oxidation in cell delivery and cell killing applications.* ACS chemical biology, 2017. **12**(5): p. 1170-1182.

18. Yan, D., J.H. Sherman, and M. Keidar, *Cold atmospheric plasma, a novel promising anti-cancer treatment modality.* Oncotarget, 2017. **8**(9): p. 15977.

19. Atkinson, J., et al., *Tocopherols and tocotrienols in membranes: a critical review.* 2008. **44**(5): p. 739-764.

20. Raederstorff, D., et al., *Vitamin E function and requirements in relation to PUFA.* British Journal of Nutrition, 2015. **114**(8): p. 1113-1122.

21. Pisoschi, A.M. and A. Pop, *The role of antioxidants in the chemistry of oxidative stress: A review.* European journal of medicinal chemistry, 2015. **97**: p. 55-74.

22. Marquardt, D., et al., *α-Tocopherol's location in membranes is not affected by their composition.* 2014. **31**(15): p. 4464-4472.

23. Fabre, G., et al., *Synergism of antioxidant action of vitamins E, C and quercetin is related to formation of molecular associations in biomembranes.* 2015. **51**(36): p. 7713-7716.

24. Ausili, A., et al., *The vertical location of α-tocopherol in phosphatidylcholine membranes is not altered as a function of the degree of unsaturation of the fatty acyl chains.* Physical Chemistry Chemical Physics, 2017. **19**(9): p. 6731-6742.

25. Qin, S.-S., Z.-W. Yu, and Y.-X.J.T.J.o.P.C.B. Yu, *Structural and kinetic properties of α-tocopherol in phospholipid bilayers, a molecular dynamics simulation study.* 2009. **113**(52): p. 16537-16546.

26. Qin, S.-S. and Z.-W.J.A.P.-C.S. Yu, *Molecular Dynamics Simulations of α-Tocopherol in Model Biomembranes.* 2011. **27**(1): p. 213-227.

27. Leng, X., et al., *α-Tocopherol is well designed to protect polyunsaturated phospholipids: MD simulations.* 2015. **109**(8): p. 1608-1618.

28. Boonnoy, P., M. Karttunen, and J.J.P.C.C.P. Wong-ekkabut, *Alpha-tocopherol inhibits pore formation in oxidized bilayers.* 2017. **19**(8): p. 5699-5704.

29. Yeagle, P.L.J.B.e.B.A.-R.o.B., *Cholesterol and the cell membrane.* 1985. **822**(3-4): p. 267-287.

30. Yeagle, P., *Cholesterol and related sterols: roles in membrane structure and function. The membranes of cells , Chap. 9.* 2016, Academic Press, Boston.

31. Saito, H. and W.J.T.J.o.P.C.B. Shinoda, *Cholesterol effect on water permeability through DPPC and PSM lipid bilayers: a molecular dynamics study.* 2011. **115**(51): p. 15241-15250.

32. Van der Paal, J., et al., *Hampering effect of cholesterol on the permeation of reactive oxygen species through phospholipids bilayer: possible explanation for plasma cancer selectivity.* 2017. **7**: p. 39526.

33. Owen, M.C., et al., *Cholesterol protects the oxidized lipid bilayer from water injury: an all-atom molecular dynamics study.* 2018. **251**(3): p. 521-534.

34. Risselada, H.J.J.B.j., *Cholesterol: The Plasma Membrane's Constituent that Chooses Sides.* 2019.

35. Schumann-Gillett, A. and M.L.J.B.e.B.A.-B. O'Mara, *The effects of oxidised phospholipids and cholesterol on the biophysical properties of POPC bilayers.* 2019. **1861**(1): p. 210-219.

36. Bennett, W.D., et al., *Molecular view of cholesterol flip-flop and chemical potential in different membrane environments.* 2009. **131**(35): p. 12714-12720.

37. Jo, S., et al., *Cholesterol flip-flop: insights from free energy simulation studies.* 2010. **114**(42): p. 13342-13348.

38. Choubey, A., et al., *Cholesterol translocation in a phospholipid membrane.* 2013. **104**(11): p. 2429-2436.

39. Thallmair, S., H.I. Ingólfsson, and S.J.J.T.j.o.p.c.l. Marrink, *Cholesterol Flip-Flop Impacts Domain Registration in Plasma Membrane Models.* 2018. **9**(18): p.

5527-5533.

40. Gu, R.-X., et al., *Cholesterol Flip-Flop in Heterogeneous Membranes.* 2019.

41. Van der Paal, J., et al., *Hampering effect of cholesterol on the permeation of reactive oxygen species through phospholipids bilayer: possible explanation for plasma cancer selectivity.* Scientific reports, 2017. **7**(1): p. 1-11.

42. Leng, X., et al., *α-Tocopherol is well designed to protect polyunsaturated phospholipids: MD simulations.* Biophysical journal, 2015. **109**(8): p. 1608-1618.

43. Kerdous, R., J. Heuvingh, and S. Bonneau, *Photo-dynamic induction of oxidative stress within cholesterol-containing membranes: shape transitions and permeabilization.* Biochimica et Biophysica Acta (BBA)-Biomembranes, 2011. **1808**(12): p. 2965-2972.

44. Bennett, W.D., et al., *Molecular view of cholesterol flip-flop and chemical potential in different membrane environments.* Journal of the American Chemical Society, 2009. **131**(35): p. 12714-12720.

45. Jo, S., et al., *Cholesterol flip-flop: insights from free energy simulation studies.* The Journal of Physical Chemistry B, 2010. **114**(42): p. 13342-13348.

46. Bennett, W.D. and D.P. Tieleman, *Molecular simulation of rapid translocation of cholesterol, diacylglycerol, and ceramide in model raft and nonraft membranes.* Journal of lipid research, 2012. **53**(3): p. 421-429.

47. Thallmair, S., H.I. Ingólfsson, and S.J. Marrink, *Cholesterol flip-flop impacts domain registration in plasma membrane models.* The journal of physical chemistry letters, 2018. **9**(18): p. 5527-5533.

48. Gu, R.-X., S. Baoukina, and D.P. Tieleman, *Cholesterol flip-flop in heterogeneous membranes.* Journal of chemical theory and computation, 2019. **15**(3): p. 2064-2070.

49. Qin, S.-S., Z.-W. Yu, and Y.-X. Yu, *Structural and kinetic properties of α-tocopherol in phospholipid bilayers, a molecular dynamics simulation study.* The Journal of Physical Chemistry B, 2009. **113**(52): p. 16537-16546.

50. Qin, S.-S. and Z.-W. Yu, *Molecular Dynamics Simulations of α-Tocopherol in Model Biomembranes.* Acta Physico-Chimica Sinica, 2011. **27**(1): p. 213-227.

51. Leng, X., F. Zhu, and S.R. Wassall, *Vitamin E has reduced affinity for a polyunsaturated phospholipid: an Umbrella sampling molecular dynamics simulations study.* The Journal of Physical Chemistry B, 2018. **122**(35): p. 8351-8358.

52. Berendsen, H.J., et al., *Interaction models for water in relation to protein hydration*, in *Intermolecular forces*. 1981, Springer. p. 331-342.

53. Bachar, M., et al., *Molecular dynamics simulation of a polyunsaturated lipid bilayer susceptible to lipid peroxidation.* The Journal of Physical Chemistry B, 2004. **108**(22): p. 7170-7179.

54. Abraham, M.J., et al., *GROMACS: High performance molecular simulations through multi-level parallelism from laptops to supercomputers.* SoftwareX, 2015. **1**: p. 19-25.

55. Bussi, G., D. Donadio, and M. Parrinello, *Canonical sampling through velocity rescaling.* The Journal of chemical physics, 2007. **126**(1): p. 014101.

56. Parrinello, M. and A. Rahman, *Polymorphic transitions in single crystals: A new molecular dynamics method.* Journal of Applied physics, 1981. **52**(12): p. 7182-7190.

57. Nosé, S. and M.J.M.P. Klein, *Constant pressure molecular dynamics for molecular systems.* 1983. **50**(5): p. 1055-1076.

58. Hess, B., et al., *LINCS: a linear constraint solver for molecular simulations.* 1997. **18**(12): p. 1463-1472.

59. Darden, T., D. York, and L. Pedersen, *Particle mesh Ewald: An N· log (N) method for Ewald sums in large systems.* The Journal of chemical physics, 1993. **98**(12): p. 10089-10092.

60. Essmann, U., et al., *A smooth particle mesh Ewald method.* The Journal of chemical physics, 1995. **103**(19): p. 8577-8593.

61. Karttunen, M., et al., *Electrostatics in biomolecular simulations: Where are we now and where are we heading?* Current topics in membranes, 2008. **60**: p. 49-89.

62. Humphrey, W., A. Dalke, and K. Schulten, *VMD: visual molecular dynamics.* Journal of molecular graphics, 1996. **14**(1): p. 33-38.

63. Knight, C.J. and J.S.J.B. Hub, *MemGen: a general web server for the setup of lipid membrane simulation systems.* 2015. **31**(17): p. 2897-2899.

64. Höltje, M., et al., *Molecular dynamics simulations of stratum corneum lipid models: fatty acids and cholesterol.* 2001. **1511**(1): p. 156-167.

65. Torrie, G.M. and J.P. Valleau, *Nonphysical sampling distributions in Monte Carlo free-energy estimation: Umbrella sampling.* Journal of Computational Physics, 1977. **23**(2): p. 187-199.

66. Kumar, S., et al., *The weighted histogram analysis method for free-energy calculations on biomolecules. I. The method.* Journal of computational chemistry, 1992. **13**(8): p. 1011-1021.

67. Bennett, W.D. and D.P.J.J.o.l.r. Tieleman, *Molecular simulation of rapid translocation of cholesterol, diacylglycerol, and ceramide in model raft and nonraft membranes.* 2012. **53**(3): p. 421-429.

68. Boonnoy, P., M. Karttunen, and J. Wong-Ekkabut, *Alpha-tocopherol inhibits pore formation in oxidized bilayers.* Physical Chemistry Chemical Physics, 2017. **19**(8): p. 5699-5704.

69. Lin, F.-H., et al., *Ferulic acid stabilizes a solution of vitamins C and E and doubles its photoprotection of skin.* Journal of Investigative Dermatology, 2005. **125**(4): p. 826-832.

70. Keidar, M., *Plasma for cancer treatment.* Plasma Sources Science and Technology, 2015. **24**(3): p. 033001.

71. Libardo, M.D.J., et al., *How does membrane oxidation affect cell delivery and cell killing?* Trends in biotechnology, 2017. **35**(8): p. 686-690.

72. Bogaerts, A., et al., *Plasma for cancer treatment: How can rons penetrate through the cell membrane? Answers from computer modeling.* Frontiers of Chemical Science and Engineering, 2019. **13**(2): p. 253-263.

CURRICULUM VITAE

NAME   Phansiri Boonnoy

DATE OF BIRTH   20 August 1989

BIRTH PLACE   Ratchaburi, Thailand

ADDRESS   Computational Biomodelling Laboratory for Agricultural Science and Technology, Faculty of Science, Kasetsart University, Bangkok 10900, Thailand

EDUCATION   B.Sc. with 1st class honored (Physics), Kasetsart University, Thailand
M.Sc. (Physics), Kasetart University , Thailand

AWARD RECEIVED   2015 Graduate Thesis Award, The Graduate School, Kasetsart University

PUBLICATION   1. Phansiri Boonnoy, Viwan Jarerattanachat, Mikko Karttunen, and Jirasak Wong-ekkabut. Bilayer Deformation, Pores & Micellation Induced by Oxidized Lipids, The Journal of Physical Chemistry Letters, Vol. 6, November 2015, pp. 4884–4888. IF:8.53
2. Phansiri Boonnoy, Mikko Karttunen, and Jirasak Wong-ekkabut. Alpha-tocopherol inhibits pore formation in oxidized bilayers, Physical Chemistry Chemical Physics, Vol. 19(8), Febuary 2017, pp. 5699-5704. IF:3.90
3. Jiramate Kitjanon, Wasinee Khuntawee, Thana Sutthibutpong, Phansiri Boonnoy, Saree Phongphanphanee, and Jirasak Wong-ekkabut*, Transferability of Polymer Chain Properties between Coarse-Grained and Atomistic Models of Natural Rubber Molecule Validated by Molecular Dynamics Simulations, Siam Physics Congress 2017 (SPC2017), IOP Conf. Series: Journal of Physics: Conf. Series, Vol. 901, 2017, 012096.
4. Phansiri Boonnoy, Mikko Karttunen*, and Jirasak Wong-ekkabut, Does alpha-tocopherol flip-flop help to protect membranes against oxidation?, The Journal of Physical Chemistry B, Vol. 122(45), October 2018, pp. 10362-10370. IF: 2.92
5. Pornkamon Nalakarn, Phansiri Boonnoy, Nililla Nisoh, Mikko Karttunen* and Jirasak Wong-ekkabut, Dependence of fullerene aggregation on lipid saturation due to a balance between entropy and enthalpy, Scientific Reports, Vol. 9, January 2019, 1037. IF: 3.99
6. Mesayamas Kongsema*, Sudtirak Wongkhieo, Mattaka Khongkow, Eric W.F. Lam, Phansiri Boonnoy, Wanwipa Vongsangnak and Jirasak Wong-ekkabut, Molecular

mechanism of Forkhead box M1 (FOXM1) inhibition by thiostrepton on breast cancer cells, Oncology Reports, Vol. 42, July 2019, pp. 953-962. IF: 3.41

7. M. Janlad, P. Boonnoy and J. Wong-ekkabut, Self-Assembly of Aldehyde Lipids in Water, The International Conference on Materials Research and Innovation 2018 (ICMARI2018), IOP Conference Series: Materials Science and Engineering, Vol. 526, 2019, 012005.

8. Phansiri Boonnoy, Viwan Jarerattanachat, Mikko Karttunen and Jirasak Wong-Ekkabut, Role of cholesterol flip-flop in oxidized lipid bilayers, Biophysical Journal, Vol. 120. 1–11, October 19, 2021. IF: 4.03

SCHOLARSHIP   The National Research Council of Thailand, Thailand Science Research and Innovation, through the Royal Golden Jubilee Ph.D. Program grant no. PHD/0204/2559